

การวิเคราะห์การแสดงออกของโปรตีนในเซลล์ผิวหนังตลอดเคื่อดำจากกรรมนุษย์ที่ได้รับ
ไฮโมซิสเทินของสารสกัดพิกัดนาโนโกลที่มีฤทธิ์ต้านอนุมูลอิสระด้วยวิธีโปรตีโอมิกส์

นายนนท์เนศ นลินรัตน์

วิทยานิพนธ์นี้เป็นส่วนหนึ่งของการศึกษาตามหลักสูตรปริญญาวิทยาศาสตรมหาบัณฑิต
สาขาวิชาชีวเวชเคมี ภาควิชาชีวเคมีและจุลชีววิทยา
คณะเภสัชศาสตร์ จุฬาลงกรณ์มหาวิทยาลัย
ปีการศึกษา 2555

บทคัดย่อและแฟ้มข้อมูลฉบับเต็มของวิทยานิพนธ์นี้พร้อมทั้งเอกสารประกอบที่เกี่ยวข้อง
เป็นแฟ้มข้อมูลของนิสิตเจ้าของวิทยานิพนธ์ที่ส่งผ่านทางบัณฑิตวิทยาลัย

The abstract and full text of theses from the academic year 2011 in Chulalongkorn University Intellectual Repository (CUIR)
are the thesis authors' files submitted through the Graduate School.

PROTEOMIC ANALYSIS OF ANTIOXIDANT EFFECTS EXHIBITED BY
PHIKUD NAVAKOT EXTRACT IN HUMAN UMBILICAL VEIN
ENDOTHELIAL CELLS UNDER HOMOCYSTEINE TREATMENT

Mr. Nonthaneth Nalinratana

A Thesis Submitted in Partial Fulfillment of the Requirements
for the Degree of Master of Science Program in Biomedical Chemistry

Department of Biochemistry and Microbiology

Faculty of Pharmaceutical Sciences

Chulalongkorn University

Academic Year 2012

Copyright of Chulalongkorn University

นนท์ชนศ นลินรัตน์ : การวิเคราะห์การแสดงออกของโปรตีนในเซลล์บุผิวหลอดเลือดดำ
 จากรกมนุษย์ที่ได้รับโฮโมซิสเทอีนของสารสกัดพิกัดนวกโฐที่มีฤทธิ์ต้านอนุมูลอิสระด้วย
 วิธีโปรตีโอมิกส์. (PROTEOMIC ANALYSIS OF ANTIOXIDANT EFFECTS
 EXHIBITED BY PHIKUD NAVAKOT EXTRACT IN HUMAN UMBILICAL VEIN
 ENDOTHELIAL CELLS UNDER HOMOCYSTEINE TREATMENT) อ.ที่ปรึกษา
 วิทยานิพนธ์หลัก : รศ.ดร.ดวงเดือน เมฆสุริยพันธ์, อ.ที่ปรึกษาวิทยานิพนธ์ร่วม : ดร.
 จันทรกานต์ พิภพมงคล, 155 หน้า.

พิกัดนวกโฐเป็นตัวยาหลักในตำรับยาหอมนวกโฐที่ใช้ในการบรรเทาอาการไหลเวียนเลือด
 ผิดปกติตามภูมิปัญญาไทย วัตถุประสงค์ของการศึกษานี้คือเพื่อค้นหาโปรตีนเป้าหมายการออกฤทธิ์
 ของสารสกัดด้วยเอทานอลของพิกัดนวกโฐ (NVK) ต่อการปกป้องเซลล์บุผิวหลอดเลือดดำจากรก
 มนุษย์ EA.hy926 จากภาวะเครียดออกซิเดชันจากโฮโมซิสเทอีน การศึกษาเบื้องต้นถึงฤทธิ์ต้าน
 อนุมูลอิสระชนิดซูเปอร์ออกไซด์ ไฮดรอกซิล ไนตริกออกไซด์ และไฮโดรเจนเปอร์ออกไซด์ พบว่า
 NVK ต้านอนุมูลอิสระทุกชนิดได้ดีเมื่อเปรียบเทียบกับฤทธิ์ของสารสกัดโฐแต่ละชนิด เมื่อทำการ
 บ่มเซลล์ EA.hy926 กับ NVK ที่ความเข้มข้น 0.05 มิลลิกรัมต่อมิลลิตรเป็นเวลา 12 ชั่วโมง ตาม
 ด้วยกระตุ้นให้เกิดภาวะเครียดออกซิเดชันด้วยโฮโมซิสเทอีนที่ความเข้มข้น 0.05 มิลลิโมลาร์เป็น
 เวลา 12 ชั่วโมง พบว่า NVK ไม่เป็นพิษต่อเซลล์ และสามารถลดปริมาณอนุมูลอิสระภายในเซลล์ได้
 เมื่อศึกษาผลต่อโปรตีนภายในเซลล์ด้วยเทคนิคอิเล็กโทรโฟริซิสแบบ 2 มิติร่วมกับเทคนิค
 แมสสเปกโตรเมตรีพบว่า NVK เปลี่ยนแปลงปริมาณโปรตีนที่เกี่ยวข้องกับกระบวนการควบคุมรี
 ดอกซ์ เมแทบอลิซึมและ chaperone เป็นต้น ขณะที่โฮโมซิสเทอีนมีผลต่อโปรตีนที่เกี่ยวข้องกับการ
 เสื่อมสภาพการทำงานของเซลล์ แต่เมื่อเซลล์ได้รับ NVK ก่อนจะได้รับโฮโมซิสเทอีนเปลี่ยนแปลง
 การแสดงออกของโปรตีน เช่น annexin A2 และ heat shock cognate 71 kD ซึ่งเกี่ยวข้องกับการ
 ปกป้องเซลล์ เมื่อนำไปวิเคราะห์ด้วยเทคนิคชีวสารสนเทศทำให้ได้แผนที่โปรตีนที่เชื่อมโยงการ
 นำส่งสัญญาณภายในเซลล์ จากเทคนิคอิมมูโนบลอตพบว่า NVK เพิ่มการแสดงออกของโปรตีน
 heme oxygenase-1 และ vascular endothelial growth factor รวมถึงกระตุ้นการทำงานของเอนไซม์
 endothelial nitric oxide synthase การศึกษานี้ทำให้ทราบถึงข้อมูลการออกฤทธิ์ของพิกัดนวกโฐ ซึ่ง
 จะเป็นหลักฐานทางวิทยาศาสตร์ในการสนับสนุนการใช้พิกัดนวกโฐในยาหอมตามภูมิปัญญาไทย

ภาควิชา.....ชีวเคมีและจุลชีววิทยา.....ลายมือชื่อนิติศ.....
 สาขาวิชา.....ชีวเวชเคมี.....ลายมือชื่ออ.ที่ปรึกษาวิทยานิพนธ์หลัก.....
 ปีการศึกษา.....2555.....ลายมือชื่ออ.ที่ปรึกษาวิทยานิพนธ์ร่วม.....

5276614533 : MAJOR BIOMEDICINAL CHEMISTRY

KEYWORDS : PHIKUD NAVAKOT / ANTIOXIDANT / HOMOCYSTEINE /
ENDOTHELIAL CELLS / PROTEOMICS

NONTHANETH NALINRATANA : PROTEOMIC ANALYSIS OF
ANTIOXIDANT EFFECTS EXHIBITED BY PHIKUD NAVAKOT EXTRACT
IN HUMAN UMBILICAL VEIN ENDOTHELIAL CELLS UNDER
HOMOCYSTEINE TREATMENT. ADVISOR : ASSOC. PROF.
DUANGDEUN MEKSURIYEN, Ph.D., CO-ADVISOR : CHANTRAGAN
PHIPHOBMONGKOL, Ph.D., 155 pp.

Phikud Navakot is a main ingredient in Yahom Navakot, Thai traditional polyherbal formula that has been widely used for treatment of circulatory disorder. In this study, the effect of Phikud Navakot ethanolic extract (NVK) was investigated on homocysteine-induced oxidative stress in human umbilical vein endothelial EA.hy926 cells. Scavenging activities against radicals of superoxide, hydroxyl, nitric oxide and hydrogen peroxide were performed. The results showed that NVK exhibited higher antioxidant activity than most of individual herbal extracts. Pre-treatment of NVK at the non-toxic concentration of 0.05 mg/mL for 12 h prior exposure to 0.05 mM homocysteine (Hcy) significantly reduced intracellular reactive oxygen species. Two-dimensional electrophoresis coupled with mass spectrometry showed that NVK alone altered the protein expression involving in redox regulation, metabolism and chaperones. Hcy altered the level of proteins involving in endothelial dysfunction. Meanwhile, pre-treatment of NVK before exposure to Hcy restored the proteins such as annexin A2, heat shock cognate 71 kD. Network analysis using bioinformatic tools such as STRING, KOBAS, and IPA[®] revealed signaling pathways affected by NVK in the absence or presence of Hcy. Additionally, immunoblot analysis showed that NVK up-regulated heme oxygenase-1 and vascular endothelial growth factor and activated endothelial nitric oxide synthase. Our investigation provides an understanding in mechanism of action of NVK, supporting the traditional use for the treatment of circulatory disorder.

Department : Biochemistry and Microbiology Student's Signature.....

Field of Study : Biomedical Chemistry Advisor's Signature.....

Academic Year : 2012 Co-advisor's Signature.....

ACKNOWLEDGMENTS

This thesis could not successfully complete without the guidance and the help of several persons who in one way or another contributed and extended their valuable assistance in the preparation and completion of this study.

First and foremost, I would like to express sincere gratitude to my thesis advisor, Associate Professor Dr. Duangdeun Meksuriyen and my co-advisor, Dr. Chantragan Phiphobmongkol for their invaluable advice, attention, motivation, encouragement, and patience. Their kindness is really appreciated. Also, I would like to thank thesis committee for their invaluable suggestion.

I wish to express my grateful thanks to Ms. Penchatr Diskul-Na-Ayudthaya and Mr. Churat Weeraphan for their assistance in 2-DE experiments. I am very thankful to Ms. Daranee Chokchaichamnankit for her assistance in LC/MS/MS analysis. I also express my grateful thanks to all members at the Laboratory of Biochemistry, Chulabhorn Research Institute whose name have not mentioned for their assistance.

I am very thankful to Dr. Sanya Hokputsa, and Associate Professor Dr. Uthai Sotanaphun for providing of Phikud Navakot extracts.

I wish to give a special thanks to Associate Professor Dr. Sa-nga Pattanakitsakul for providing human umbilical vein endothelial EA.hy926 cells for the preliminary study. I also thank to Pharmaceutical Research Instrument Center and Chulalongkorn University Drug and Health Products Innovation Promotion Center (CU.D.HIP), for providing scientific equipments for this study.

I am very thankful to all members at the Department of Biochemistry and Microbiology, Faculty of Pharmaceutical Sciences for their kindness and assistance.

Finally, I wish to express my infinite thank to my family, who always love, understand and support everything in my life.

This work was financially supported by TRF Master Research Grant (TRF MAG Window I: MRG545S094), National Research Council of Thailand (NRCT 2011-33) and the 90th Anniversary of Chulalongkorn University Fund (Ratchadaphisedksomphot Endowment Fund). I also thank Suwan Osoth Co., Ltd. for partly providing a fellowship.

CONTENTS

	Page
ABSTRACT IN THAI.....	iv
ABSTRACT IN ENGLISH.....	v
ACKNOWLEDGEMENTS.....	vi
CONTENTS.....	vii
LIST OF TABLES.....	viii
LIST OF FIGURES.....	xi
LIST OF ABBREVIATIONS.....	xiii
CHAPTER	
I INTRODUCTION.....	1
II LITERATURE REVIEW.....	6
III MATERIALS AND METHODS.....	15
IV RESULTS AND DISCUSSION.....	30
V CONCLUSIONS.....	84
REFERENCES.....	87
APPENDICES.....	111
APPENDIX A.....	112
APPENDIX B.....	119
VITA.....	155

LIST OF TABLES

Table		Page
1	Codes of nine crude drugs in Phikud Navakot and their part used.....	20
2	Steady-state levels of proteins in NVK-treated cells identified by LC/MS/MS.....	51
3	KOBAS analysis of differentially expressed proteins in NVK-treated cells.....	57
4	Steady-state levels of proteins in Hcy-treated cells identified by LC/MS/MS.....	63
5	KOBAS analysis of differentially expressed proteins in Hcy-treated cells.....	69
6	Summary of changed proteins which affected by treatment of NVK, Hcy and NVK+Hcy.....	74
7	The percentage of $O_2^{\cdot-}$ scavenging activities of AD.....	119
8	The percentage of $O_2^{\cdot-}$ scavenging activities of AL.....	119
9	The percentage of $O_2^{\cdot-}$ scavenging activities of AP.....	120
10	The percentage of $O_2^{\cdot-}$ scavenging activities of AS.....	120
11	The percentage of $O_2^{\cdot-}$ scavenging activities of LC.....	121
12	The percentage of $O_2^{\cdot-}$ scavenging activities of NJ.....	121
13	The percentage of $O_2^{\cdot-}$ scavenging activities of PK.....	122
14	The percentage of $O_2^{\cdot-}$ scavenging activities of SC.....	122
15	The percentage of $O_2^{\cdot-}$ scavenging activities of TC.....	123
16	The percentage of $O_2^{\cdot-}$ scavenging activities of NVK.....	123
17	The percentage of H_2O_2 scavenging activities of AD.....	124
18	The percentage of H_2O_2 scavenging activities of AL.....	124
19	The percentage of H_2O_2 scavenging activities of AP.....	125

Table	Page
20 The percentage of H ₂ O ₂ scavenging activities of AS.....	125
21 The percentage of H ₂ O ₂ scavenging activities of LC.....	126
22 The percentage of H ₂ O ₂ scavenging activities of NJ.....	126
23 The percentage of H ₂ O ₂ scavenging activities of PK.....	127
24 The percentage of H ₂ O ₂ scavenging activities of SC.....	127
25 The percentage of H ₂ O ₂ scavenging activities of TC.....	128
26 The percentage of H ₂ O ₂ scavenging activities of NVK.....	128
27 The percentage of OH [•] scavenging activities of AD.....	129
28 The percentage of OH [•] scavenging activities of AL.....	129
29 The percentage of OH [•] scavenging activities of AP.....	130
30 The percentage of OH [•] scavenging activities of AS.....	130
31 The percentage of OH [•] scavenging activities of LC.....	131
32 The percentage of OH [•] scavenging activities of NJ.....	131
33 The percentage of OH [•] scavenging activities of PK.....	132
34 The percentage of OH [•] scavenging activities of SC.....	132
35 The percentage of OH [•] scavenging activities of TC.....	133
36 The percentage of OH [•] scavenging activities of NVK.....	133
37 The percentage of NO [•] scavenging activities of AD.....	134
38 The percentage of NO [•] scavenging activities of AL.....	134
39 The percentage of NO [•] scavenging activities of AP.....	135
40 The percentage of NO [•] scavenging activities of AS.....	135
41 The percentage of NO [•] scavenging activities of LC.....	136
42 The percentage of NO [•] scavenging activities of NJ.....	136
43 The percentage of NO [•] scavenging activities of PK.....	137

Table	Page
44 The percentage of NO [•] scavenging activities of SC.....	137
45 The percentage of NO [•] scavenging activities of TC.....	138
46 The percentage of NO [•] scavenging activities of NVK.....	138
47 The EC ₅₀ values of O ₂ ^{•-} , H ₂ O ₂ , OH [•] and NO [•] scavenging activities of ethanolic extracts of individual herbs and NVK.....	139
48 The EC ₅₀ values of O ₂ ^{•-} , H ₂ O ₂ , OH [•] and NO [•] scavenging activities of water extracts of individual herbs and NVK.....	140
49 The combination index values of O ₂ ^{•-} , H ₂ O ₂ , OH [•] and NO [•] scavenging activities of ethanolic and water extracts.....	141
50 The percentage of cell viability of NVK.....	141
51 The percentage of DCF fluorescence of NVK.....	142
52 The percentage of cell viability of Hcy.....	142
53 The percentage of DCF fluorescence of Hcy for 0.5, 1, 2 and 3 h.....	143
54 The percentage of DCF fluorescence of Hcy for 6, 12 and 24 h.....	144
55 The percentage of DCF fluorescence of NVK pre-treatment at the various concentrations for 12 h prior to 1 mM Hcy for 1 h.....	145
56 The percentage of cell viability of NVK pre-treatment at the various concentrations for 12 h prior to 0.05 mM Hcy for 12 h.....	146
57 The percentage of DCF fluorescence of NVK pre-treatment at the various concentrations for 12 h prior to 0.05 mM Hcy for 12 h.....	147
58 Identified proteins obtained from LC/MS/MS and MASCOT database.....	147
59 Relative ratio of NVK on induction of HIF-1 α in EA.hy926 cells.....	151
60 Relative ratio of NVK on induction of Nrf2 in EA.hy926 cells.....	152
61 Relative intensity ratio of HO-1 expression by NVK treatment.....	152
62 Relative intensity ratio of expression of antioxidant enzymes by NVK treatment.....	153
63 Relative intensity ratio of VEGF expression by NVK treatment.....	153
64 Relative intensity ratio of Akt phosphorylation by NVK treatment.....	154

Table		Page
65	Relative intensity ratio of eNOS phosphorylation by NVK treatment..	154

LIST OF FIGURES

Figure		Page
1	Conceptual framework of the antioxidant role of NVK in endothelial cells under Hcy treatment.....	3
2	EC ₅₀ values for O ₂ ^{•-} scavenging activity.....	31
3	EC ₅₀ values for H ₂ O ₂ scavenging activity.....	33
4	EC ₅₀ values for OH [•] scavenging activity.....	35
5	EC ₅₀ values for NO [•] scavenging activity.....	36
6	CI values of the antioxidant activities were compared between the ethanolic and water extracts of NVK.....	38
7	Concentration- and time-dependent studies of NVK on cell viability determined by MTT assay.....	40
8	Concentration- and time-dependent studies of NVK on intracellular ROS determined by DCFH-DA assay.....	42
9	Concentration- and time-dependent studies of Hcy on cell viability determined by MTT assay.....	43
10	Concentration- and time-dependent studies of Hcy on intracellular ROS determined by DCFH-DA assay.....	45
11	Effect of NVK on ROS and viability under 1-h Hcy treatment.....	47
12	Effect of NVK on ROS and viability under 12-h Hcy treatment.....	48
13	Representative 2-DE gels of proteins from cells exposed to NVK.....	49
14	Functional categories of the changed proteins in NVK-treated cells..	53
15	Relative spot intensities of identified proteins from NVK-treated cells compared to control.....	54
16	Network analysis of identified proteins from NVK-treated cells using STRING.....	55
17	Representative 2-DE gels of proteins from cells exposed to Hcy.....	62

Figure		Page
18	Functional categories of the changed proteins in Hcy-treated cells....	65
19	Relative spot intensities of identified proteins from Hcy-treated cells compared to control group (untreated).....	66
20	Network analysis of identified proteins from Hcy-treated cells using STRING.....	67
21	Representative 2-DE gels of proteins from the cells exposed to NVK before expures to Hcy.....	71
22	Relative spot intensities of same proteins in NVK pretreatment followed by Hcy group compared to either NVK or Hcy groups.....	72
23	Network analysis of identified proteins from cells exposed to NVK before expures to Hcy using STRING.....	73
24	Time-dependent study of HIF-1 α and Nrf2 induction by NVK treatment.....	78
25	Concentration-dependent study of HO-1 expression by NVK treatment.....	79
26	Concentration-dependent study of antioxidant enzyme expression by NVK treatment.....	80
27	VEGF expression affected by NVK.....	82
28	Time-dependent study on phosphorylation of eNOS and Akt by NVK treatment.....	83
29	Possible mechanism of NVK in the (A) absence and (B) presence of Hcy in endothelial cells.....	85

LIST OF ABBREVIATIONS

%	percentage
A	absorbance
A549 cells	human lung carcinoma cells
ABTS	2,2-azino-bis(3-ethylbenzothiazoline-6-sulfonic acid)
AD	<i>Angelica dahurica</i>
AGEs	advanced glycation end products
Akt	protein kinase B
AL	<i>Atractylodes lancea</i>
ANOVA	analysis of variance
AP	<i>Artemisia pallens</i>
APS	ammonium persulfate
ARE	antioxidant response element
AS	<i>Angelica sinensis</i>
ATCC	American Type Culture Collection
ATP	adenosine triphosphate
BSA	albumin from bovine serum
°C	Celsius
Ca ²⁺	calcium
CaCl ₂	calcium chloride
CAT	catalase
CCl ₄	carbon tetrachloride
CHAPS	3-[(3-cholamidopropyl) dimethylammonio]-1-propanesulfonate
ChREBP	carbohydrate response element binding protein
CI	combination index
CO ₂	carbon dioxide
COX	cyclooxygenase
DCF	2',7'- dichlorofluorescein
DCFH	2',7'- dichlorodihydrofluorescein

DCFH-DA	2',7'- dichlorodihydrofluorescein diacetate
2-DE	two-dimensional electrophoresis
DHAP	dihydroxyacetone phosphate
DMEM	Dulbecco's modified Eagle's medium
DMSO	dimethyl sulfoxide
DNA	deoxyribonucleic acid
DPPH	2, 2-diphenyl-1-picrylhydrazyl
DTT	dithiothreitol
EA.hy926 cells	immortalized human umbilical vein endothelial cells
EC ₅₀	half maximal effective concentration
ECL	enhanced chemiluminescence
ECV304 cells	transformed human umbilical vein endothelial cells
EDTA	ethylenediaminetetraacetic acid
EF-tu	elongation factor Tu
eNOS	endothelial nitric oxide synthase
ER	endoplasmic reticulum
ERK	extracellular signal-regulated kinase
<i>et al.</i>	<i>et alii</i> , and others
F	fluorescence intensity
F1,6P	β-D-fructose 1,6-bisphosphate
FBS	fetal bovine serum
FeCl ₃	ferric (III) chloride
FRAP	ferric reducing antioxidant power
GADP	D-glyceraldehyde 3-phosphate
GAPDH	glyceraldehyde 3-phosphate dehydrogenase
GPx	glutathione peroxidase
GRP78	glucose-regulated protein 78 kD
GSH	glutathione
GST	glutathione-S-transferase
GST-P	glutathione-S-transferase class Pi
h	hour

HCl	hydrochloric acid
Hcy	homocysteine
HepG2 cells	human hepatocellular carcinoma cells
HIF-1 α	hypoxia inducible factor-1 α
hnRNPA1L2	heterogeneous nuclear ribonucleoprotein A1-like 2
hnRNPA2B1	heterogeneous nuclear ribonucleoproteins A2/B1
hnRNPH1	heterogeneous nuclear ribonucleoprotein H
H ₂ O ₂	hydrogen peroxide
HO-1	heme oxygenase-1
HPLC	high performance liquid chromatography
HRP	horseradish peroxidase
Hsc70	heat shock cognate 71 kD
Hsp70	heat shock protein 70 kD
HUVEC cells	human umbilical vein endothelial cells
IC ₅₀	half maximal inhibitory concentration
ICAM-1	intercellular adhesion molecule 1
IEF	isoelectric focusing
IL-1 β	interleukin-1 beta
iNOS	inducible nitric oxide synthase
IPA	Ingenuity Pathway Analysis
IPG	immobilized pH gradient
JNK	c-Jun N-terminal kinases
kD	kilodalton
KEGG	Kyoto Encyclopedia of Genes and Genomes
KOBAS	KEGG Orthology Based Annotation System
LC	<i>Ligusticum chuanxiong</i>
LC	liquid chromatography
M	molar
mA	milliampere
MALDI-TOF	matrix-assisted laser desorption/ionisation-time of flight
MAPK	mitogen-activated protein kinase

MBP1	myc promoter-binding protein
MDA	malondialdehyde
MEK	MAPK/ERK kinase
mg	milligram
min	minute
mL	milliliter
mM	millimolar
Mn-SOD	manganese superoxide dismutase
mRNA	messenger ribonucleic acid
MS	mass spectrometry
MTT	3-(4, 5-dimethylthiazol-2-yl)-2, 5-diphenyltetrazolium bromide
MW	molecular weight
NaCl	sodium chloride
NADH	nicotinamide adenine dinucleotide
NADPH	nicotinamide adenine dinucleotide phosphate
NBT	nitrotetrazolium blue chloride
NF- κ B	nuclear factor kappa-light-chain-enhancer of activated B cells
NH ₄ HCO ₃	ammonium bicarbonate
NJ	<i>Nardostachys jatamansi</i>
NL	non-linear
nLC	nanoflow liquid chromatography
NO	nitric oxide
NO [•]	nitric oxide radical
NOS	nitric oxide synthase
NPM	nucleophosmin
Nrf2	nuclear factor (erythroid-derived 2)-like 2
NVK	Phikud Navakot ethanolic extract
O ₂ ^{•-}	superoxide radical
OH [•]	hydroxyl radical

ONOO ⁻	peroxynitrite
PAGE	polyacrylamide gel electrophoresis
PANTHER	Protein analysis through evolutionary relationships
PBS	phosphate-buffered saline
PC12 cells	rat adrenal medulla pheochromocytoma cells
PDGF	platelet-derived growth factor
PDI	protein disulfide-isomerase
PDIA3	protein disulfide-isomerase A3
PEP	phosphoenolpyruvate
2PG	2-phosphoglycerate
pH	negative logarithm of hydrogen ion concentration
pI	isoelectric point
PID	Pathway interaction database
PK	<i>Picrorhiza kurrooa</i>
PKC	protein kinase C
PKM	pyruvate kinase M1/M2
PMS	phenazine methosulfate
PTM	post-translational modification
PVDF	polyvinylidene fluoride
RAW264.7 cells	murine leukaemic monocyte macrophage cells
RIPA	radioimmunoprecipitation assay
RNS	reactive nitrogen species
ROS	reactive oxygen species
rpm	revolutions per minute
s	second
SC	<i>Saussurea costus</i>
SDS	sodium dodecyl sulfate
S.E.M.	standard error of mean
SFPQ	splicing factor proline- and glutamine-rich
SNP	sodium nitroprusside
SOD	superoxide dismutase

STRING	Search Tool for the Retrieval of Interacting Genes/proteins
TBA	2-thiobarbituric acid
TBARS	thiobarbituric acid-reactive substances
TBS-T	tris-buffered saline-tween 20
TC	<i>Terminalia chebula</i>
TCA	trichloroacetic acid
TCP-1	T-complex protein 1
TEMED	N,N,N',N'-tetramethylethylenediamine
TNF- α	tumor necrosis factor- α
tPA	tissue plasminogen activator
TPI	triosephosphate isomerase
μ A	microampere
μ L	microliter
μ M	micromolar
UV	ultraviolet
V	volt
v/v	volume by volume
VEGF	vascular endothelial growth factor
vWF	von Willebrand factor
X5P	xylulose-5-phosphate

CHAPTER I

INTRODUCTION

According to the World Health Organization, cardiovascular diseases are the leading causes of death and disability in the world. Over 80% of cardiovascular death takes place in low- and middle-income countries. Ministry of Public Health of Thailand reported that cardiovascular diseases, which referred to atherosclerosis, heart disease and hypertension, have been the leading cause of death in 2006-2010 (Bureau of Policy and Strategy, 2011). The major pathogenesis of cardiovascular diseases is endothelial dysfunction, leading to development of atherosclerosis. Epidemiologic studies reveal that hyperhomocysteinaemia, where the plasma level of homocysteine (Hcy) is higher than 0.1 mM, is associated with endothelial dysfunction (Domagala *et al.*, 1998). High level of Hcy can impair endothelial function through various mechanisms especially increase in oxidative stress (Perna *et al.*, 2003). Since the oxidative stress can injure endothelial cells, a number of herbal extracts and antioxidant compounds have been tested as agents to restore endothelial function (Laght *et al.*, 2000). Several herbal extracts and natural compounds were found to have protective effect against Hcy-induced endothelial dysfunction such as garlic extract (Weiss *et al.*, 2006), *Astragalus membranaceus* extract (Zhang *et al.*, 2007) and ginsenoside Rb1 (Zhou *et al.*, 2005). Therefore, herbal extracts may be an alternative source for therapeutic agents.

According to Thai traditional knowledge, the medicinal herbs when used in combination would bring the better therapeutic efficacy than single herb which is called a synergistic effect (Williamson, 2001). Yahom, one of Thai polyherbal formulae primarily used for treating circulatory disorder, has been included in the List of Herbal Medicinal Products of Thailand (National Drug Committee of Thailand, 2011). Yahom consists of 54 herbs including Phikud Navakot, which is a set of an equal proportion of nine herbs. Phikud Navakot consists of roots of *Angelica dahurica* (Fisch.) Benth. & Hook.f. (Kot Soa, Apiaceae), *A. sinensis* (Oliv.) Diels (Kot Chiang, Apiaceae) and *Saussurea costus* (Falc.) Lipsch. (Kot Kradoo, Asteraceae), the rhizomes of *Atractylodes lancea* (Thunb.) DC. (Kot Kamao, Asteraceae), *Ligusticum chuanxiong* Hort. (Kot Huabua, Apiaceae) and *Picrorhiza kurroa* Royle ex Benth.

(Kot Kanprao, Scrophulariaceae), the roots and rhizomes of *Nardostachys jatamansi* (D. Don) DC. (Kot Jatamansi, Valerianaceae), the aerial parts of *Artemisia pallens* Walls ex DC. (Kot Chulalumpa, Asteraceae) and the galls of *Terminalia chebula* Retz. (Kot Pungpla, Combretaceae). Several scientific findings support the traditional use of Yahom in treatment of circulatory disorder. Yahom increased the cerebral blood flow in rats under regional vasodilation (Jariyapongskul *et al.*, 2006). Water extract of Yahom increased aortic ring and atrial contraction (Suvitayavat *et al.*, 2005). Phikud Navakot was hypothesized to be a major active ingredient in Yahom since several Yahom formulae were consisted of crude drugs in Phikud Navakot. Moreover, Phikud Navakot ethanolic extract (NVK) did not show treatment-related mortality in rats, suggesting that NVK may be relatively safe from toxicity (Kengkoom *et al.*, 2012). However, the effect of NVK on Hcy-induced oxidative stress has not been investigated elsewhere. Endothelial cells, a main target of Hcy, were used as a model in this study.

Conceptual framework

Hcy increased oxidative stress in endothelial cells by generation of superoxide radical ($O_2^{\bullet-}$) via auto-oxidation and induction of nicotinamide adenine dinucleotide phosphate (NADPH) oxidase (Tyagi *et al.*, 2005) (Figure 1), which subsequently converted to hydrogen peroxide (H_2O_2) by superoxide dismutase (SOD). Hydrogen peroxide was further detoxified to H_2O and O_2 by glutathione peroxidase (GPx) or catalase (CAT). However, H_2O_2 is also converted by Fenton reaction to generate hydroxyl radical (OH^{\bullet}) which is highly reactive. Increase of these reactive oxygen species (ROS) caused endothelial damage. In response to ROS, several antioxidant enzyme systems (Dreger *et al.*, 2009) and transcription factors including hypoxia inducible factor-1 α (HIF-1 α) (Haddad *et al.*, 2000) as well as nuclear factor (erythroid-derived 2)-like 2 (Nrf2) are triggered (Surh *et al.*, 2008), resulting in expression of proteins in response to oxidative stress such as heme oxygenase-1 (HO-1) and vascular endothelial growth factor (VEGF). This study hypothesized that treatment with NVK might protect endothelial cells from Hcy-induced oxidative stress through its ability to scavenge $O_2^{\bullet-}$, H_2O_2 , OH^{\bullet} and NO^{\bullet} , as well as alter the transcription factors including HIF-1 α and Nrf2, which regulate protein expression of

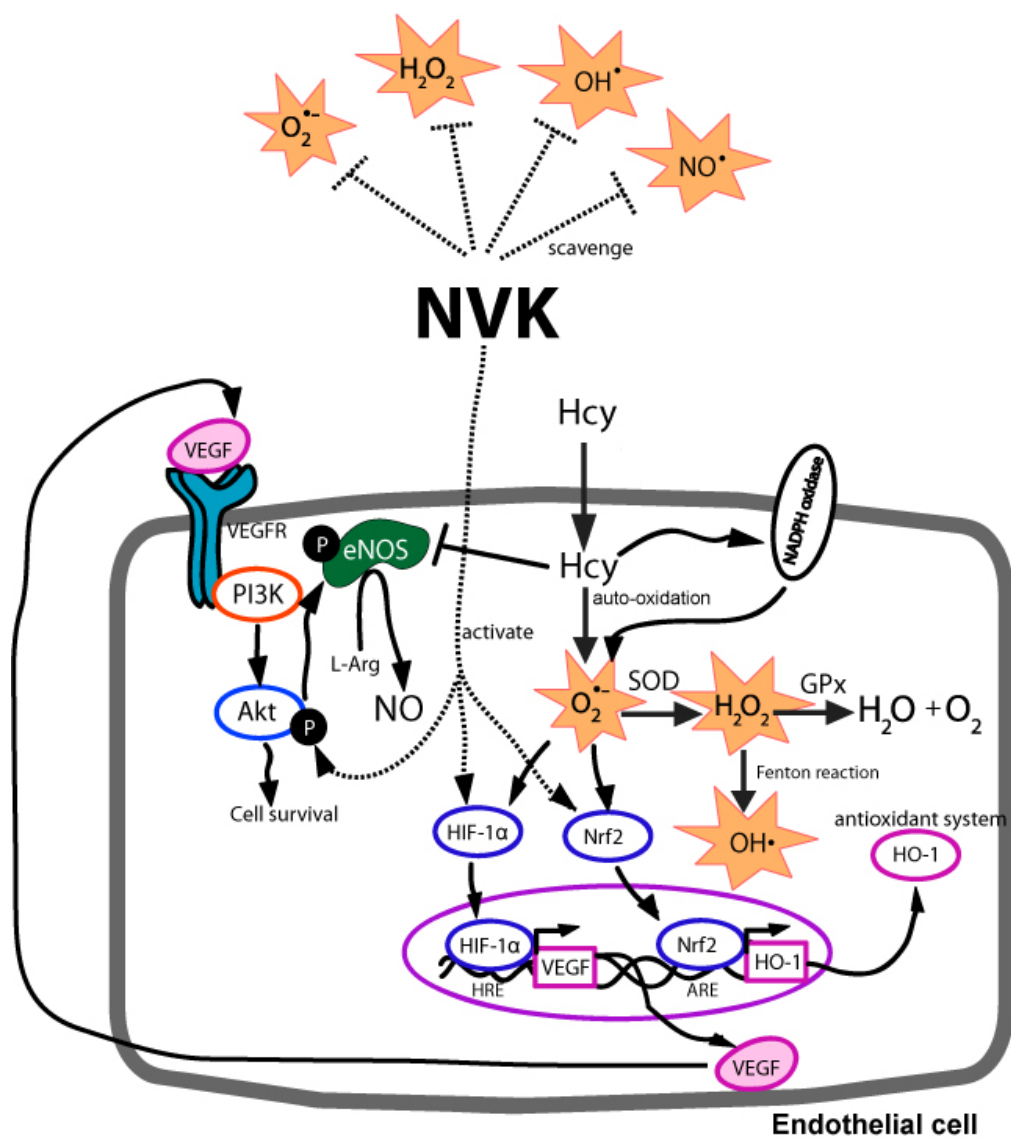


Figure 1. Conceptual framework of the antioxidant role of NVK in endothelial cells under Hcy treatment.

antioxidant enzymes, VEGF and HO-1. NVK might also activate protein kinase B (PKB or Akt) which phosphorylates endothelial nitric oxide synthase (eNOS), resulting in the production of nitric oxide (NO) as a vasorelaxant. We therefore hypothesized that NVK might play a role in restoration of endothelial function.

Objectives

1. To determine scavenging activities against ROS and RNS of NVK in cell-free system.
2. To investigate the effect of NVK on viability and intracellular ROS level in EA.hy926 cells in the absence or presence of Hcy.
3. To investigate the effect of NVK on proteomic profile in EA.hy926 cells in the absence or presence of Hcy.

Scope of study

In this study, the effect of scavenging activities against $O_2^{\bullet-}$, H_2O_2 , OH^{\bullet} and NO^{\bullet} of NVK were investigated in cell-free system. Intracellular ROS level attenuated by NVK at the nontoxic concentrations was determined. To investigate proteomic profile affected by NVK in the absence or presence of Hcy, two-dimensional electrophoresis (2-DE) was performed. Liquid chromatography coupled with ion trap mass spectrometry (LC/MS/MS) and MASCOT database were used to identify the changed proteins in the cells treated with NVK in the absence or presence of Hcy. To confirm the expression of proteins involving in cellular oxidative homeostasis, immunoblot analysis was performed.

Experimental design

The scavenging activities against $O_2^{\bullet-}$, H_2O_2 , OH^{\bullet} and NO^{\bullet} of NVK were performed using the assays of nitrotetrazolium blue (NBT) reduction, guaiacol, deoxyribose and Griess, respectively. To find out the non-toxic concentrations of NVK, 3-(4, 5-dimethylthiazol-2-yl)-2, 5-diphenyltetrazolium (MTT) reduction assay was performed. Pre-treatment of the cells with NVK at the non-toxic concentrations in the absence or presence of Hcy was performed to measure intracellular ROS level using 2',7'- dichlorodihydrofluorescein diacetate (DCFH-DA) assay. The effective

concentrations of NVK resulting in restoring cellular ROS were selected for the detection of proteomic profile induced by NVK in the absence or presence of Hcy using 2-DE, LC/MS/MS and MASCOT database. Identified protein lists were subjected to pathway analysis using bioinformatic tools. The annotated proteins of interest affected by NVK were confirmed using Western blot analysis.

Contributions of the study

1. Information to support traditional use of Phikud Navakot, probably a major active constituent of Yahom Navakot for treating circulatory disorder.
2. Understanding the underlying mechanism of Phikud Navakot in maintaining homeostasis of vascular system.

CHAPTER II

LITERATURE REVIEW

Endothelial function

Endothelial cells line the luminal side of blood vessels and play a critical role in the regulatory a variety of physiological functions such as regulation of coagulation, adhesion of leukocytes, secretion of growth factors to control vascular smooth muscle cells and pericyte growth, response to vascular stimuli and control vascular tone (Behrendt and Ganz, 2002). Endothelial cells regulate vascular tone and blood pressure by control the synthesis of vasodilator substances such as NO (Brandes *et al.*, 2000) and vasoconstriction substances such as endothelin-1 and thromboxane A₂ (Morris *et al.*, 2010). The synthesis of NO can be triggered by various substances such as norepinephrine and sheer stress (Ohno *et al.*, 1993) via several signaling pathways. One of these is the activation of Akt (Dimmeler *et al.*, 1999) which phosphorylates eNOS, resulting in the production of NO from L-arginine. Another pathway is the increase in cytoplasmic Ca²⁺ via G protein-coupled receptors (Venema *et al.*, 1996) by binding to calmodulin, resulting in activation of eNOS. NO plays not only in relaxation of vascular smooth muscle cells but also inhibition of platelet aggregation, leukocyte adhesion (De Caterina *et al.*, 1995) and inhibition of apoptosis in endothelial cells (Lee *et al.*, 2005). Loss of NO level due to impairment of eNOS activity and eNOS expression, lacking of L-arginine and formation of peroxynitrite (ONOO⁻) by reaction of NO with O₂⁻ (Forstermann *et al.*, 2010) causes endothelial dysfunction.

Several factors such as diabetes, smoking, oxidative stress and hyperhomocysteinemia can impair endothelial function (Wotherspoon *et al.*, 2003). Endothelial dysfunction is thought to be a major event in the development of atherosclerosis (Domagala *et al.*, 1998).

Oxidative stress in endothelial cell function

ROS such as O₂⁻, OH[•] including H₂O₂, and RNS such as NO[•] and ONOO⁻ are considered to play an important role in cardiovascular pathology including endothelial dysfunction (Forstermann *et al.*, 2010). In normal endothelial cells,

biochemical sources of ROS are mitochondrial respiration, xanthine oxidase, lipoxygenase, cyclooxygenase (COX), cytochrome P450s, NADPH oxidases, NOS, and other peroxidase enzymes (Cai, 2005). In response to oxidative stress, several antioxidant enzymes such as SOD first catalyzes the dismutation of $O_2^{\cdot-}$ to H_2O_2 . In mammalian cells, there are 2 isoforms of intracellular SODs depending on their cofactors. SOD contains copper and zinc as its cofactor, [Cu,Zn]-SOD (SOD1) found in cytosol, and manganese as its cofactor, [Mn]-SOD (SOD2) presented in mitochondria. H_2O_2 is subsequently reduced to water by GPx and CAT. Excess H_2O_2 can be converted to OH^{\cdot} by highly reactive Fenton reaction (Wolin, 1996). In addition, the elevated level of ROS can also trigger the signaling proteins including transcription factors such as Nrf2 and HIF-1 α , which are essential for induction of genes encoding oxidative stress-responsive proteins. Under normal conditions, Nrf2 is found mainly in the cytosol. When oxidative stress occurred by elevated level of ROS and RNS, Nrf2 rapidly translocated into nucleus and regulated the antioxidant response (Itoh *et al.*, 2004). After translocation of Nrf2 into the nucleus, Nrf2 formed a complex and bound to antioxidant response element (ARE) which was located in the promoter and subsequently initiated the transcription of cytoprotective genes (Nguyen *et al.*, 2003). Proteins which regulated by Nrf2 are SOD, GPx, glutathione S-transferase (GST), CAT, HO-1 and thioredoxin (Surh *et al.*, 2008).

Other transcription factor is HIF-1 α which plays an essential role in cellular oxygen homeostasis (Semenza *et al.*, 1999). HIF-1 α functions as a master regulator in response to oxygen level by induction the transcription of more than 60 proteins, including VEGF to promote angiogenesis or cell survival (Semenza *et al.*, 1999). In normoxia, HIF-1 α rapidly degraded by ubiquitin-proteasome pathway, whereas hypoxia blocks degradation leading to accumulation and translocation into nucleus. Several growth factors and endogenous substances are known to stabilize HIF-1 α under normoxia, including NO (Palmer *et al.*, 2000).

Metabolism of homocysteine and its role in cardiovascular disease

Hcy is an intermediate in methionine metabolic pathway (Selhub, 1999). The deficiency of some cofactors such as vitamin B₆ and B₁₂ (Perla-Kajan *et al.*, 2007) and the genetic deficiency of some enzymes such as cysteine β -synthase in

methionine metabolism (Lalouschek *et al.*, 1999) may cause hyperhomocysteinemia. Normal plasma concentration and mildly elevated level of Hcy are ranging from 5 - 15 μM and 15 - 30 μM , respectively (Hankey and Eikelboom, 1999). Plasma level of Hcy higher than 0.1 mM is considered as severe hyperhomocysteinemia which is associated with premature vascular disease (Thambyrajah and Townend, 2000).

At cellular level, Hcy induced toxicity in endothelial cells by increasing intracellular ROS (McDowell and Lang, 2000). Incubation of Hcy (20 - 100 μM) for 24 h increased the mRNA expression of NADPH oxidase while reduced the expression of thioredoxin, resulting in an increase in intracellular ROS in rat heart microvascular endothelial cells (Tyagi *et al.*, 2005). Furthermore, an increase in intracellular ROS directly triggered the auto-oxidation of Hcy to generate $\text{O}_2^{\cdot-}$ (Hogg, 1999; McDowell and Lang, 2000). Hcy (1 mM) reduced phosphorylation of Akt and eNOS in HUVEC cells (Yan *et al.*, 2010) and NO level in ECV304 cells (Lin *et al.*, 2007). The expression of cationic amino acid transporter, for L-arginine transportation into the cell, decreased in Hcy-treated bovine aortic endothelial cells, resulting in lacking of NO precursor (Jin *et al.*, 2007).

Antioxidant activity and protective role against oxidative stress of herbs in Phikud Navakot

Several studies reported the protective effect of herbs used in Phikud Navakot and their active substances. *Angelica dahurica* has been widely used as an antipyretic and analgesic for cold, headaches and toothaches (Piao *et al.*, 2004). The ethanolic extract of *A. dahurica* exhibited good OH^{\cdot} scavenging activity (Xu *et al.*, 2011) and increased HO-1 activity and expression in asthmatic mice (Lee *et al.*, 2007). The ethanolic and water extracts exhibited moderate Fe^{2+} chelating activity (Xu *et al.*, 2011). Chemical constituents of *A. dahurica* contained furanocoumarin derivatives such as imperatorin, isoimperatorin, oxypeucedanin and 8-hydroxybergapten (Piao *et al.*, 2004; Lee *et al.*, 2011). Imperatorin increased vasodilation in mouse thoracic aorta by increasing NO level (Nie *et al.*, 2009). Isoimperatorin reduced TNF- α induced ROS generation in EA.hy926 cells and prevented TNF- α induced monocyte cell adhesion by inhibition of extracellular signal-regulated kinase (ERK), protein kinase C (PKC) and Akt phosphorylation (Moon *et al.*, 2011). Isoimperatorin also

induced transcription of retinoic X receptor (Liu *et al.*, 2011) which stimulated tissue plasminogen activator (tPA) gene expression in HUVEC cells (Kooistra *et al.*, 1995).

Atractylodes lancea is used as traditional treatment against rheumatic diseases, digestive disorders, night blindness and influenza (Resch *et al.*, 2001). The methanolic and water extracts of *A. lancea* contained low phenolic content, resulting in poor antioxidant activity (Cai, 2004). Phytochemical investigations of *A. lancea* showed the presence of polyacetylenes, sesquiterpenoids (Resch *et al.*, 2001) and sesquiterpene glycosides (Kitajima *et al.*, 2003). The major sesquiterpenes were atractylon, β -eudesmol and atractydin (Chen *et al.*, 2009; Hasada *et al.*, 2010). However, β -eudesmol (50 - 100 μ M) was found to inhibit proliferation and migration of HUVEC cells stimulated by basic fibroblast growth factor through the blockade of the ERK phosphorylation pathway (Tsuneki *et al.*, 2005). Atractylon (0.01, 0.1 and 1.0 mg/mL) moderately scavenged DPPH radicals and significantly reduced *tert*-butyl hydroperoxide-induced lipid peroxidation in primary cultured hepatocytes (Hwang *et al.*, 1996).

Artemisia pallens has been widely used in folk medicine as antihelmintic antibacterial and antifungal agents, and treatment of diabetes mellitus (Niranjan *et al.*, 2009). The methanolic extract of *A. pallens* exhibited DPPH and NO[•] scavenging activities (Ruikar *et al.*, 2011). The 50% ethanolic extract of *A. pallens* showed good OH[•] scavenging activity (Suresh *et al.*, 2011). However, the effect of *A. pallens* on endothelial cell function was rarely studied. Phytochemical studies revealed the presence of polyphenols such as gallic acid, chlorogenic acid, ferulic acids, rutin and quercetin (Niranjan *et al.*, 2009) and arbutin (Garai *et al.*, 2012), which exhibited high antioxidant abilities and cytoprotection. The methanolic extract of *A. pallens* also showed ability to reduce blood glucose level in hyperglycemic rats, while the water extract was inactive (Subramoniam *et al.*, 1996).

Both *Ligusticum chuanxiong* and *Angelica sinensis* have been widely used for the treatment of circulatory disorders in traditional Chinese medicine (Cheng *et al.*, 2008). The protective effect against H₂O₂ in ECV304 cells was found in ethyl ether extract of mixed *L. chuanxiong* and *A. sinensis* (1:1) by increasing enzyme activities of SOD, GPx and CAT (Hou *et al.*, 2004). The water extract of *L. chuanxiong* and *A. sinensis* exhibited poor OH[•] antioxidant activities (Li *et al.*, 2004; Liao *et al.*, 2008).

Major chemical components of *L. chuanxiong* were essential oils, alkaloids, phenolic acids, polysaccharides and proteins (Zhang *et al.*, 2003). The water-soluble crude polysaccharide extract from *L. chuanxiong* showed moderate reducing power and scavenging activities against DPPH, $O_2^{\cdot-}$ and OH^{\cdot} (Yuan *et al.*, 2008). The crude essential oil extract of *L. chuanxiong* showed good DPPH and 2,2-azinobis(3-ethylbenzothiozoline-6-sulfonic acid) (ABTS) scavenging activities (Jeong *et al.*, 2009). Ferulic acid, found in both *L. chuanxiong* and *A. sinensis* (Yan *et al.*, 2005), exhibited good antioxidant activities against ABTS and NO^{\cdot} , while inactive against $O_2^{\cdot-}$ and OH^{\cdot} (Maurya *et al.*, 2010). Ferulic acid also decreased radiation-induced intracellular ROS in HUVEC cells by Nrf2 activation, resulting in restoration of glutathione (GSH) level and up-regulation of HO-1 (Ma *et al.*, 2010). The expression of VEGF, platelet-derived growth factor and HIF-1 α was up-regulated in ferulic acid-treated HUVEC cells (Lin *et al.*, 2010). Tetramethylpyrazine isolated from *L. chuanxiong* increased protein expression of HO-1 and decreased NADPH oxidase activity in rat renal tubular cells (Sue *et al.*, 2009). Tetramethylpyrazine also inhibited angiotensin 2-induced ROS generation in HUVEC cells (Lee *et al.*, 2005). In addition, butylidenephthalide and ligustilide derivatives were found in volatile oil of *L. chuanxiong* and *A. sinensis*. Dihydroxylicustilide protected H_2O_2 -injured HUVEC cells by increase in SOD activity and NO level, and decrease in malondialdehyde (MDA) level (Li *et al.*, 2013). Z-ligustilide inhibited apoptotic cell death in H_2O_2 -treated PC12 cells (Yu *et al.*, 2008). The polysaccharide crude extract of *A. sinensis* increased SOD, GPx and CAT activities in liver of CCl_4 -fed rats (Yu *et al.*, 2013) and heart of myocardial-injured rats (Zhang *et al.*, 2010). *A. sinensis* extracted with 20% ethanol exhibited better DPPH scavenging activities than water extract which were correlated with higher ferulic acid and total phenolic contents (Huang *et al.*, 2008). The essential oil fraction, containing coniferyl ferulate, of *A. sinensis* showed DPPH and ABTS radical scavenging activities with less potent than ascorbic acid (Li *et al.*, 2007). Senkyunolide isolated from *L. chuanxiong* increased HO-1 expression in H_2O_2 -treated HepG2 cells (Qi *et al.*, 2010).

Nardostachys jatamansi has been described in Ayurveda medicine for its use in mental disorders, insomnia, hyperlipidemia, hypertension and heart diseases (Sharma and Singh, 2012). *N. jatamansi* extracted with 70% ethanol showed the good

scavenging activities against DPPH, $O_2^{\cdot-}$, OH^{\cdot} and NO^{\cdot} similar to ascorbic acid while H_2O_2 scavenging activity was inactive (Sharma and Singh, 2012). The protective effects of *N. jatamansi* alcoholic extracts on restoration of SOD, GPx and CAT activities were found in H_2O_2 -induced oxidative stress in rat glioma cells (Dhuna *et al.*, 2013), doxorubicin-induced cardiac damage in rats (Subashini *et al.*, 2006), brain of stressed rats (Lyle *et al.*, 2009) and brain of haloperidol-induced catalepsy rats (Rasheed *et al.*, 2010). Essential oils in *N. jatamansi* such as patchoulol, ledene oxide and globulol showed good antioxidant activity against DPPH (Parveen *et al.*, 2011).

Picrorhiza kurrooa has been traditionally used for treatment of liver disorder, fever, dyspepsia and chronic diarrhea (Rajkumar *et al.*, 2011). The methanolic extract of *P. kurrooa* showed high DPPH scavenging activity and ferric reducing antioxidant power (FRAP), which were correlated with high total phenolic contents (Guleria *et al.*, 2013). The methanolic and water extracts of *P. kurrooa* exhibited promising antioxidant potentials against DPPH and OH^{\cdot} , and high ability to inhibit lipid peroxidation (Rajkumar *et al.*, 2011). *P. kurrooa* alcoholic extract showed good scavenging activities against DPPH, $O_2^{\cdot-}$ and NO^{\cdot} (Govindarajan *et al.*, 2003). Oral administration of methanolic and water extracts of *P. kurrooa* attenuated the levels of NO^{\cdot} , $O_2^{\cdot-}$, $ONOO^{\cdot-}$ and lipid peroxidation and restored enzyme activities of SOD, GPx, GST, glutathione reductase and CAT in the pancreas of alloxan-induced diabetic rats (Chauhan *et al.*, 2008). Restoration of antioxidant enzyme activities was also found in gastric ulcerated rats fed with ethanolic extract of *P. kurrooa* (Ray *et al.*, 2002). Picroliv isolated from *P. kurrooa* increased HIF-1 α and VEGF expression in HUVEC cells (Gaddipati *et al.*, 1999a) and prevented cerebral injury by up-regulation of VEGF and insulin like growth factor-1 and its receptor in cerebral hypoxia (Gaddipati *et al.*, 1999b). Picroliv also enhanced endothelial cell migration, resulting in angiogenesis promotion in *ex vivo* rat aorta ring model (Singh *et al.*, 2007). Tannins such as gallic acid, ellagic acid and isochebulic acid isolated from *P. kurrooa* strongly inhibited COX and lipid peroxidation (Zhang *et al.*, 2004).

Saussurea costus has been used as traditional medicine for abdominal pain and tenesmus (Choi *et al.*, 2012). Moderate DPPH scavenging activity and reducing power of ethanolic extract of *S. costus* was reported, which was correlated with total flavonoid contents (Chang *et al.*, 2012). The methanolic extract of *S. costus* was

found to possess moderate scavenging activity against DPPH (Butkhup and Samappito, 2011). *S. costus* extracted with 50% ethanol exhibited good scavenging activities against $O_2^{\cdot-}$ as well as NO^{\cdot} and inhibited lipid peroxidation in rat liver homogenate (Pandey *et al.*, 2005). Active constituents isolated from *S. costus* such as dehydrocostus lactone and santamarin exhibited cytoprotective effects against oxidative stress. Dehydrocostus lactone increased HO-1 expression *via* Nrf2 regulation in H_2O_2 -treated HepG2 cells (Jeong *et al.*, 2007) and inhibited the activation of NF- κ B, resulting in suppression of NO production from inducible NOS (iNOS) in lipopolysaccharide-treated murine macrophage RAW264.7 cells (Jin *et al.*, 2000). Santamarin, a sesquiterpene lactone, also increased HO-1 expression by activation of nuclear Nrf2 translocation in RAW264.7 cells (Choi *et al.*, 2012).

Terminalia chebula has been widely used in traditional medicine and regarded as the king of Ayurveda medicine (Lee *et al.*, 2007). The antioxidant activities of *T. chebula* were extensively studied. The ethanolic extract of *T. chebula* exhibited the potent scavenging activities against DPPH, $O_2^{\cdot-}$, H_2O_2 , OH^{\cdot} and NO^{\cdot} (Sabu *et al.*, 2002; Cheng *et al.*, 2003; Hazra *et al.*, 2010; Manosroi *et al.*, 2010; Chang *et al.*, 2012; Arya *et al.*, 2013). Water extract of *T. chebula* exhibited the potent scavenging activities against DPPH, $O_2^{\cdot-}$, H_2O_2 , OH^{\cdot} and NO^{\cdot} (Naik *et al.*, 2004; Lee *et al.*, 2005; Walia *et al.*, 2009). *T. chebula* extract increased SOD, GPx and CAT activities and inhibited lipid peroxidation in kidney of aged rats (Mahesh *et al.*, 2009) and in heart of isoproterenol-induced oxidative stress rats (Suchalatha *et al.*, 2005). *T. chebula* methanolic extract and its chebulic acid prevented endothelial dysfunction by inhibition of advanced glycation end products (AGEs) formation and reduction of AGEs-induced ROS in HUVEC cells (Lee *et al.*, 2011). Crude tannin extracts isolated from *T. chebula* increased VEGF expression, resulting in wound healing promotion in rats (Li *et al.*, 2011).

EA.hy926 cell line as a model for the study of endothelial function

From the role of endothelial cells in the regulation of various vascular biological processes, the endothelial cell culture has been widely used to study molecular function for understanding the new insight in cardiovascular diseases. The culture of primary endothelial cells such as HUVEC cells has some limitation such as

the short lifespan and variation from batch to batch due to various origins. Several endothelial cell lines were established for the study of vascular biology. The advantage of these cell lines are the long-life span, well characterization, and stable presenting endothelial behavior. Among the immortalized cell lines, Ea.hy926 cell line was the most frequently used and best characterized (Bouïs *et al.*, 2001; Baranska *et al.*, 2005). Ea.hy926 cell line has been established from the fusion of HUVEC cells and human lung carcinoma cell line A549 (Edgell *et al.*, 1983) with endothelial cell phenotypes such as von Willebrand factor (vWF), tPA, plasminogen activator inhibitor-1, tissue factor, and thrombomodulin (Bouïs *et al.*, 2001). Comparative study between HUVEC cells and various popular cell lines showed that the positive expression of endothelial marker proteins, vWF, CD31, VEGF receptor, and the uptake of low-density lipoprotein were observed only in HUVEC and EA.hy926 cells (Unger *et al.*, 2002). EA.hy926 cells showed the up-regulation of intercellular adhesion molecule 1 (ICAM-1) in response to TNF- α and interleukin-1 beta (IL-1 β) (Unger *et al.*, 2002). These indicated that EA.hy926 cells exhibited most of phenotype similar to primary endothelial cells. Several studies used EA.hy926 cell line as a model to investigate endothelial cell function affected by natural compounds such as genistein (Fuchs *et al.*, 2006), eicosapentaenoic acid (Gousset-Dupont *et al.*, 2007), luteolin and cynaroside (Li *et al.*, 2004) and olive oil (Manna *et al.*, 2009).

Proteomics and bioinformatics as tools for signaling network analysis

Proteomics is the large-scale study of proteins. There are 2 approaches to separate the mixture of proteins *e.g.* 2-DE and LC approaches. The 2-DE was based on separation by two properties of proteins in two dimensions. In first dimension, mixtures of proteins were separated by isoelectric point (pI) which called isoelectric focusing (IEF). Since protein was resolved, MS was performed to acquire the fragments of peptides. The set of peptide fragments was subjected to search against MASCOT database. To investigate the association among the identified proteins, bioinformatic tools and cellular pathway databases were required in data analysis. There are many pathway analysis tools available such as STRING (<http://string-db.org/>) and KOBAS (<http://kobas.cbi.pku.edu.cn/home.do>). The association of these

proteins was reported as direct and indirect protein-protein interaction (Franceschini *et al.*, 2013) and merging into the canonical cellular pathways (Xie *et al.*, 2011).

Since traditional medicines including natural compounds are extensively studied to provide scientific evidences for supporting the traditional uses or finding drug candidates, 2-DE was used as a tool for understanding the complex mechanisms at the cellular and molecular levels. For example, epidemiological studies suggested that soy and its active isoflavone such as genistein could protect endothelial cells from oxidative stress-induced damage. To clarify this action, the effects of soy extract and genistein in Hcy-treated EA.hy926 cells was investigated using 2-DE coupled with matrix-assisted laser desorption/ionisation-time of flight (MALDI-TOF) MS (Fuchs *et al.*, 2005; Fuchs *et al.*, 2006). Proteomic analysis revealed that soy extract and genistein changed expression of proteins involved anti-atherosclerotic properties, which could pave the way for further study in molecular pathway. From 2-DE, purposed mechanism of ouabain on HUVEC cell proteome was revealed (Qiu *et al.*, 2007). The water extract of *Salvia miltiorrhiza* which exhibited antioxidant effects was subjected to 2-DE and pathway analysis to investigate the target proteins and pathway. The result showed that the extract modulated protein carbonylation and altered the proteins involved in redox regulation and atherosclerosis (Hung *et al.*, 2009). Therefore, proteomics and bioinformatics could be the powerful tools to screen the target molecules of the natural compound actions and elucidate the underlying mechanisms of their effects.

CHAPTER III

MATERIALS AND METHODS

Equipments

- Centrifuge (Allegra X-12 R, Zentrifugen, Germany)
- CO₂ incubator (3121, Forma Scientific Inc, Massachusetts, USA)
- Electrophoresis apparatus
 - Mighty small II SE250/SE260 (Hoefer Inc., California, USA)
 - Mini Trans-Blot[®] Electrophoretic Transfer cell (Bio-Rad, USA)
- Hemocytometer (Bright-line, Hausser Scientific, Pennsylvania, USA)
- ImageJ software (National Institute of Health, Maryland, USA)
- ImageMaster 2D platinum 7.0 software (GE Healthcare, Sweden)
- ImageScanner III (GE Healthcare, Sweden)
- Ion trap mass spectrometer coupled with CaptiveSpray ion source (amaZon speed[™] ion trap, Bruker Daltonics, Massachusetts, USA)
- Isoelectric focussing (IEF) system (Ettan[™] IPGphor[™] 3, GE Healthcare, Sweden)
- Microplate reader (Perkin elmer, Victor 3, Massachusetts, USA)
- Nanoflow liquid chromatography (nLC) system (Thermo Scientific, Yokohama, Japan)
 - Analytical column: EASY-column 10 cm, ID 75 μm, 3μm particle size, C18-A2
 - EASY-nLC II system
 - Pre-column: EASY-column 2 cm, ID 100μm, 5μm particle size, C18-A1
- Phase-contrast inverted microscope (CK30, Olympus, Tokyo, Japan)
- Power supply (EC570-90, Thermo Electron corporation, Massachusetts, USA)
- Spectrophotometer (Spectronic Genesys 5, New York, USA)
- Strip holder 7 cm (GE Healthcare, Uppsala, Sweden)

Materials

- Cell culture dish 100 mm (Cat. no. 430167, Corning Inc., USA)
- Cell culture flask (Corning Inc., USA)

- 25 cm² Rectangular cell culture flask (Cat. no. 430168)
- 75 cm² Rectangular cell culture flask (Cat. no. 430641)
- FluoroTrans® polyvinylidene fluoride (PVDF) transfer membrane (Cat. no. BSP0161, Pall Life Sciences, USA)
- Hyperfilm™ enhanced chemiluminescence (ECL) (Cat no. 28906838, Amersham, Buckinghamshire, UK)
- Immobiline™ DryStrip pH 3-10 non-linear (NL), 7 cm (Cat no. 17-6001-11 GE Healthcare, Sweden)
- 6-well plate (Cat. no. 65, Corning Inc., USA)
- 96-well plate (Cat. no. 371, Corning Inc., USA)

Reagents

- Acrylamide (Cat. no. 13H0609, Sigma-Aldrich, Missouri, USA)
- Agarose (Cat. no. 1840000, BDH Chemical, England)
- Albumin from bovine serum (BSA) (Cat. no. A7906, Sigma-Aldrich, Missouri, USA)
- Ammonium persulfate (APS) (Cat. no. 949 A471617, Merck, Darmstadt, Germany)
- Ascorbic acid (Cat. no. 95210, Fluka Chemicals, Steinheim, Germany)
- Bromophenol blue (Cat. no. 135869, Merck, Darmstadt, Germany)
- 3-[(3-Cholamidopropyl) dimethylammonio]-1-propanesulfonate (CHAPS) (Cat. no. 17-1314-01, GE Healthcare, Buckinghamshire, UK)
- Coomassie blue R250 (Cat. no. BD100-25, Fisher Biotech, New Jersey, USA)
- 2-Deoxy-D-ribose (Cat. no. 31170, Sigma-Aldrich, Missouri, USA)
- 2',7'- Dichlorodihydrofluorescein diacetate (DCFH-DA) (Cat. no. D6883, Sigma-Aldrich, Missouri, USA)
- Dimethyl sulfoxide (DMSO) (Cat. no. 60153, Merck, Darmstadt, Germany)
- 3-(4, 5-dimethylthiazol-2-yl)-2, 5-diphenyltetrazolium bromide (MTT) (Cat. no. M5655, Sigma-Aldrich, Missouri, USA)
- Dithiothreitol (DTT) (Cat. no. 76H0975, Sigma-Aldrich, Missouri, USA)
- Dulbecco's modified Eagle's medium (DMEM) (Cat. no. 12800-058, Gibco, Auckland, New Zealand)

- ECL Prime™ Western blotting detection reagent (Cat. no. RPN2232, Amersham, Buckinghamshire, UK)
- Ethylenediaminetetraacetic acid (EDTA) (Cat. no. E6758, Sigma-Aldrich, Missouri, USA)
- Ferric (III) chloride (FeCl₃) (Cat. no. UN1773, Merck, Darmstadt, Germany)
- Ferulic acid (Cat. no. 128708, Sigma, Missouri, USA)
- Fetal bovine serum (FBS) (Cat. no. SV30160.02, Hyclone, Cramlington, UK)
- Glycerol (Cat. no. 453752, Carlo Erba, Milan, Italy)
- Glycine (Cat. no. G/0800/60, Fisher Scientific, Leicestershire, UK)
- Griess reagent (modified) (Cat. no. G4410, Sigma-Aldrich, Missouri, USA)
- Guaiacol (Cat. no. G5502, Sigma-Aldrich, Missouri, USA)
- D,L-Homocysteine (Hcy) (Cat. no. H4628, Sigma, Missouri, USA)
- Hydrogen peroxide (H₂O₂) (Cat. no. H/1750/17, Fisher Scientific, California, USA)
- Immobilized pH gradient (IPG) buffer™ pH 3-10 NL (Cat. no. 17-6000-87, GE Healthcare, Buckinghamshire, UK)
- Iodoacetamide (Cat. no. RPN6302, GE Healthcare, Buckinghamshire, UK)
- Mannitol (Cat. no. M4125, Sigma-Aldrich, Missouri, USA)
- Methanol (Cat. No. 1.06009, Merck, Darmstadt, Germany)
- Mouse monoclonal antibody to β-actin HRP conjugated (Cat. no. ab20272, Abcam, Cambridge, England)
- N, N'-Methylenebisacrylamide (Cat. no. 14607-2, Sigma-Aldrich, Missouri, USA)
- β-Nicotinamide adenine dinucleotide, reduced disodium salt (NADH) (Cat. no. N6005, Sigma-Aldrich, Missouri, USA)
- Nitrotetrazolium blue chloride (NBT) (Cat. no. N6876, Sigma-Aldrich, Missouri, USA)
- PageRuler™ pre-stain protein ladder (Cat. No. SM0671, Fermentas, Rockford, USA)
- Penicillin-streptomycin (Cat. no. 15140-122, Gibco, Auckland, New Zealand)
- Peroxidase from horseradish - Type I (Cat. no. P8125, Sigma-Aldrich, Missouri, USA)

- Protease cocktail inhibitor (Cat. no. P8340, Sigma-Aldrich, Missouri, USA)
- Quercetin (Cat. no. Q0125, Sigma, Missouri, USA)
- Rabbit polyclonal antibody (Abcam, Cambridge, England)
 - Akt (Cat. no. ab6076)
 - Akt (phospho S473) (Cat. no. ab66138)
 - CAT (Cat. no. ab16731)
 - eNOS (Cat. no. ab5589)
 - eNOS (phospho S1177) (Cat. no. ab22604)
 - glyceraldehyde 3-phosphate dehydrogenase (GAPDH) (Cat. no. ab9483)
 - GPx1 (Cat. no. ab16831)
 - HO-1 (Cat. no. ab85309)
 - Nrf2 (Cat. no. ab31163)
 - SOD1 (Cat. no. ab16831)
 - VEGF (Cat. no. ab46154)
- Rabbit polyclonal antibody to HIF-1 α (H-206) (Cat. no. sc-10790, Santa Cruz Biotechnology, Texas, USA)
- Servalyl™ carrier ampholytes 3-10 (Cat. no. 42940.01, Serva, Heidelberg, Germany)
- Sodium deoxycholate (Cat. no. D6750, Sigma-Aldrich, Missouri, USA)
- Sodium dodecyl sulfate (SDS) (Cat. no. L57119160 741, Merck, Darmstadt, Germany)
- Sodium nitroprusside dihydrate (SNP) (Cat. no. 71778, Sigma-Aldrich, Missouri, USA)
- Sucrose (Cat. no. K14076651, Merck, Darmstadt, Germany)
- SuperSignal™ West Femto (Cat. no. 34095, Thermo Scientific, Rockford, USA)
- Swine polyclonal antibody anti-rabbit HRP (Cat. no. P0217, Dako, Glostrup, Denmark)
- N,N,N',N'-Tetramethylethylenediamine (TEMED) (Cat. no. 38C-0080, Sigma-Aldrich, Missouri, USA)
- Thiourea (Cat. no. 2779784, Merck, Darmstadt, Germany)
- 2-Thiobarbituric acid (TBA) (Cat. no. T5500, Sigma-Aldrich, Missouri, USA)

- Trichloroacetic acid (Cat. no. 1.00807.0250, Merck, Darmstadt, Germany)
- Tris-(hydroxymethyl)aminomethane (Cat. no. T1503, Sigma-Aldrich, Missouri, USA)
- Triton X-100 (Cat. no. 93420, Fluka, St. Gallen, Switzerland)
- Trypsin from porcine pancreas (Cat. no. T4799, Sigma-Aldrich, Missouri, USA)
- Trypsin, sequencing grade (Cat. no. V511A, Promega, Wisconsin, USA)
- Tween-20 (Cat. no. BD337-500, Fisher Biotech, NJ, USA)
- Urea (Cat. no. 15604, Riedel-de Haën, Seelze, Germany)

Methods

Plant materials

The codes of nine crude drugs in Phikud Navakot were shown in Table 1. Roots of AD, AS, SC, rhizomes of AL, LC, PK, roots and rhizomes of NJ, aerial parts of AP and galls of TC were purchased in October 2009 from traditional drugstores in Bangkok, Thailand. Crude drugs of AD, AL, AS, LC, NJ, PK, SC and TC were identified by Dr. Sanya Hokputsa of Phytochemical Research Group, Research and Development Institute, Government Pharmaceutical Organization. Meanwhile, AP was identified by Associate Professor Dr. Uthai Sotanaphun of Department of Pharmacognosy, Faculty of Pharmacy, Silpakorn University.

Preparation of the extracts

The extracts of nine crude drugs used in cell-free assays were kindly provided by Dr. Sanya Hokputsa. Briefly, each dried crude drug was powdered and sieved through No. 40 mesh. The powdered herbs (1 kg each) were extracted with 2 × 5 L of either 50% ethanol or water under reflux for 3 h. The ethanolic and water extract of Phikud Navakot, as the combinations of nine herbs in equal proportion, was prepared and extracted with the same procedure as above. The extracts were then spray-dried or freeze-dried.

Phikud Navakot ethanolic extract (NVK) used in cell-based assays was kindly provided by Associate Professor Dr. Uthai Sotanaphun. Briefly, NVK was prepared by mixing the powders containing equal proportion of nine herbs. The powder was

Table 1. Codes of nine crude drugs in Phikud Navakot and their part used

Crude drug	Scientific name	Family	Part used	Code
Kot Soa	<i>Angelica dahurica</i>	Apiaceae	root	AD
Kot Kamao	<i>Atractylodes lancea</i>	Asteraceae	rhizome	AL
Kot Chulalumpa	<i>Artemisia pallens</i>	Asteraceae	aerial part	AP
Kot Chiang	<i>Angelica sinensis</i>	Apiaceae	root	AS
Kot Huabua	<i>Ligusticum chuanxiong</i>	Apiaceae	rhizome	LC
Kot Jatamansi	<i>Nardostachys jatamansi</i>	Valerianaceae	root and rhizome	NJ
Kot Kanprao	<i>Picrorhiza kurrooa</i>	Scrophulariaceae	rhizome	PK
Kot Kradook	<i>Saussurea costus</i>	Asteraceae	root	SC
Kot Pungpla	<i>Terminalia chebula</i>	Combretaceae	gall	TC

extracted by maceration with 80% ethanol (100 g of dried powder per 1 L of 80% ethanol) for overnight, followed by reflux for 3 h twice which was further combined and evaporated to dryness using rotary evaporator.

Stock solutions of NVK were prepared by dissolving 1 g of the extract in 5 mL of DMSO to give a concentration of 200 mg/mL. The stock solutions were aliquoted and stored at -20°C until use. For cell treatment, stock solution was diluted in complete DMEM containing DMSO (0.5% final concentration) in all experiment of cell treatment.

Antioxidant assays of the extracts

Superoxide radical scavenging assay

Generation of $O_2^{\cdot-}$ was based on the non-enzymatic NADH/PMS system. The $O_2^{\cdot-}$ scavenging activity was spectrophotometrically detected by the reduction of NBT according to previously reported method (Fernandes *et al.*, 2004). The assay was performed in 96-well plate. The reaction mixture in each well contained 60 μ L of 166 μ M NADH, 60 μ L of 43 μ M NBT, 20 μ L of extract at various concentrations dissolved in double-distilled water and 60 μ L of 2.7 μ M PMS. All other reagents were dissolved in 80 mM potassium phosphate buffer. After incubation for 8 min at room temperature, the absorbance was measured in a microplate reader at 560 nm against the appropriate blank solutions. Quercetin was used as a positive control. The percentage of $O_2^{\cdot-}$ scavenging was calculated from following equation:

$$\% \text{ superoxide scavenging} = (A_{\text{control}} - A_{\text{sample}}) / A_{\text{control}} \times 100.$$

Where A_{control} is the absorbance of the vehicle control group, consisting of reaction mixture without the extract, and A_{sample} is the absorbance of reaction mixture when mixed with the extract.

Hydrogen peroxide scavenging assay

Scavenging activity against H_2O_2 was determined using guaiacol method (Choi *et al.*, 2007) with slight modification. The assay was performed in 96-well plate. The reaction mixtures contained 0.01% guaiacol solution, 0.5 mM H_2O_2 , extract at various concentrations dissolved in double-distilled water and 1 U/mL horseradish peroxidase in potassium phosphate buffer pH 7.4. After incubation for 30

min at room temperature, the absorbance was measured in a microplate reader at 450 nm against the appropriate blank solutions. Quercetin was used as a positive control. The percentage of H₂O₂ scavenging was calculated from following equation:

$$\% \text{ hydrogen peroxide scavenging} = (A_{\text{control}} - A_{\text{sample}}) / A_{\text{control}} \times 100.$$

Where A_{control} is the absorbance of the vehicle control group which consists of reaction mixture without sample, and A_{sample} is the absorbance of reaction mixture when mixed with sample.

Hydroxyl radical scavenging assay

Scavenging activity against OH[•] was determined using deoxyribose method (Fernandes *et al.*, 2004; Halliwell *et al.*, 1987). The OH[•] were generated by a Fenton system (H₂O₂/FeCl₃-EDTA/ascorbic acid) degraded deoxyribose leading to thiobarbituric acid-reactive substances (TBARS) formation. Reaction mixtures contained, in a final volume of 1 mL, 2.8 mM 2-deoxy-D-ribose, 10 mM potassium phosphate buffer pH 7.4, extract at various concentrations, Fe³⁺-EDTA (10 mM FeCl₃ and 10.4 mM EDTA premixed before addition to reaction mixture), 0.1 mM H₂O₂ and 0.1 mM ascorbic acid. After incubation at 37°C for 1 h, 1 mL of 2.8% (w/v) trichloroacetic acid and 1 mL of 1% (w/v) TBA were added, and the mixture was heated in a water bath at 100°C for 15 min. The absorbance was measured at 532 nm against the appropriate blank solutions. All tests were performed three times. Mannitol, a classical OH[•] scavenger, was used as a positive control (Yan *et al.*, 1998). The percentage of OH[•] scavenging was calculated from following equation:

$$\% \text{ hydroxyl radical scavenging} = (A_{\text{control}} - A_{\text{sample}}) / A_{\text{control}} \times 100.$$

Where A_{control} is the absorbance of the vehicle control group which consists of reaction mixture without sample, and A_{sample} is the absorbance of reaction mixture when mixed with sample.

Nitric oxide radical scavenging assay

The NO[•] was generated by SNP and further interacted with oxygen to create nitrite ions that can be detected with Griess reagent. The assay was performed in 96-well plate according to a previous method (Mandal *et al.*, 2009) with slight modification. Briefly, 20 µL of extracts at various concentrations were incubated with

80 μL of 4 mM SNP dissolved in phosphate-buffered saline (PBS) pH 7.4 at room temperature under light. After 2.5 h incubation, 100 μL of Griess reagent was added and the mixture was color-developed for 10 min in the dark. The absorbance of pink solution was measured at 560 nm against the appropriate blank solutions. Quercetin was used as a positive control. The percentage of NO^{\bullet} scavenging was calculated from following equation:

$$\% \text{ nitric oxide scavenging} = (A_{\text{control}} - A_{\text{sample}}) / A_{\text{control}} \times 100.$$

Where A_{control} is the absorbance of the vehicle control group which consists of reaction mixture without sample, and A_{sample} is the absorbance of reaction mixture when mixed with sample.

Calculation of synergistic effect

The interaction among herbs was evaluated using the combination index (CI) according to the following equation:

$$\text{CI} = \sum_{j=1}^9 (C)_j / (\text{EC}_{50})_j$$

Where CI is the combination index for n herbs at 50% scavenging effect and j represents each herb. C is the proportionality of the concentration of each of n herbs that exerts EC_{50} in combination. This is calculated as the EC_{50} divided by 9 based on the contents in equal proportions of nine herbs in NVK. The CI values of < 1 , 1 and > 1 indicate synergistic, additive and antagonistic effects, respectively (Chou, 2006).

Cell culture

Human umbilical vein endothelial EA.hy926 cell line (CRL-2922) was purchased from American Type Culture Collection (ATCC) (Virginia, USA). The cells with a seeding density of 1×10^5 cells/mL were cultured in DMEM medium supplemented with 10% FBS and 1% penicillin-streptomycin at 37°C in 5% CO_2 incubator. Medium was changed every 2 - 3 days. The cells were cultured until confluence and subcultured every 3 - 4 days using 1 mM EDTA and 0.25% trypsin in phosphate-buffered saline (PBS).

Determination of cell viability using MTT reduction assay

The effect on cell viability was evaluated by the reduction of MTT (Carmichael *et al.*, 1987) by mitochondrial succinate dehydrogenase to produce the purple formazan crystals in the cells, indicating viable cells. The cells were seeded at density of 1×10^5 cells/mL in 96-well plate. After 24-h incubation for allowing the cells attached to the plate, the cells were treated with NVK (0.002 - 1 mg/mL) or Hcy (0.005 - 5 mM) for 6, 12 and 24 h. In study of the effect of NVK on Hcy-treated cells, the cells were pre-treated with NVK (0.001 - 0.5 mg/mL) for 12 h, and then exposed to Hcy at the selected concentration and incubation time. The medium containing NVK or Hcy was replaced by MTT solution (0.4 mg/mL) in DMEM medium and incubated for 4 h. The MTT solution was removed and DMSO was added to the wells to dissolve the formazan crystals into purple solution. The absorbance of the solution was measured in a microplate reader at 570 nm against the appropriate blank solutions. The percentage of cell viability was calculated from following equation:

$$\% \text{ cell viability} = A_{\text{sample}} / A_{\text{control}} \times 100.$$

Where A_{control} is the absorbance of the vehicle control group, and A_{sample} is the absorbance of treated group. The half maximal inhibitory concentration (IC_{50}) value was used to evaluate the toxicity of NVK and Hcy.

Determination of intracellular ROS level using DCFH-DA assay

Intracellular ROS was determined by DCFH-DA assay (Wang and Joseph, 1999). DCFH-DA entered the cells and was hydrolyzed by plasma esterase to non-fluorescent 2',7'- dichlorodihydrofluorescein form (DCFH). The highly fluorescent DCF which oxidized from DCFH by the intracellular ROS was spectrofluorometrically detected. The fluorescence intensity indicated the intracellular ROS level. The cells were seeded at a density of 1×10^5 cells/mL in 96-well plate. After 24-h incubation for allowing the cells attached to the plate, the cells were treated with NVK (0.002 - 1 mg/mL) for 6, 12 and 24 h, or with Hcy (0.01 - 2 mM) for 0.5, 1, 2, 3, 6, 12 and 24 h. In study of the effect of NVK on Hcy-treated cells, the cells were pre-treated with NVK (0.001 - 0.5 mg/mL) for 12 h, and then exposed to Hcy at the selected concentration and incubation time to induce intracellular ROS. The medium containing NVK or Hcy was removed. The cells were washed twice with

cold PBS and loaded with 100 μ L of 5 μ M DCFH-DA in PBS at 37°C for 30 min, and then washed twice with cold PBS. The fluorescence intensity was measured in microplate reader at an excitation wavelength of 485 nm and an emission wavelength of 535 nm. The fluorescence intensity in each groups were expressed in the percentage of control as calculated from following equation:

$$\% \text{ control} = F_{\text{sample}} / F_{\text{control}} \times 100.$$

Where F_{control} is the fluorescence intensity of the vehicle control group, and F_{sample} is the fluorescence intensity of treated group.

Proteomic analysis using 2-dimensional electrophoresis

2-DE was used to study the effect of NVK on proteomic profile in Hcy-treated cells. The cells pre-treated with NVK for 12 h and exposed to Hcy for 12 h. The cells were seeded at a density of 1×10^5 cells/mL in 100 mm culture dishes. After 24-h incubation for allowing the cells attached to the dish, the cells were treated with NVK (0.05 mg/mL) or/and Hcy (0.05 mM) for 12 h. The cells were washed three times with ice-cold 0.25 M sucrose. After adding the 0.25 M sucrose, cells were scraped off the dish with a rubber cell scraper. The cell suspension was transferred to the 1.5 mL centrifuge tube and subsequently centrifuged at 2400 rpm for 10 min to collect the cell pellets. To extract the cellular protein, the lysis buffer (7 M urea, 2 M thiourea, 4% CHAPS, 5% ampholytes, 40 mM DTT and 1% cocktail protease inhibitor) was added to the cell pellets and allowed to stand for 1 h. After centrifugation at 12000 rpm for 15 min, the supernatant was collected and subsequently determined the protein concentration by Bradford method.

Proteins (150 μ g) were mixed with rehydration buffer and applied to 7 cm Immobiline DryStrip pH 3 - 10 NL, which were rehydrated for overnight (12 - 16 h) at room temperature. Rehydrated strips were applied to IEF system to perform the first dimensional electrophoresis at 50 μ A per strip with running condition: 300 V for 30 min, 1000 V for 30 min, 5000 V for 1.5 h and 5000 V for 3 h. Focused IPG strips were equilibrated in the equilibration buffer (50 mM Tris-HCl pH 6.8, 6 M urea, 30% glycerol, 1% SDS) containing 1% DTT for 15 min, followed by the equilibration buffer containing 2.5% iodoacetamide instead of DTT for 15 min. For the second dimensional electrophoresis, the equilibrated IPG strips were placed to 12.5% SDS-

PAGE (10 × 10.5 × 1.5 mm) and covered with 0.5% agarose sealing solution containing bromophenol blue dye. The SDS-PAGE was carried out at 12 mA per gel until the bromophenol blue dye reached the lower edge of the gel. The protein spots on gels were visualized with Coomassie blue staining (1% Coomassie blue R250, 40% MeOH and 10% acetic acid). The stained gels were destained with destain solution (40% MeOH and 10% acetic acid) to remove excess dyes and scanned with ImageScanner 3. Protein spots were quantified using ImageMaster 2D platinum software.

Comparative analysis of 2-DE gels image

2-DE gel images obtained from each condition (control, NVK-treated cells, Hcy-treated cells and NVK in Hcy-treated cells) were analyzed using ImageMaster 2D platinum. In each condition, images from at least three independent experiments were grouped into similar class. Protein spots on these gels were detected using the detection parameters which were adjusted to 5 for minimum area, 5 for smooth and 25 for saliency. The detected protein spots in the same class were matched together and defined with the same number. Analysis mode of the software was used to report the average percentage of protein volume for each class. The matched spots from each class were matched again to compare the intensity of each spot between classes and the average ratios were reported. The statistical analysis, one-way analysis of variance (ANOVA), was used to indicate the significance of differential protein spots ($p < 0.05$). Moreover, protein spot, which only presented in each class, was also considered to be differential protein spot. The protein spots which significantly changed were subjected to identify the protein.

In-gel tryptic digestion

The selected protein spots were cut out from the gels and transferred to 1.5 mL centrifuge tubes (Srisomsap *et al.*, 2010). The pieces of gels were washed with 0.1 M NH_4HCO_3 in 50% acetonitrile to remove Coomassie blue dye until the gel pieces were colorless. The completely dried gel pieces were reduced by adding reducing buffer solution (0.1 M NH_4HCO_3 , 10 mM DTT and 1 mM EDTA) and incubated at 60°C for 45 min. After cooling, the reducing buffer solution was replaced by the

alkylating solution (100 mM iodoacetamide in 0.1 M NH_4HCO_3 solution). After incubation in the dark at room temperature for 30 min, the alkylating solution was removed. The gel pieces were washed three times for 10 min each time with 50% acetonitrile. After the gel pieces were completely dried, the digesting buffer (0.05 M Tris-HCl, 10% acetonitrile, 1 mM CaCl_2 , pH 8.5 and 1% trypsin) was added to the gel pieces and incubated at 37°C for overnight. The solution was collected and the remaining gel pieces were added by 2% trifluoroacetic acid, 1 mM CaCl_2 in 0.05 M Tris-HCl buffer pH 8.5 and 2.5% formic acid in acetonitrile to extract the remaining proteins. This extract was pooled with previous solution and dried for being subject to mass spectrometric analysis.

Protein identification by LC/MS/MS

Protein identification was carried out using nLC system coupled with ion trap MS equipped with a electrospray ion source. Trypsinized peptides were concentrated and desalted on a C18 column. Eluents A and B were 0.1% formic acid in water and 0.1% formic acid in acetonitrile, respectively. Sample (6 μL) was injected into nano-LC system for separation at a flow rate of 0.5 $\mu\text{L}/\text{min}$ for 30 min using gradients system: 0 min 95% A, 20 min 60% A, 20.5 min 5% A, 29 min 5% A and 29.5 min 95% A, followed by MS/MS analysis using 1.0 s automatic scan rate with 0.1 s interscan delay. Parent mass peaks ranging from 50 to 3000 m/z were selected for MS/MS analysis. The collision energy was fixed at 1300 V. AutoMSⁿ was applied with SMART isolation and fragmentation (at 60% amplitude), and scan ranges were automatically scaled to the individual precursor mass in each MS/MS spectrum. The Bruker proteomics database system Compass 1.4 was used for MS/MS data processing, which was then analyzed using the MASCOT search tool on the Matrix Science site (<http://www.matrixscience.com/>). MS/MS data were searched against SwissProt database for *Homo sapiens* taxonomy. The search parameters were set as follows: peptide mass tolerance = 1.2 Da; MS/MS ion mass tolerance = 0.2 Da; enzyme set as trypsin and allowance was set up to 1 missed cleavages; peptide charges were limited to 1+, 2+ and 3+. The proteins were identified with $p < 0.05$ and MASCOT scores >25 were considered as promising hits.

Bioinformatic tools

To elucidate the pathway of differentially expressed proteins obtained from 2-DE and MS/MS, the combination of bioinformatic tools such as STRING (<http://string-db.org/>), KOBAS (<http://kobas.cbi.pku.edu.cn/home.do>) and IPA[®] (<http://www.ingenuity.com/products/ipa>) was used. The identified proteins were uploaded as a list of Uniprot entry number. The interaction of each protein was searched against human databases with the default parameters. The association of these proteins was reported as direct and indirect protein-protein interaction, related literatures and merging into the canonical cellular pathways.

Immunoblot analysis

After incubation with NVK or Hcy, the cells were washed three times with ice-cold PBS and were scraped off the dish with a rubber cell scraper. The cell suspension was transferred to a 1.5 mL centrifuge tube and subsequently centrifuged at 2400 rpm for 10 min to collect cell pellets. To extract the cellular protein, radio-immunoprecipitation assay (RIPA) lysis buffer (50 mM Tris, 150 mM NaCl, 0.1% SDS, 0.5% sodium deoxycholate, 1% Triton-X100 and 1% cocktail protease inhibitor) was added to the cell pellets and allowed to stand for 1 h. After centrifugation at 12000 rpm for 15 min, the supernatant was collected and subsequently determined the protein concentration by Bradford method.

Proteins (20 μ g) were mixed with 5 \times sample buffer and loaded each well of SDS-PAGE (12.5% SDS-PAGE for detection of SOD, GPx, CAT, HO-1, VEGF, Nrf2 and Akt and 8% SDS-PAGE for detection of HIF-1 α and eNOS). The proteins were separated with the applied voltage of 90 V until bromophenol blue dye reached the lower edge of the gel. The separated proteins on the gels were subsequently electrotransferred onto PVDF membranes by the applied voltage of 45 V for 2 h.

The blots were blocked for 2 h at room temperature with 5% BSA in TBS-T buffer (10 mM Tris-HCl, pH 7.4, 150 mM NaCl with 0.1% Tween 20) and then incubated with rabbit polyclonal primary antibodies for SOD (1:3000), GPx (1:3000), CAT (1:3000), HO-1 (1:1000), VEGF (1:1000), Nrf2 (1:1000), HIF-1 α (1:1000), Akt (1:1000), p-Akt (1:1000), eNOS (1:500) and p-eNOS (1:1000) in 3% BSA in TBS-T buffer overnight at 4°C. The blots were washed 5 times for 5 min each time with TBS-

T buffer to remove the excess antibody and incubated with secondary antibody with HRP-conjugated (1:3000) in 3% BSA in TBS-T buffer for 1 h at room temperature. After washing with TBS-T buffer 5 times for 5 min, the protein bands were detected by using ECL detection solution and followed by exposure the membrane to X-ray films. The bands on the X-ray film were quantitative analyzed by ImageJ software. The mouse monoclonal antibodies for β -actin (1:5000) and rabbit polyclonal antibody for GAPDH (1:1000) were used to normalize as the loading control.

Statistical analysis

All data are expressed as the mean \pm standard error of the mean (S.E.M.) of at least three independent experiments. Each was performed in triplicate. Comparisons among groups were evaluated using multiple group comparisons, and identified significantly differences using ANOVA with a post hoc test. Student's *t*-test was used to compare significant difference between two groups. Differences were considered as being significant at $p < 0.05$ and $p < 0.01$.

CHAPTER IV

RESULTS AND DISCUSSIONS

ROS and RNS scavenging activity of NVK and single herb Superoxide radical scavenging activity

$O_2^{\cdot-}$ is the by-product in electron transport chain caused an increase in cellular oxidative stress. Substance which can eliminate $O_2^{\cdot-}$ results in reduction of oxidative stress. To investigate the ability of the extract to quench $O_2^{\cdot-}$ from reaction mixture, NBT reduction assay was performed. The $O_2^{\cdot-}$ scavenging activities of all extracts were in a concentration dependent manner and the EC_{50} values were calculated (Figure 2). Quercetin was used as a positive control, showing an EC_{50} value of $14.28 \pm 0.42 \mu\text{g/mL}$ ($42.21 \pm 1.255 \mu\text{M}$), which was in agreement with a previous report (Mandal *et al.*, 2011). Comparison among all extracts, the highest activities were found in both ethanolic and water extracts of TC, exhibiting EC_{50} values of 12.00 ± 1.14 and $10.50 \pm 1.05 \mu\text{g/mL}$, respectively. High activities were also found in PK, NVK, AP and NJ, exhibiting EC_{50} values ranging from 28.60 to 80.69 $\mu\text{g/mL}$, while moderate activities was observed in LC, AD and AS with EC_{50} values ranging from 130.99 to 378.31 $\mu\text{g/mL}$. The poorest activities were found in AL and SC, exhibiting EC_{50} values greater than 1 mg/mL.

The results were in accordance with a previous report, demonstrating that high $O_2^{\cdot-}$ scavenging activity was found in methanolic extract of TC fruit (Hazra *et al.*, 2010). The water extract also showed high $O_2^{\cdot-}$ scavenging activity but less potent than methanolic extract of TC (Cheng *et al.*, 2003). High $O_2^{\cdot-}$ scavenging activity was also found in methanolic extract of PK (Russo *et al.*, 2002; Govindarajan *et al.*, 2003), which was probably due to picroliv, picroside-I and kutkoside as previously reported (Chander *et al.*, 1992). The ethanolic extract of NJ showed good scavenging activities against $O_2^{\cdot-}$ (Sharma and Singh, 2012). Interestingly, both ethanolic and water extracts of AP showed high $O_2^{\cdot-}$ scavenging activity, exhibiting EC_{50} values of 75.29 ± 4.65 and $61.16 \pm 2.30 \mu\text{g/mL}$, which has not been reported elsewhere. Phytochemical study of AP extracted with 50% methanol-water revealed the presence of gallic acid, protocatechuic acid, chlorogenic acid, ferulic acids, rutin, quercetin and

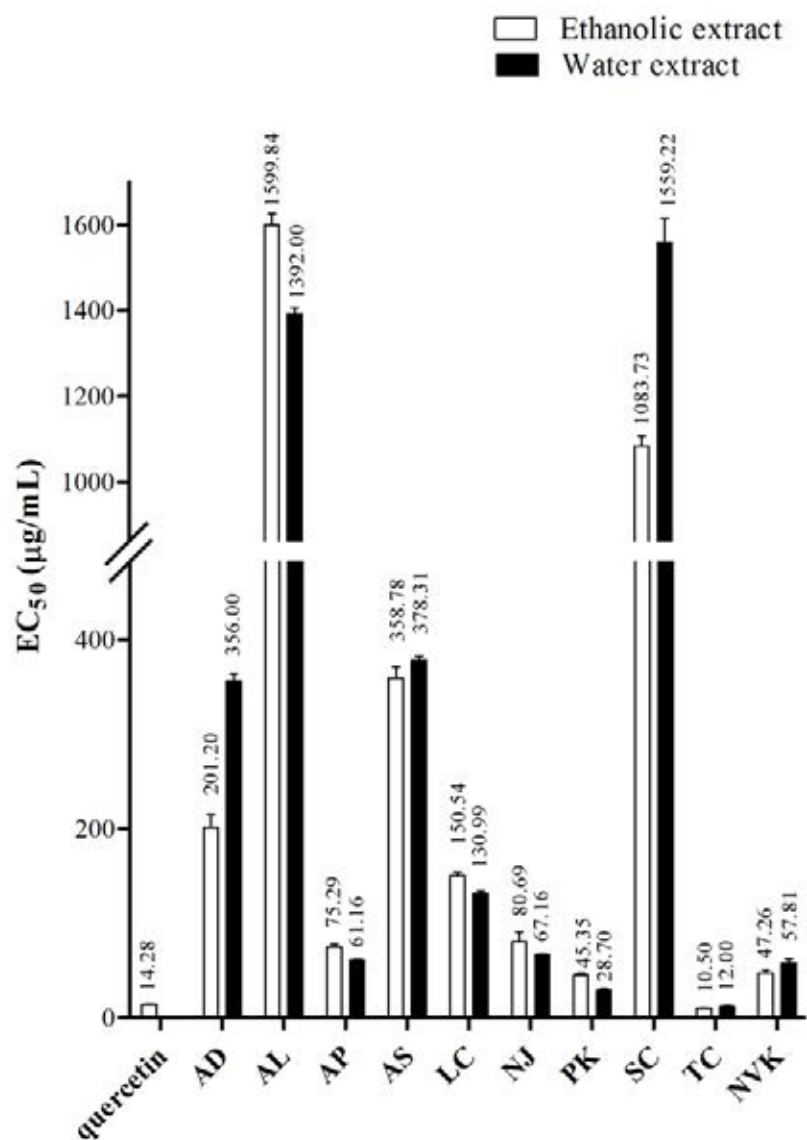


Figure 2. EC₅₀ values for O₂^{•-} scavenging activity of NVK extracted with 50% ethanol and water as compared to AD, AL, AP, AS, LC, NJ, PK, SC and TC. Quercetin was used as a positive control. Results were expressed as mean ± S.E.M (n = 3). Each performed in triplicate.

kaempferol (Niranjan *et al.*, 2009). The presence of gallic acid (Yoshiki *et al.*, 2001) and quercetin (Mandal *et al.*, 2011) might be responsible for $O_2^{\cdot-}$ scavengers in AP. Therefore, the potent $O_2^{\cdot-}$ scavenging activity of NVK might arise from TC, PK and AP.

Hydrogen peroxide scavenging activity

H_2O_2 is a product from neutralization of $O_2^{\cdot-}$ by intracellular SOD. Using guaiacol method, all extracts exhibited scavenging activities against H_2O_2 in a concentration-dependent manner (Figure 3). There was a large difference in H_2O_2 scavenging activity among each extracts with EC_{50} values ranging from 21.28 to 3016.00 $\mu\text{g/mL}$. The most potent activity was found in both ethanolic and water extracts of TC (EC_{50} 21.28 ± 0.29 and 22.35 ± 0.48 $\mu\text{g/mL}$, respectively) followed by NVK (EC_{50} 132.32 ± 15.16 and 248.52 ± 7.65 $\mu\text{g/mL}$, respectively) (Figure 3). Meanwhile, AD, LC, AP, PK and NJ showed moderate activity with EC_{50} values ranging from 501.91 to 896.71 $\mu\text{g/mL}$, respectively (Figure 3). Similar to $O_2^{\cdot-}$ scavenger, the poor H_2O_2 scavenger was also found in AL, AS and SC with EC_{50} values ranging from 1 to 3 mg/mL. The EC_{50} value of quercetin, used as a positive control, was 15.62 ± 0.06 $\mu\text{g/mL}$ (46.18 ± 1.883 μM).

From our results, both ethanolic and water TC extracts similarly exhibited high scavenging activity against H_2O_2 , which was in accordance with a previous study, revealing that TC fruits extracted with methanol, 95% ethanol and water could scavenge H_2O_2 with similar EC_{50} values in HRP-luminol- H_2O_2 system (Chang and Lin, 2012). Though atractylochromene isolated from AL was reported to exhibit good H_2O_2 scavenging activity (Heilmann *et al.*, 1998), our result revealed that AL showed the poorest activity (Figure 3). Based on our extraction procedure, atractylochromene in AL might be present in very minute quantity, resulting poor antioxidant activity.

Hydroxyl radical scavenging activity

The OH^{\cdot} , generated by Fenton reaction from H_2O_2 , are the most reactive species and can damage most biomolecules such as lipids, DNA and proteins. Unlike $O_2^{\cdot-}$ and H_2O_2 which can be neutralized by SOD, GPx and CAT, OH^{\cdot} cannot be eliminated by any enzymatic reaction (Manda *et al.*, 2009). Therefore, antioxidant

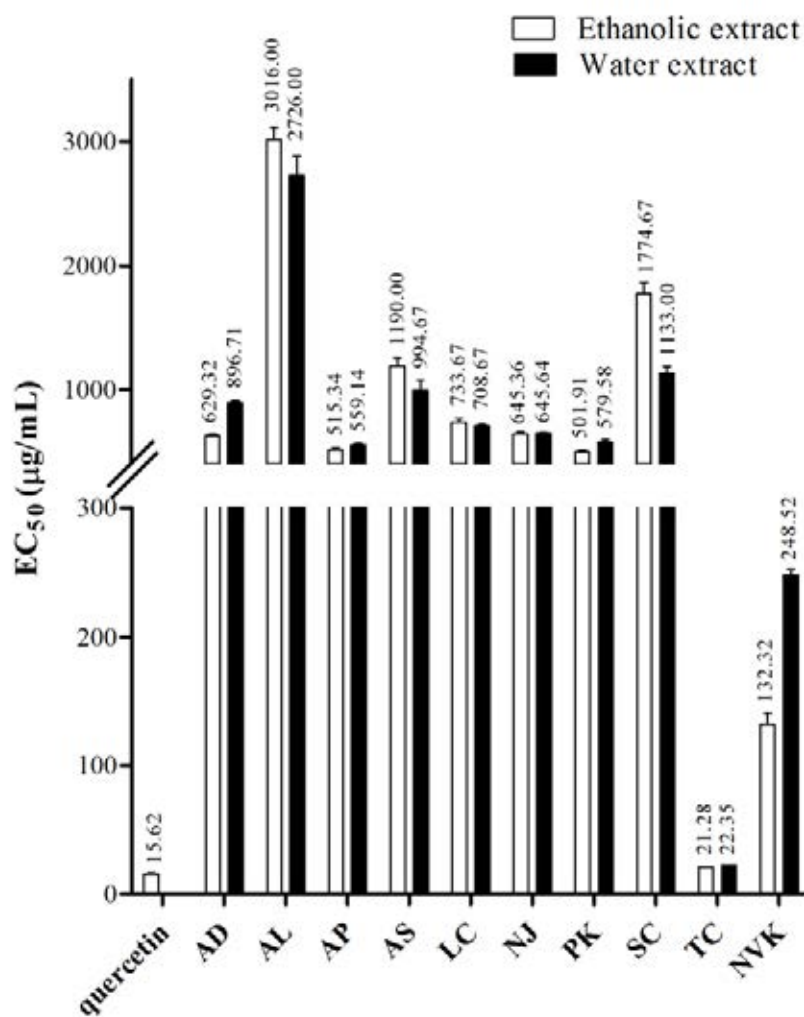


Figure 3. EC₅₀ values for H₂O₂ scavenging activity of NVK extracted with 50% ethanol and water as compared to AD, AL, AP, AS, LC, NJ, PK, SC and TC. Quercetin was used as a positive control. Results were expressed as mean ± S.E.M (n = 3). Each performed in triplicate.

was required for elimination of OH^\bullet . The ability of the extract to scavenge OH^\bullet was performed using deoxyribose assay. Again, the ethanolic and water extracts of TC were the most potent activity (EC_{50} 9.99 ± 1.03 and 7.63 ± 0.36 $\mu\text{g/mL}$, respectively) followed by NVK (EC_{50} 26.99 ± 1.47 and 40.42 ± 2.51 $\mu\text{g/mL}$, respectively) (Figure 4). Mannitol, a positive control, exhibited the EC_{50} value of 442.51 ± 2.22 $\mu\text{g/mL}$ which was similar to a previous report (EC_{50} 571.45 ± 20.12 $\mu\text{g/mL}$) (Hazra *et al.*, 2008). Meanwhile, AD, AP, NJ, PK and SC also showed higher OH^\bullet scavenging activities than mannitol (EC_{50} ranging from 81.86 ± 2.81 to 325.54 ± 12.78 $\mu\text{g/mL}$).

Our results were in accordance with a previous report, demonstrating that high OH^\bullet scavenging activities were found in several herbs in Phikud Navakot. The highest activity was found in TC, which might be due to high phenolic contents (Sabu *et al.*, 2002; Cheng *et al.*, 2003; Hazra *et al.*, 2010). Interestingly, SC with poor activities against both $\text{O}_2^{\bullet-}$ and H_2O_2 , had the OH^\bullet scavenging activity higher than most of single herbs except TC. This activity might be due to the reducing power of sesquiterpene lactone isolated from SC (Chang *et al.*, 2012), leading to poorly active in Fenton reaction. Good OH^\bullet scavenging activities of AP, NJ and PK were also reported (Rajkumar *et al.*, 2011; Suresh *et al.*, 2011; Sharma and Singh, 2012).

Nitric oxide scavenging activity

NO^\bullet is an important cellular signaling molecule. The toxicity of NO^\bullet caused by reaction with $\text{O}_2^{\bullet-}$ to produce reactive ONOO^\bullet , leading to serious toxic reactions with biomolecules (Forstermann, 2010). The ability of the extract to scavenge NO^\bullet was performed using Griess assay. Quercetin was used as a positive control (EC_{50} 11.06 ± 0.63 $\mu\text{g/mL}$, 32.68 ± 1.859 μM) (Figure 5), which was in agreement with a previous report (Ebrahimzadeh *et al.*, 2009). Surprisingly, AD, possessing moderate potency against ROS, exhibited the highest scavenging activity against NO^\bullet , exhibiting EC_{50} values of 30.67 ± 4.16 and 70.00 ± 13.53 $\mu\text{g/mL}$ for ethanolic and water extracts, respectively (Figure 5). Both ethanolic and water extracts of TC, LC, NVK, and AP also showed high NO^\bullet scavenging activities (EC_{50} values ranging from 68.33 to 135.67 $\mu\text{g/mL}$, respectively). The poorest ability to scavenge NO^\bullet was found in AS (Figure 5).

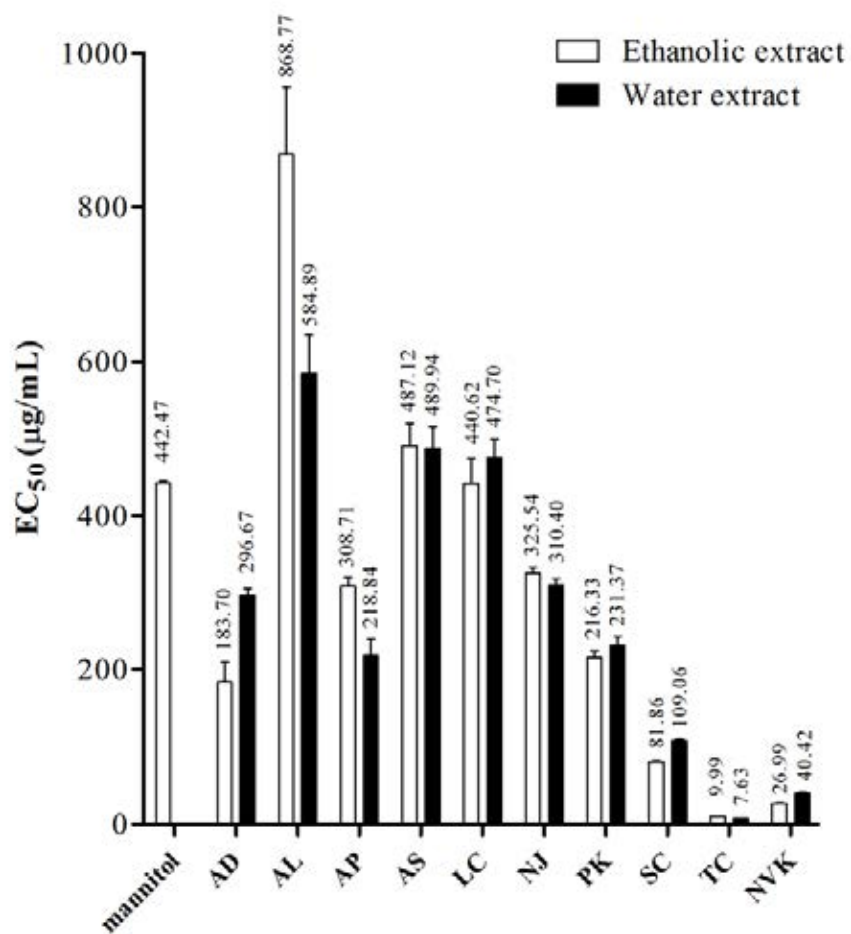


Figure 4. EC₅₀ values for OH• scavenging activity of NVK extracted with 50% ethanol and water as compared to AD, AL, AP, AS, LC, NJ, PK, SC and TC. Mannitol was used as a positive control. Results were expressed as mean ± S.E.M (n = 3). Each performed in triplicate.

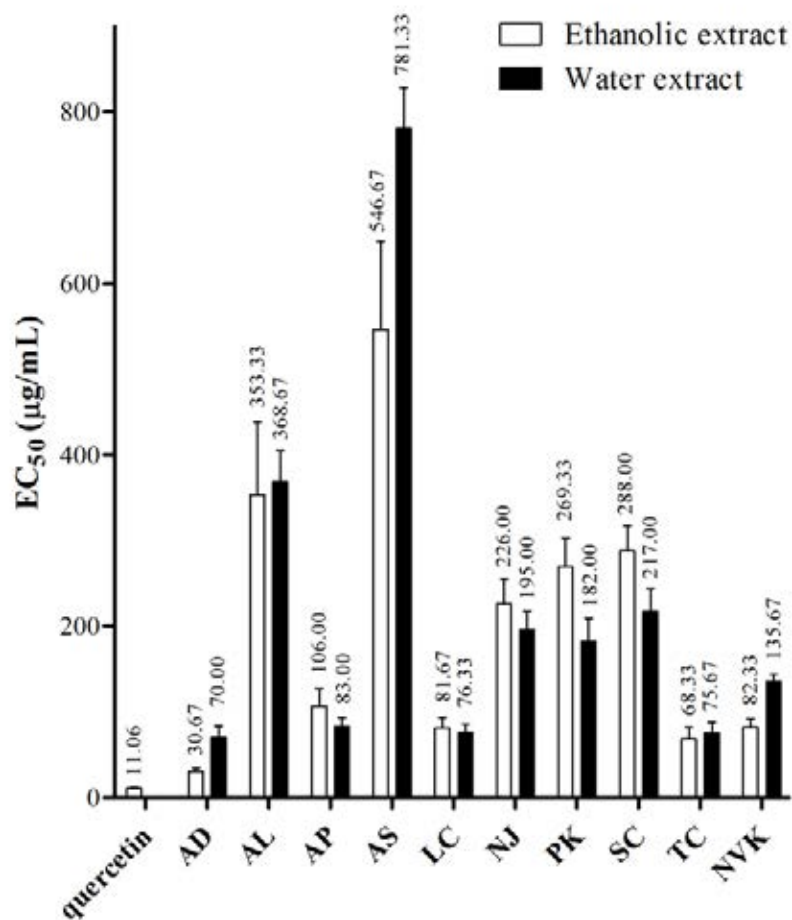


Figure 5. EC₅₀ values for NO• scavenging activity of NVK extracted with 50% ethanol and water as compared to AD, AL, AP, AS, LC, NJ, PK, SC and TC. Quercetin was used as a positive control. Results were expressed as mean ± S.E.M (n = 3). Each performed in triplicate.

From our results, good NO[•] scavenging activity of NVK (Figure 5) might arise from AD, AP, LC and TC which exhibited potent scavenging activities. TC was previously reported to exhibit high NO[•] scavenging activity (Hazra *et al.*, 2010). However, the NO[•] scavenging activities of all herbs in Phikud Navakot have not been reported elsewhere. These activities might be due to the presence of active compounds in each herb. The presence of polyphenols such as gallic acid, ferulic acids and quercetin might be responsible for NO[•] scavenging activity in AP (Niranjan *et al.*, 2009). Ferulic acid, which also found in LC, exhibited good antioxidant activities against NO[•] (Maurya *et al.*, 2010).

Synergistic study

The extracts were found to have different potency of scavenging activities against O₂^{•-}, H₂O₂, OH[•] and NO[•]. TC remarkably exhibited the most potent activities and AL had the poorest activities in all tested assays. Meanwhile, the scavenging activity of NVK was greater than most of individual herb extracts except TC. This might be due to herb-herb interaction. Thus, the CI value was used to determine the interaction among nine herbs in terms of synergistic, additive or antagonistic effects. The ethanolic extract of NVK significantly exhibited the synergistic antioxidant activities against all tested ROS and RNS with CI values lesser than 1.0 (Figure 6). Meanwhile, the water extract of NVK showed a somewhat irregular pattern of antioxidant activities as follows: synergistic effect against OH[•] (CI = 0.73), antagonistic effect against H₂O₂ (CI = 1.51) and additive effect against O₂^{•-} and NO[•] (CI ≈ 1).

According to EC₅₀ values, the scavenging activities of the ethanolic extracts were significantly more potent than of the water extracts (Figure 2-5). This implied that the antioxidant constituents were likely water-insoluble. Previous study reported that the ethyl acetate extract of herb pair containing *Astragalus membranaceus* and *Glycyrrhiza uralensis* exhibited the synergistic effect, while the water extract showed the antagonism (Li *et al.*, 2011) due to the increase in total flavonoid and phenolic contents in the herb pair (Li *et al.*, 2011). The interaction of epicatechin and quercetin-3β-glucoside in each herb was found to possess the synergistic antioxidative effect (Hidalgo *et al.*, 2010). This was in agreement with our result, confirming that

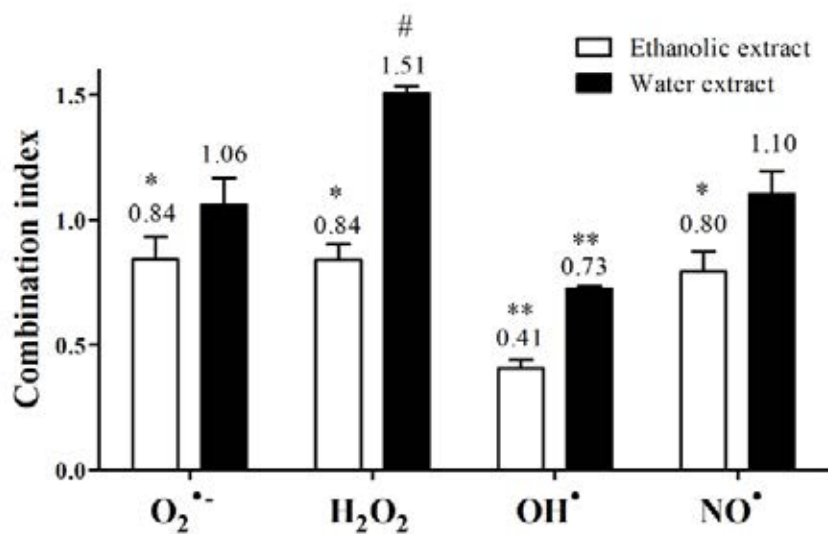


Figure 6. CI values of the antioxidant activities were compared between the ethanolic and water extracts of NVK. Results were expressed as mean \pm S.E.M. from three independent experiments performed in triplicate. Significance of CI values lower than 1 was indicated as * $p < 0.05$ and ** $p < 0.01$. # indicated the significance of CI values higher than 1 ($p < 0.05$).

the polarity of solvent used in extraction process was largely responsible for synergistic or antagonistic effects. Some phenolic compounds such as chlorogenic and gallic acids found in TC (Manosroi *et al.*, 2010) are not stable to high pH (Friedman and Jürgen, 2000). Based on our observation, the percent yield of the extract obtained from combining the powder of nine herbs was higher than the sum of yield from each extract. These implied that the extraction process of combining herbs, consisting of many active substances, might alter the acid-base environment (van Acker *et al.*, 1996), resulting in the improvement of stability and solubility of active constituents.

Our results revealed that the antioxidant activities of the ethanolic extract of NVK were more potent than the water extract and the importance of the combination of nine herbs which was essential to confer maximal antioxidant activity due to the synergistic effect. Therefore, the ethanolic extract of NVK was chosen and further subjected to cell-based experiments.

Effect of NVK on viability of EA.hy926 cells

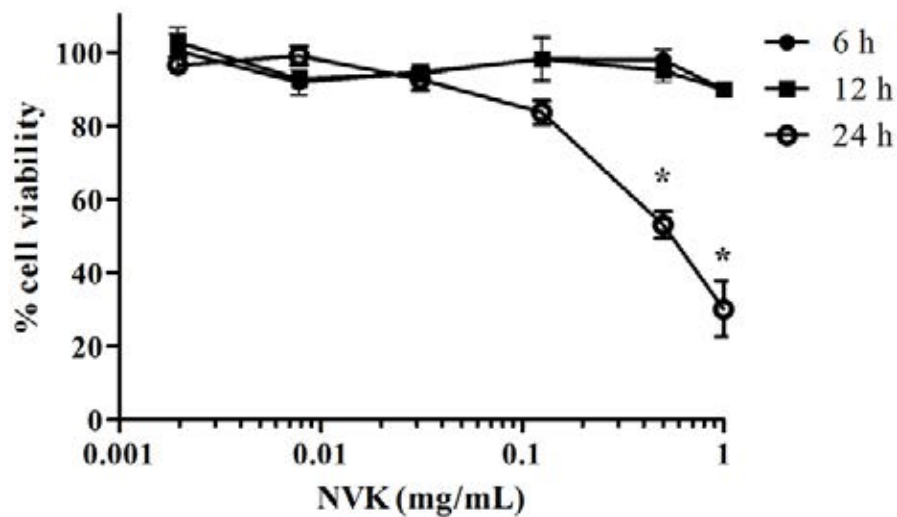
To determine nontoxic concentration of NVK, cell viability was determined using MTT assay. The results showed that NVK at concentrations below 1 mg/mL for 6- and 12-h treatment was not toxic to the cells, while 24-h treatment with NVK at the concentration above 0.2 mg/mL was significantly toxic (Figure 7A), exhibiting an IC_{50} value of 0.555 ± 0.071 mg/mL (Figure 7B).

Among herbs in NVK, TC and PK were previously reported to have not only antioxidant activity but also toxicity. The ethanolic extract of TC fruit and its active constituents such as gallic acid, ethyl gallate, luteolin and tannic acid showed toxicity against malignant cell lines with IC_{50} values at $\mu\text{g/mL}$ level (Saleem *et al.*, 2002). However the toxicity on normal cells has not been reported elsewhere. The nontoxic concentrations of NVK were chosen for further study on intracellular ROS effect.

Effect of NVK on intracellular ROS

According to the antioxidant potential of NVK in cell-free system, intracellular ROS level affected by NVK was then determined using DCFH-DA assay. The intracellular ROS was significantly decreased after the cells were treated

(A)



(B)

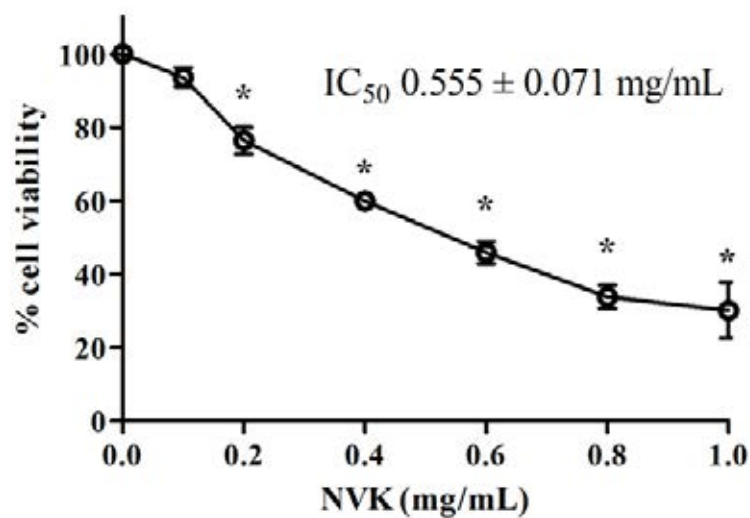


Figure 7. Concentration- and time-dependent studies of NVK on cell viability determined by MTT assay. The cells were treated with (A) NVK at the concentrations of 0.002, 0.008, 0.031, 0.125, 0.50 and 1.00 mg/mL for 6, 12 and 24 h and (B) NVK at the concentrations of 0.1, 0.2, 0.4, 0.6, 0.8 and 1.0 mg/mL for 24 h with an IC_{50} value. Results were presented as mean \pm S.E.M. ($n = 3$). Each performed in triplicate. * indicated the significant difference when compared to the vehicle control group ($p < 0.05$).

with NVK at the concentration above 0.2 mg/mL for 24 h (Figure 8) due to the loss of cell viability (Figure 7B). The result suggested that NVK at the non-toxic concentration itself did not affect the intracellular ROS level in normal cellular condition. Therefore, NVK at concentration lower than 0.2 mg/mL was used for further studies.

Effect of Hcy on cell viability

In order to determine appropriate condition to induce oxidative stress in EA.hy926 cells, the effect of Hcy on cell viability was determined using MTT assays. Concentration- and time-dependent studies revealed that after 24-h treatment of Hcy at concentrations higher than 5 mM became significantly toxic to the cells, exhibiting 76.81 ± 1.99 % cell viability (Figure 9).

Elevated plasma concentration of Hcy was considered as a risk factor of atherosclerosis (Bautista *et al.*, 2002). Normal plasma concentration and mildly elevated level of Hcy range 5 - 15 μ M and 15 - 30 μ M, respectively (Hankey and Eikelboom, 1999). Plasma level of Hcy higher than 0.1 mM was considered as severe hyperhomocysteinaemia which was associated with premature vascular disease (Thambyrajah and Townend, 2000). Hcy at the concentrations between 1 - 10 mM were found to induce concentration-dependent damage of endothelial cells. Treatment with 2.5 mM Hcy (Sipkens *et al.*, 2012) or 3 mM Hcy (Zhang *et al.*, 2001) induced apoptotic cell death in HUVEC cells, while 1 mM Hcy reduced viability of ECV304 cells (Lin *et al.*, 2007). Meanwhile, 20-h incubation of 0.05 - 0.5 mM Hcy did not affect the viability of EA.hy926 cells and human brain endothelial cells (Kam *et al.*, 2012). Cytotoxicity of Hcy on endothelial cells was mainly related to an increase in oxidative stress via uncoupling of NOS activity (Topal *et al.*, 2004), increase in NADPH oxidase protein expression (Tyagi *et al.*, 2005) and auto-oxidation of Hcy (McDowell and Lang 2004). Hence, the effect of Hcy on intracellular ROS was further investigated.

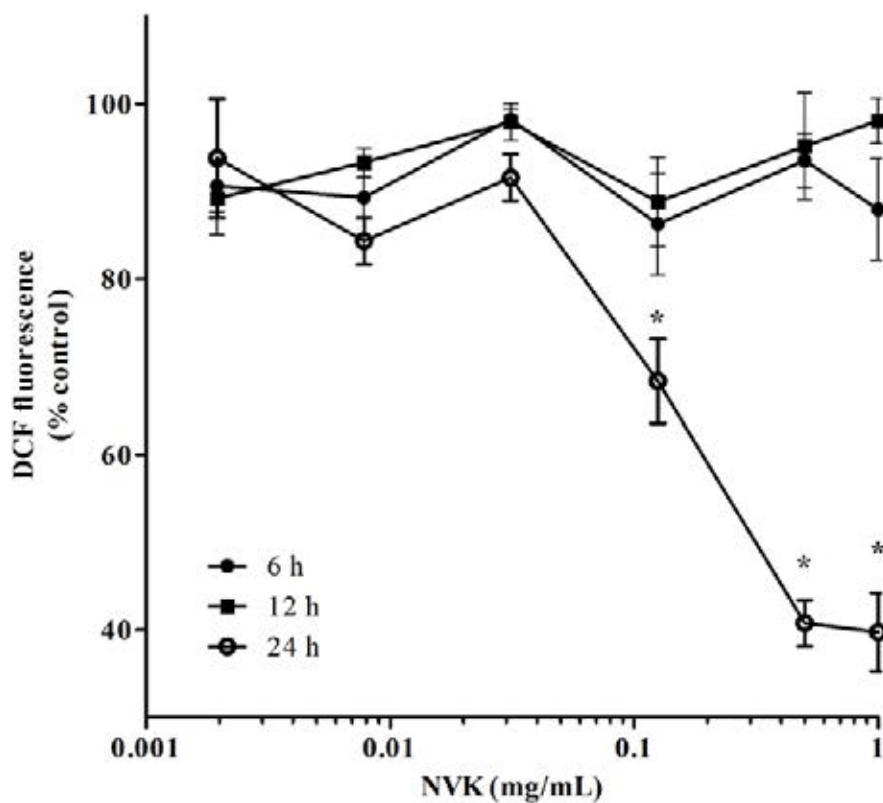


Figure 8. Concentration- and time-dependent studies of NVK on intracellular ROS determined by DCFH-DA assay. The cells were treated with NVK at the concentrations of 0.002, 0.008, 0.031, 0.125, 0.50 and 1.00 mg/mL for 6, 12 and 24 h. Results were shown as mean \pm S.E.M. ($n = 3$). Each performed in triplicate. * indicates the significant difference when compared to the control group ($p < 0.05$).

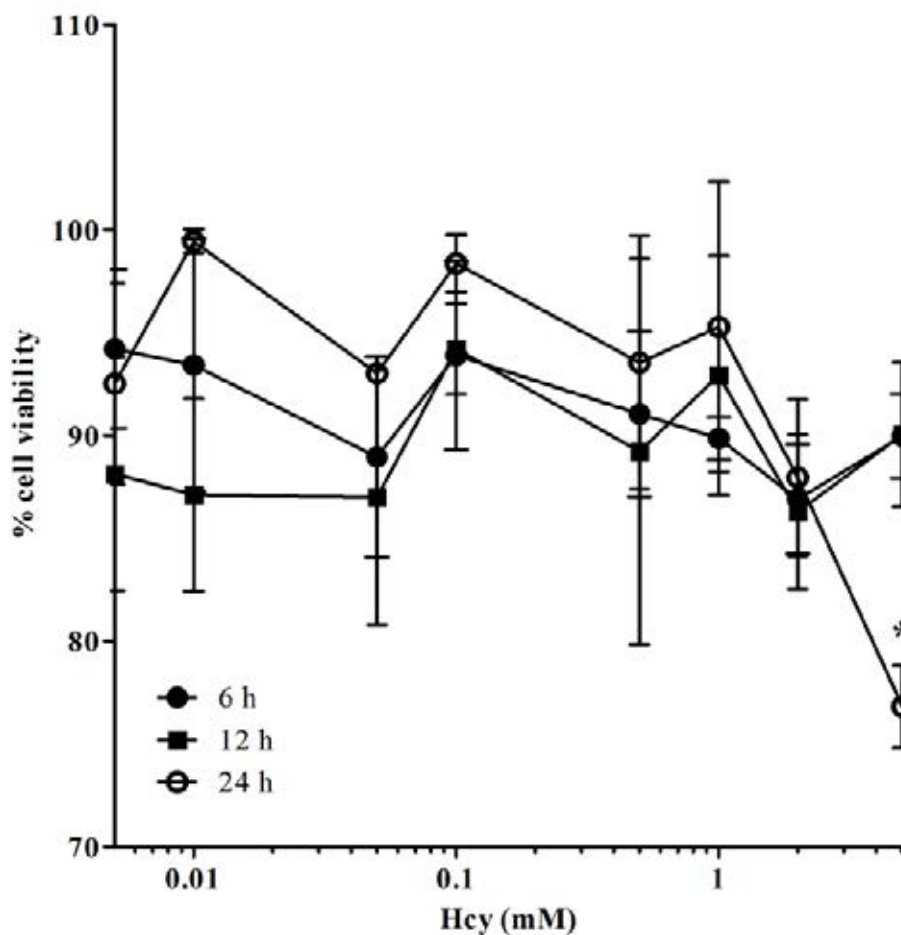


Figure 9. Concentration- and time-dependent studies of Hcy on cell viability determined by MTT assay. The cells were treated with Hcy at the concentrations of 0.005, 0.01, 0.05, 0.1, 0.5, 1, 2 and 5 mM for 6, 12 and 24 h. Results were shown as mean \pm S.E.M. ($n = 3$). Each performed in triplicate. * indicates the significant difference when compared to the control group ($p < 0.05$).

Effect of Hcy on intracellular ROS

To evaluate the effect of Hcy on intracellular ROS, the cells were exposed to Hcy at various concentrations and incubation times. Hcy at the nontoxic concentrations significantly showed a biphasic increase in intracellular ROS after 1- and 12-h exposure (Figure 10).

Short duration of Hcy treatment led to generate $O_2^{\bullet-}$ by auto-oxidation in various cell types such as HUVEC cells (Bao *et al.*, 2009; Zou *et al.*, 2010), human megakaryocytic cells (Austin *et al.*, 1998) and T lymphocytes (Zhang *et al.*, 2002). The rate of Hcy auto-oxidation rapidly occurred within 2 h (Hogg, 1999) due to thiol moiety, which was subsequently oxidized by the transition metal ion to a thiyl radical. The thiyl radical can react with other Hcy molecule to generate radical intermediate which further reduces oxygen to $O_2^{\bullet-}$ (McDowell and Lang, 2000). Therefore, a rapid burst of ROS within 1 h induced by Hcy in our study might be due to the auto-oxidation of Hcy.

Furthermore, the increase in intracellular ROS after 12-h exposure to Hcy might be due to the induction of both activity and expression of proteins involving in oxidative stress such as of NADPH oxidase in microvascular endothelial cells treated with 40 μ M Hcy for 6 - 24 h (Tyagi *et al.*, 2005), HUVEC cells treated with 1 mM Hcy for 24 h (Dong *et al.*, 2005) and HUVEC cells treated with 2.5 mM Hcy for 6 h (Sipkens *et al.*, 2011). Activation of NADPH oxidase activity was observed in rat malignant glioma cells treated with 80 μ M Hcy for 16 h (Yi *et al.*, 2004). Moreover, Hcy increased oxidative stress by inhibition of L-arginine uptake in HUVEC cells (Jin *et al.*, 2007), resulting in generation of $O_2^{\bullet-}$ by induction of uncoupled eNOS reaction (Topal *et al.*, 2004).

Therefore, 1 mM Hcy with 1-h brief exposure and 0.05 mM Hcy with 12-h exposure were selected for induction of oxidative stress in EA.hy926 cells.

Effect of NVK on intracellular ROS in Hcy-treated cells

To determine whether NVK attenuated oxidative stress, the effect of NVK on intracellular ROS in Hcy-treated cells was determined. Pre-treatment with NVK at the concentration of 0.05 mg/mL for 12 h prior exposure to Hcy (1 mM) for 1 h significantly reduced ROS compared to Hcy-treated cells without affecting cell

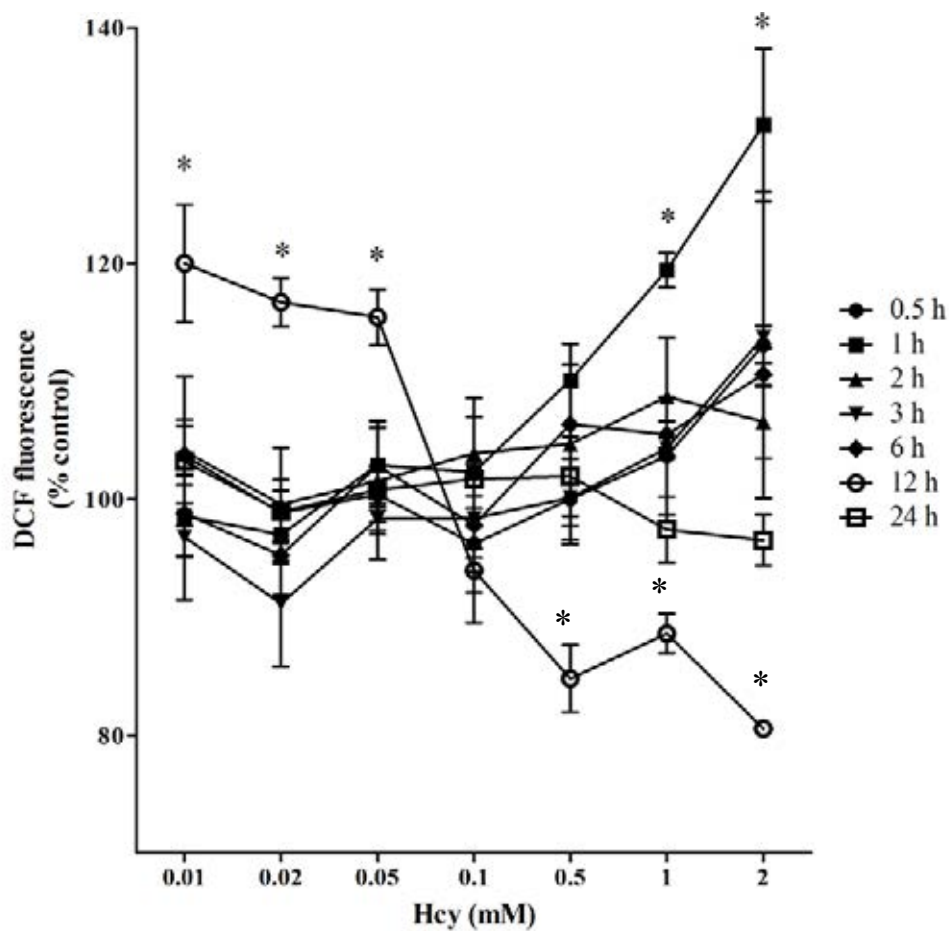


Figure 10. Concentration- and time-dependent studies of Hcy on intracellular ROS determined by DCFH-DA assay. The cells were treated with Hcy at the concentrations of 0.01, 0.02, 0.05, 0.1, 0.5, 1 and 2 mM for 0.5, 1, 2, 3, 6, 12 and 24 h. Results were shown as mean \pm S.E.M. ($n = 3$). Each performed in triplicate. * indicates the significant difference when compared to the control group ($p < 0.05$).

viability (Figure 11). Additionally, NVK (0.05 mg/mL) significantly decreased ROS when treated with 0.05 mM Hcy for 12 h with a slight decrease in cell viability ($78.32 \pm 9.54 \%$) but not significantly different when compared to Hcy-treated group (Figure 12). However, NVK (0.5 mg/mL) significantly decreased viability in cells treated with 1 mM Hcy for 1 h (Figure 11) or 0.05 mM Hcy for 12 h (Figure 12), resulting in significant decrease in ROS.

NVK and Hcy alone at the indicated concentrations and incubation times did not affect the viability (Figure 7 and 9). When cells were pre-treated with NVK (0.2 and 0.5 mg/mL) followed by Hcy, the cell viability was significantly reduced. This implied that high concentration of NVK also injured EA.hy926 cells or made the cells more susceptible to oxidative stress. Therefore, the reduction of DCF fluorescence intensity in cells treated with NVK (0.2 and 0.5 mg/mL) might be due to the loss of cell viability (Figures 11, 12). Meanwhile, reduction of DCF fluorescence intensity in the cells pre-treated with NVK (0.005, 0.01 and 0.05 mg/mL) might result from antioxidant effect of the NVK (Figure 6). The result showed that pre-treatment of NVK (0.05 mg/mL) could reduce intracellular ROS when induced by both 1-h and 12-h incubation of Hcy. This suggested that NVK had the protective effect on the cells against oxidative stress induced by the short- or long-time exposure to Hcy. Therefore, NVK at the concentration of 0.05 mg/mL, with a significant reduction of ROS in Hcy-treated cells, was subjected to the study of proteomic profile.

Molecular response of EA.hy926 cells towards NVK treatment

Proteomic profile of NVK-treated cells using 2-DE

To identify proteins or pathways by which NVK might affect, the extracted proteins from untreated (control) and NVK-treated cells were compared using 2-DE to verify differential protein expression. The steady-state level of proteins changed after exposure to NVK. More than 344 and 346 protein spots were resolved per 2-DE gel from total cell lysate of control and NVK-treated cells, respectively (Figure 13). Treatment with NVK (0.05 mg/mL) for 12 h, the intensity of 197 of 344 spots decreased, while 147 spots increased. Total 27 spots, showing statistically different compared to control, were selected to identify the proteins using LC/MS/MS (Figure 13). Results from MASCOT database revealed that total 27 spots could be

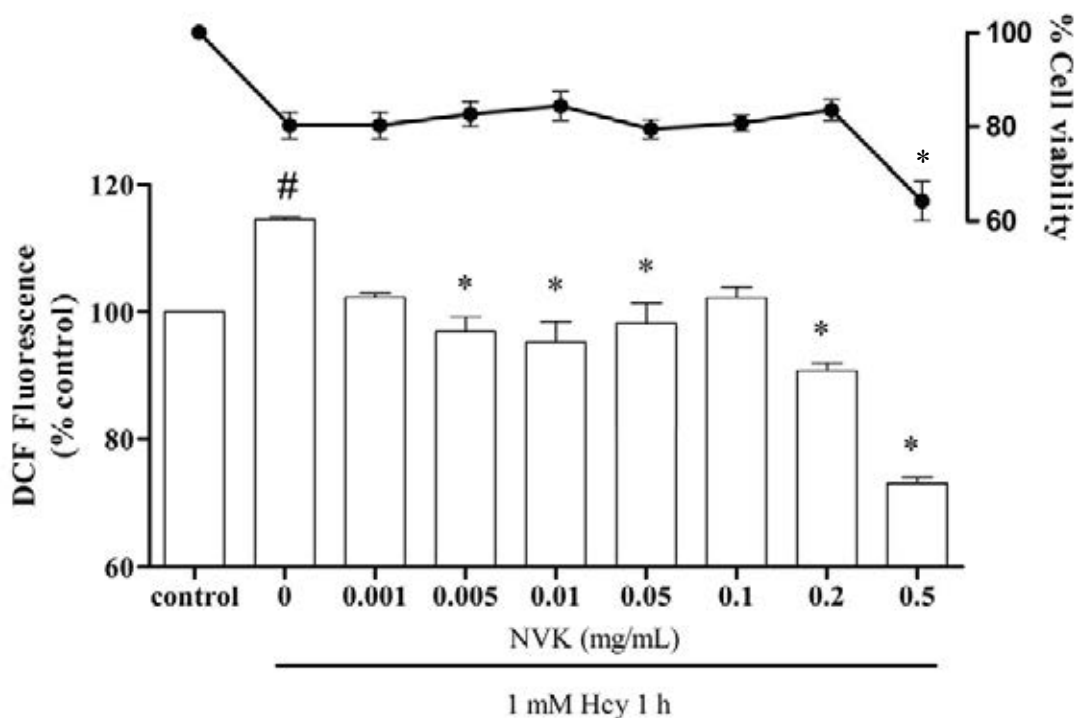


Figure 11. Effect of NVK on ROS and viability under 1-h Hcy treatment. Cells were pre-treated with NVK at the indicated concentrations for 12 h and were subsequently exposed to Hcy (1 mM) for 1 h. Bar graph and left axis represented the intracellular ROS. Line graph and right axis represented the cell viability. Results were shown as mean \pm S.E.M. ($n = 3$). Each performed in triplicate. # indicates the significant difference when compared to the control group ($p < 0.05$). * indicates the significant difference when compared to the Hcy-treated group ($p < 0.05$).

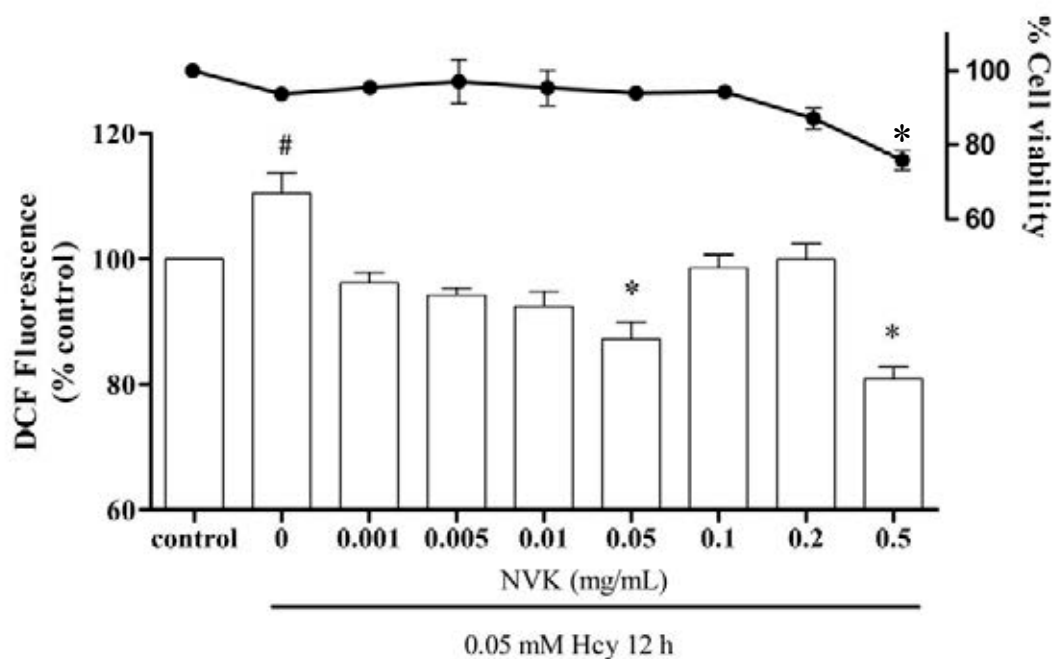


Figure 12. Effect of NVK on ROS and viability under 12-h Hcy treatment. Cells were treated with NVK at the indicated concentrations for 12 h and were subsequently exposed to Hcy (0.05 mM) for 12 h. Bar graph and left axis represented the intracellular ROS. Line graph and right axis represented the cell viability. Results were shown as mean \pm S.E.M. ($n = 3$). Each performed in triplicate. # indicates the significant difference when compared to the control group ($p < 0.05$). * indicates the significant difference when compared to the Hcy-treated group ($p < 0.05$).

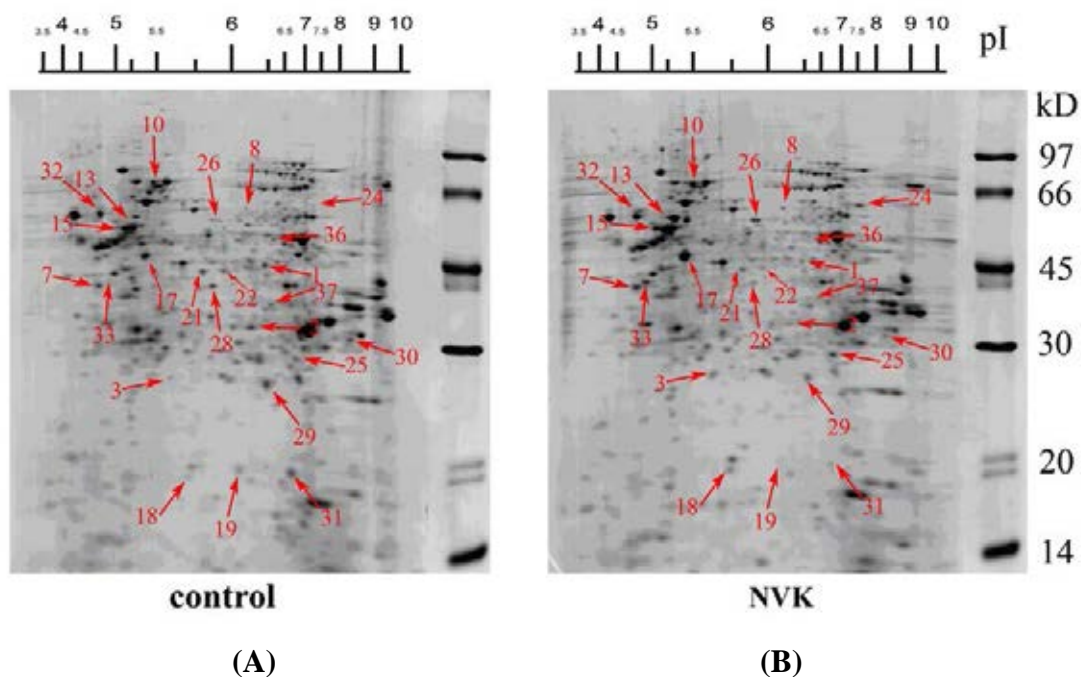


Figure 13. Representative 2-DE gels of proteins from cells exposed to NVK. Proteins (150 μ g) were separated on non-linear IPG strips pH 3 - 10 NL for the first dimension and 12.5% SDS-PAGE for the second dimension of separation. Coomassie blue stained gels of proteins from (A) untreated cells (B) cells treated with NVK (0.05 mg/mL) for 12 h. The proteins spots numbered were excised, subjected to tryptic digestion and identified using LC/MS/MS analysis. Similar results were obtained in 4 independent experiments.

identified to 22 proteins (Table 2). According to the protein function, they were categorized into 7 types involving in protein synthesis (28%), cytoskeleton proteins (21%), redox regulation (13%), metabolism (13%), chaperones (13%), annexins (8%) and other proteins (4%) (Figure 14). Eight proteins down-regulated by NVK were annexin A1, annexin A2, prelamin-A/C, α -enolase, splicing factor proline- and glutamine-rich (SFPQ), heterogeneous nuclear ribonucleoproteins A2/B1 (hnRNPA2B1), heterogeneous nuclear ribonucleoprotein A1-like 2 (hnRNPA1L2) and elongation factor Tu (EF-tu). Thirteen up-regulated proteins were glutathione S-transferase Pi (GST-P), protein disulfide-isomerase (PDI), endoplasmic reticulum protein 1 (TCP-1), heat shock cognate 71 kD (Hsc70), vimentin, β -tubulin, β -actin, stathmin, pyruvate kinase isozymes M1/M2 (PKM), triosephosphate isomerase (TPI), heterogeneous nuclear ribonucleoprotein H (hnRNPH1) and lipocalin-1 (Figure 15 and Table 2). Notably, nucleophosmin (NPM) (spot no. 33, Figure 13B), was only found in the NVK-treated cells. These proteins were subjected to investigate the protein-protein interaction in pathway analysis.

Our result showed that some spots presented the same proteins which might due to post-translational modification (PTM) or alternative splicing (Kamath *et al.*, 2011; Lengqvist *et al.*, 2011). For example, α -enolase was found more than one spot (spot no. 21 and 22, Figure 13). This event also occurred in several proteomic studies (Ha *et al.*, 2005; Rubporn *et al.*, 2009; Shao *et al.*, 2012).

Pathway analysis of identified proteins from NVK-treated cells using bioinformatic tools

To elucidate the pathway of differentially expressed proteins obtained from 2-DE and LC/MS/MS, the combination of bioinformatic tools such as STRING, KOBAS and IPA[®] was used. The list of 22 proteins (Table 2) was uploaded. The association of these proteins was reported as direct and indirect protein-protein interaction (Franceschini *et al.*, 2013) and merging into the canonical cellular pathways (Xie *et al.*, 2011). Network analysis using STRING showed that the protein-protein interaction (Figure 16) affected by NVK was related to several cellular processes such as oxidative stress, modulation of transcription factors with client proteins, glycolysis and anti-apoptosis.

Table 2. Steady-state levels of proteins in NVK-treated cells identified by LC/MS/MS.

Spot no.	Protein identity	UniProt no.	Theoretical		Fold change	MASCOT score	Cellular location
			MW (kD)	pI			
Annexin							
1	Annexin A1	P04083	39	6.6	-2.81	427	cell membrane; cytoplasm
2	Annexin A2	P07355	39	7.6	-2.20	153	cell membrane; cytoplasm
Redox regulation							
3	Glutathione <i>S</i> -transferase P	P09211	24	5.4	+1.95	134	cytoplasm; mitochondria
4	Superoxide dismutase [Cu-Zn]	P00441	16	5.7	-0.97	89	cytoplasm
Chaperones							
7	Endoplasmic	P14625	93	4.8	+1.89	267	ER
8	T-complex protein 1, subunit beta	P78371	58	6.0	+1.87	226	cytoplasm
10	Heat shock cognate 71 kD protein	P11142	71	5.4	+2.04	457	cytoplasm
32	Protein disulfide-isomerase	P07237	57	4.8	+1.89	548	cell membrane; ER
Cytoskeleton							
13	Vimentin	P08670	54	5.1	+6.25	879	cytoplasm
15	Tubulin beta-4A	P04350	50	4.8	+2.65	172	cytoplasm
17	Actin, beta	P60709	42	5.3	+2.64	260	cytoplasm
18	Stathmin	P16949	17	5.8	+1.72	131	cytoplasm
19	Prelamin-A/C	P02545	74	6.6	-1.69	156	nucleus
Metabolism							
21	Alpha-enolase	P06733	47	7.0	-1.75	243	cytoplasm; nucleus
22	Alpha-enolase	P06733	47	7.0	-2.09	181	cytoplasm; nucleus

Table 2. (continued)

Spot no.	Protein identity	UniProt no.	Theoretical		Fold change	MASCOT score	Cellular location
			MW (kD)	pI			
23	Pyruvate kinase isozymes M1/M2	P14618	58	8.0	+2.62	215	cytoplasm; nucleus
24	Alpha-enolase	P06733	47	7.0	-1.87	265	cytoplasm; nucleus
25	Triosephosphate isomerase	P60174	31	5.7	+1.90	152	cytoplasm
Protein synthesis							
26	Heterogeneous nuclear ribonucleoprotein H	P31943	49	5.9	+3.02	227	nucleus
28	Splicing factor, proline- and glutamine-rich	P23246	76	9.5	-2.47	116	nucleus
29	Heterogeneous nuclear ribonucleoprotein H	P31943	49	5.9	-1.78	121	nucleus
30	Heterogeneous nuclear ribonucleoproteins A2/B1	P22626	37	9.1	-1.95	201	nucleus
31	Heterogeneous nuclear ribonucleoprotein A1-like 2	Q32P51	34	9.1	-1.87	98	nucleus
33	Nucleophosmin	P06748	33	4.6	only in NVK	78	cytoplasm; nucleus
36	Elongation factor Tu, mitochondrial	P49411	50	7.3	-2.49	203	mitochondria
Other proteins							
37	Lipocalin-1	P31025	19	5.4	+2.01	107	cytoplasm

UniProt: Universal Protein Resource (<http://www.uniprot.org/>)

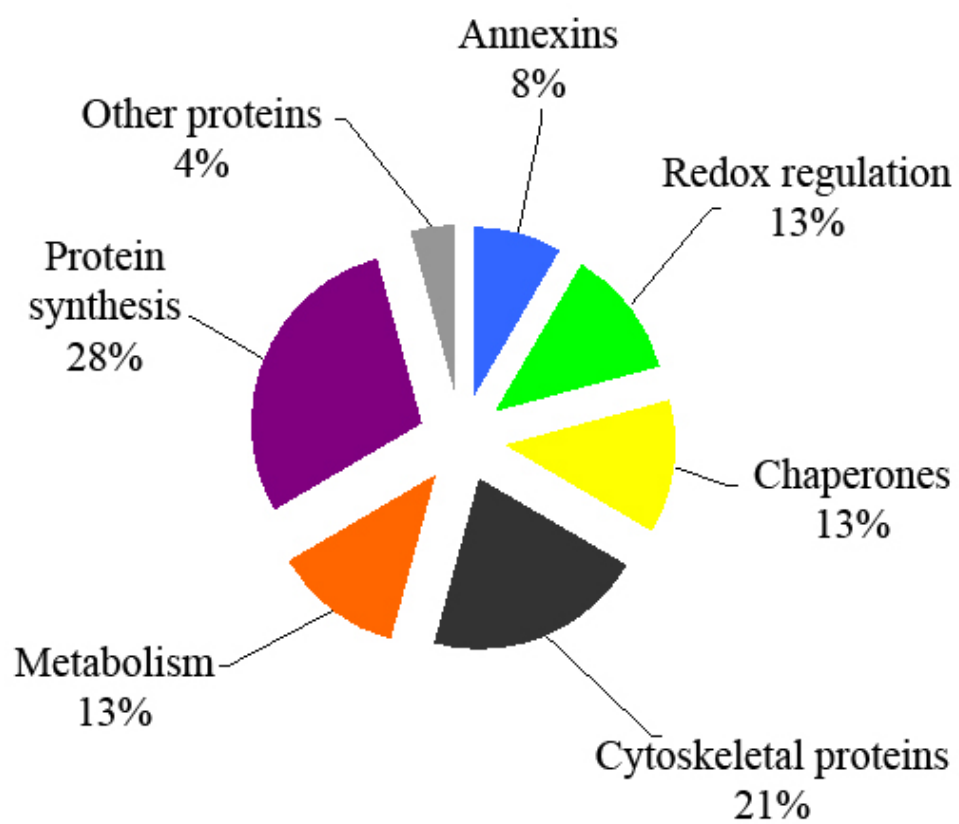


Figure 14. Functional categories of the changed proteins in NVK-treated cells.

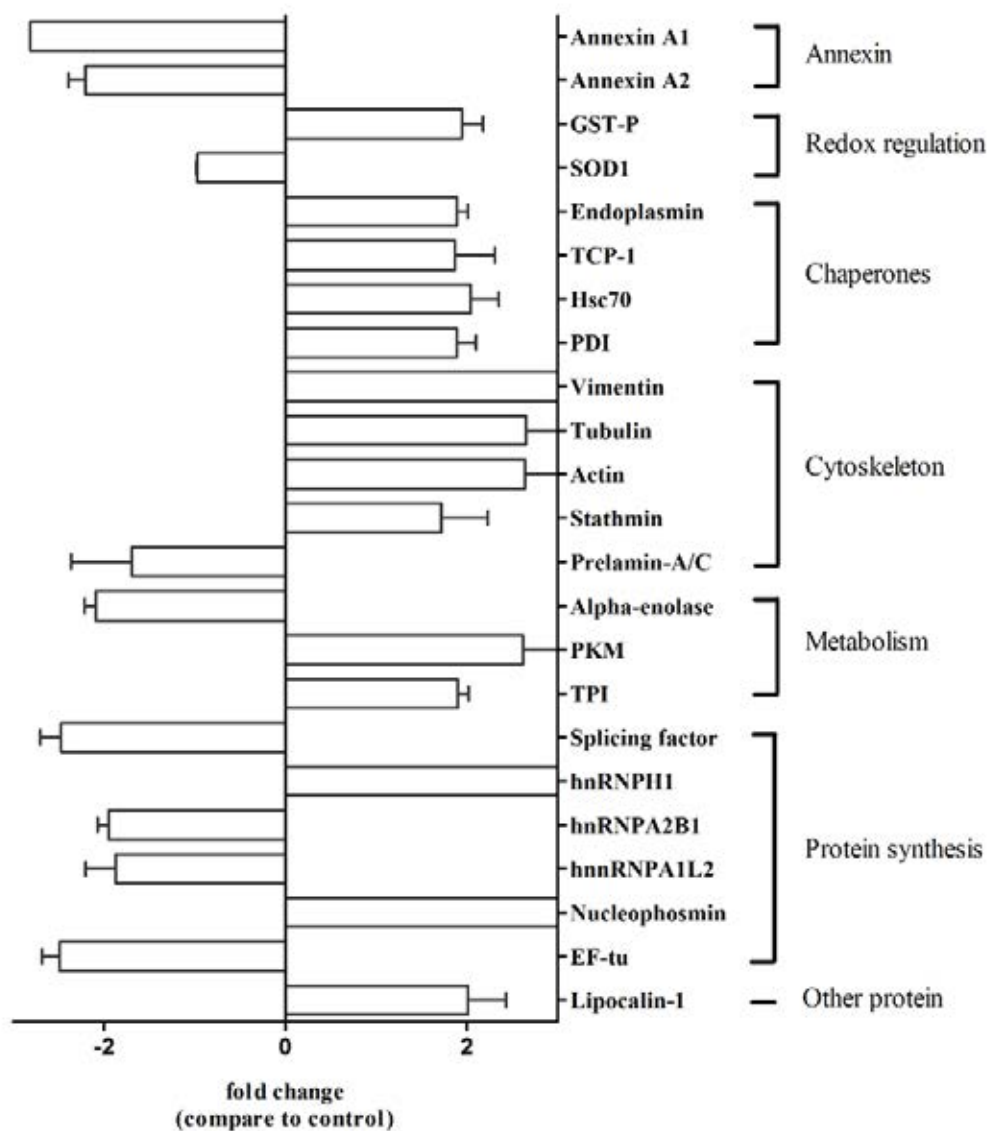


Figure 15. Relative spot intensities of identified proteins from NVK-treated cells compared to control.

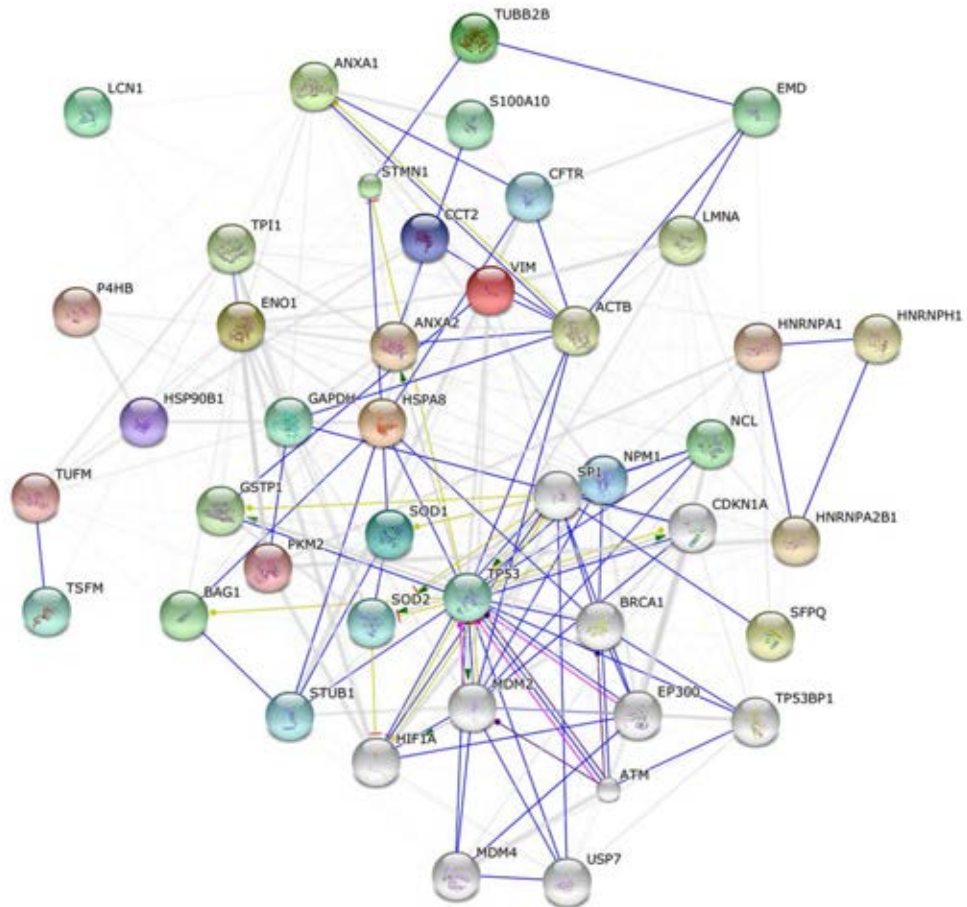


Figure 16. Network analysis of identified proteins from NVK-treated cells using STRING. Each node represented the proteins. The association of these proteins was reported as direct and indirect protein-protein interaction.

KOBAS analysis implicated that the altered proteins involved in aurora B signaling, glycolysis/gluconeogenesis, HIF-1 α transcription factor network and cytoskeletal regulation by Rho GTPase ($p < 0.05$) (Table 3). However, due to small number of data obtained from 2-DE, the number of samples, which could be merged together into the same cellular pathways, was also little (Table 3). From our results, only one or two proteins could be merged into each pathway which consisting of a large number of molecules, resulting in low percent coverage in each pathway.

Annexin A1 and annexin A2 are calcium-dependent phospholipid binding proteins, were both decreased in NVK-treated cells. The diverse biological actions of annexin A1 were reported. In immune system, annexin A1, which was primarily intracellular protein, was produced by endothelial cells as an anti-inflammatory factor (Rodrigo *et al.* 2004) by inhibition of phospholipase A2 (Kim *et al.*, 1994). Annexin A1 has also been identified as a secreted molecule. When leukocytes adhered onto endothelial cells, annexin A1 was released and bound to formyl peptide receptor to inhibit the interaction between leukocytes and endothelial cells (Perretti *et al.*, 2002; Gil *et al.*, 2006). The secretion of annexin A1 was also triggered from some substances such as glucocorticoid and dexamethasone (Comera and Russo-Marie, 1995) to produce anti-inflammatory effects. The secretion of annexin a1 might result in decrease of intracellular annexin A1 level.

Annexin A2 was found to promote tPA-mediated activation of plasminogen to plasmin (Peterson *et al.*, 2003). Binding of annexin A2 to S100A10 protein localized to cell membrane (He *et al.*, 2008) was triggered by signals such as heat, cytokines or thrombin to be phosphorylated by Src-like kinase (Deora *et al.*, 2004). The overexpression of annexin A2 caused hyperfibrinolytic hemorrhagic condition (Menell *et al.*, 1999). The decrease of annexin A2 might cause a decrease in fibrinolytic activity. However, fibrinolytic activity in normal blood condition was found to be low (Fearnley and Lackner, 2008). Hence, annexin A2 might not play an explicit role in normal condition.

GST-P, which is a redox regulation protein, was up-regulated in NVK-treated cells. GST-P catalyzed the conjugation between reduced glutathione and exogenous

Table 3. KOBAS analysis of differentially expressed proteins in NVK-treated cells.

KOBAS pathway	Database	No. of sample	Background proteins	% coverage in pathway	<i>p</i> -value
aurora B signaling	PID Curated	3	39	7.69	0.013
glycolysis I	BioCyc	3	22	13.64	0.022
HIF-1- α transcription factor network	PID Curated	3	65	4.62	0.023
cytoskeletal regulation by Rho GTPase	PANTHER	3	68	4.41	0.044
glycolysis / gluconeogenesis	KEGG	3	65	4.62	0.044

PID: Pathway Interaction Database (<http://pid.nci.nih.gov/>)

BioCyc (<http://biocyc.org/>)

PANTHER: Protein analysis through evolutionary relationships (<http://www.pantherdb.org/>)

KEGG: Kyoto Encyclopedia of Genes and Genomes (www.genome.jp/kegg/)

or endogenous hydrophobic electrophiles (Tew *et al.*, 2011). Since mitochondria are one of the major sources of cellular oxidative stress, GST-P, localized in both cytoplasm and mitochondria, serves as the protective mechanism against the oxidative imbalance in mitochondria (Goto *et al.*, 2009) by increasing glutathione level.

Treatment with NVK up-regulated the expression of chaperone proteins such as endoplasmic reticulum chaperone, TCP-1, Hsc70 and PDI (Figure 15). These chaperone proteins primarily act to aid protein folding process and are found in endoplasmic reticulum (ER), since protein synthesis often occurs in this area (Ellis, 2006). Some of chaperones were also found in cytoplasm (Houry, 2001).

Similar to mitochondria, ER environment is a more oxidizing environment than cytoplasm (Sevier and Kaise, 2002). In normal condition, protein folding primarily occurs in ER. However, under ER stress condition, the formation of disulfide crosslink was impaired, resulting in protein misfolding and leaving cytosolic cysteine residues susceptible to oxidation (Cumming *et al.*, 2004). PDI, a chaperone, catalyzes the formation of disulfide crosslink in the protein folding process (Gruber *et al.*, 2006). The up-regulation of PDI has been reported to promote protein refolding and cytoprotective against ER stress condition (Conn *et al.*, 2004). The up-regulation of PDI in NVK-treated cells may prevent protein misfolding before exposure to oxidative stress.

Endoplasmic reticulum chaperone is Ca^{2+} -binding molecular chaperone in the processing and transport of secreted proteins in ER and anti-apoptotic process due to ER stress (Reddy *et al.*, 1999; Bando *et al.*, 2004). Endoplasmic reticulum chaperone can be up-regulated by HIF-1 α in response to hypoxia (Paris *et al.*, 2005) and usually co-expressed with 78 kD glucose-regulated protein (GRP78) in cellular protection response to oxidative stress (Østergaard *et al.*, 2009; Wu *et al.*, 2009). However, our result demonstrated that only up-regulation of endoplasmic reticulum chaperone not GRP78 was observed in NVK-treated cells.

TCP-1 played a role in assisting the folding of proteins upon ATP hydrolysis (Seo *et al.*, 2010). TCP-1 was known to involve in biogenesis and folding of cytoskeletal proteins such as tubulin, actin and cofilin (Liang and MacRae, 1997). The study reported that TCP-1 was a protein that expressed in response to hypoxia in human aortic endothelial cells (Ning *et al.*, 2004).

Hsc70, a constitutively expressed Hsp70 family member, is a chaperone involved in the folding and trafficking of client proteins (Tsukahara *et al.*, 2000). Recent study showed a role of Hsc70 in response to oxidative stress (Dastoor *et al.*, 2000). Similar to endoplasmic reticulum chaperones, Hsc70 also had a protective effect against ER stress-induced cell apoptosis by promoting protein refolding (Gupta *et al.*, 2010). Hsc70 prevented the processing of pro-caspases 9 and inhibited JNK activity, resulting in cellular prevention from apoptosis (Mosser *et al.*, 2000). Moreover, Hsc70 was a chaperone involving in Akt-mediated cell survival in response to VEGF and Akt-mediated eNOS activation in HUVEC cells (Shiota *et al.*, 2010).

The protein expression of PKM and TPI were up-regulated, while α -enolase was down-regulated in NVK-treated cells (Figure 15). PKM, TPI and α -enolase are enzymes in glucose metabolism (Okar *et al.*, 2001). In glycolysis, D-glucose was phosphorylated before converting to β -D-fructose 1,6-bisphosphate (F1,6P), which was further converted by aldolase to D-glyceraldehyde 3-phosphate (GADP) and dihydroxyacetone phosphate (DHAP). DHAP was rapidly converted by TPI into GADP, which was further converted by several steps to 2-phosphoglycerate (2PG). In this step, α -enolase converted 2PG into phosphoenolpyruvate (PEP) and further to the final product pyruvate by PKM. Since α -enolase was down-regulated by NVK, the accumulation of 2PG occurred. Furthermore, the accumulation of 2PG reversed back to F1,6P and triggered the pathway switching from glycolysis to pentose phosphate pathway, resulting in the formation of xylulose-5-phosphate (X5P).

Recent studies showed that X5P activated the translocation of carbohydrate response element binding protein (ChREBP) into nucleus and bound to *HIF1A* promoter to activate transcription of HIF-1 α (Haase *et al.*, 2010; Isoe *et al.*, 2010). HIF-1 α activated the transcription of over 40 target genes including *TPI*, *α -enolase*, *PKM*, *NPM* and *GST-P* (Wiesener and Maxwell, 2003; Brix *et al.*, 2012).

The activation of HIF-1 α mainly occurred when endothelial cells under hypoxic condition or stimulated by growth factors, cytokines and some glycolytic products (Isoe *et al.*, 2010). Some studies also reported that HIF-1 α was activated by active natural products such as ferulic acid (Lin *et al.*, 2010), quercetin (Jeon *et al.*, 2008; Radreau *et al.*, 2009) and picroliv (Gaddipati *et al.*, 1999). After activation,

cytoplasmic HIF-1 α translocated into nucleus and heterodimerized with aryl hydrocarbon receptor nuclear translocator and bound to the nuclear binding site, followed by transactivation of target genes (Chilov *et al.*, 1999).

Treatment with NVK significantly down-regulated α -enolase (Figure 15). Interestingly, α -enolase gene (*ENO1*), encodes not only α -enolase (48 kD) localized in cytoplasm, but also Myc promoter-binding protein (MBP1) (37kD) localized in nucleus (Feo *et al.*, 2000). This might explain why 3 spots were found in α -enolase on the 2-DE gel (spot no. 21, 22 and 24, Figure 13) due to different molecular weights and pI values. Amino acid sequence alignment showed 79 % identity between α -enolase and MBP1. The computed MW and pI values of α -enolase was 47 kD and 7.00, respectively, while of MBP1 were 36 kD and 5.93, respectively (Table 2). These suggested that NVK also down-regulated MBP1 which suppressed the expression of proteins involving in cell proliferation, differentiation and cell survival by *c-myc* promoter binding (Feo *et al.*, 2000), resulted in preventing the transcription initiation by c-Myc. Down-regulation of MBP1 by NVK led to increase NPM expression which was regulated by c-Myc (Li *et al.*, 2008). Moreover, the protein expression of NPM was regulated by not only c-Myc but also HIF-1 α (Li *et al.*, 2004). NPM was considered as an anti-apoptotic protein due to its ability to inactivate p53 in mouse skin epithelial cell line (Dhar *et al.*, 2009). The anti-apoptotic roles of NPM were observed on hypoxic cell death in human fibroblast cells (Li *et al.*, 2004) and UV-induced cell death in mouse fibroblast cells (Wu *et al.*, 2002). NPM was up-regulated when treated HUVEC cells with salvianolic acid B, which was a cardioprotective compound extracted from *Salviae miltiorrhizae* (Chang *et al.*, 2011). Up-regulation of NPM (Figure 15) might have a protective role in oxidative stress-induced cell damage.

Our results revealed that NVK could regulate the expression of proteins involving in cellular protection from oxidative stress, which were in accordance with previous studies of natural products. Treatment of genistein, an isoflavone from soy, up-regulated TCP-1, endoplasmic reticulum chaperone and GST-P and down-regulated PKM in EA.hy926 cells (Fuchs *et al.*, 2005). TCP-1 and NPM were up-regulated in salvianolic acid B-treated HUVEC cells (Chang *et al.*, 2011). These reports suggested the protective roles of these proteins in endothelial cells.

The result demonstrated that changed proteins (Table 2) in NVK-treated cells were supposed to be regulated by transcription factors HIF-1 α and Nrf2. Nrf2 is the one of major transcription factor that response to cellular oxidative stress (Kensler *et al.*, 2007). Nrf2 binds to antioxidant response elements (ARE) in promoter region of target genes and up-regulates several cytoprotective proteins and antioxidant enzymes such as SOD, GPx, GST, CAT and HO-1 (Surh *et al.*, 2008). To elucidate HIF-1 α or Nrf2 activated by NVK, the effect on protein expression was further investigated by immunoblot analysis.

Proteomic profile of Hcy-treated cells using 2-DE

Hcy (0.05 mM) for 12 h significantly increased intracellular ROS in EA.hy926 cells (Figure 10). The effect of Hcy on the proteomic profile was investigated using 2-DE. The results showed that up to 326 protein spots could be resolved from the gels of Hcy-treated cells. Total 22 protein spots were significantly changed (Figure 17, Table 4) and were categorized into 7 groups (Figure 18) involving in protein synthesis (23%), metabolism (14%), chaperone (22%), cytoskeleton (9%), redox regulation (18%), annexins (9%) and other proteins (5%). Five up-regulated proteins were GST-P, SOD, TPI, calreticulin and lipocalin-1 (Figure 19). Ten down-regulated proteins were annexin A2, protein disulfide-isomerase A3 (PDIA3), PDI, α -enolase, PKM, Hsc70, GRP78, EF-Tu and hnRNPA1L2. Notably, seven spots were lost in Hcy-treated group which were annexin A1, stathmin, endoplasmin, TCP-1, hnRNPH1 and NPM. The group of vimentin fragments was obviously altered the pattern (spot no. 13, Figure 17).

Pathway analysis of identified proteins from Hcy-treated cells

The list of 26 proteins (Table 4) was uploaded onto STRING and KOBAS. The network analysis using STRING showed the protein-protein interactions (Figure 20). Protein expression altered by Hcy was related to oxidative stress, modulation of transcription factors and their client proteins, glycolysis, apoptosis and chaperones.

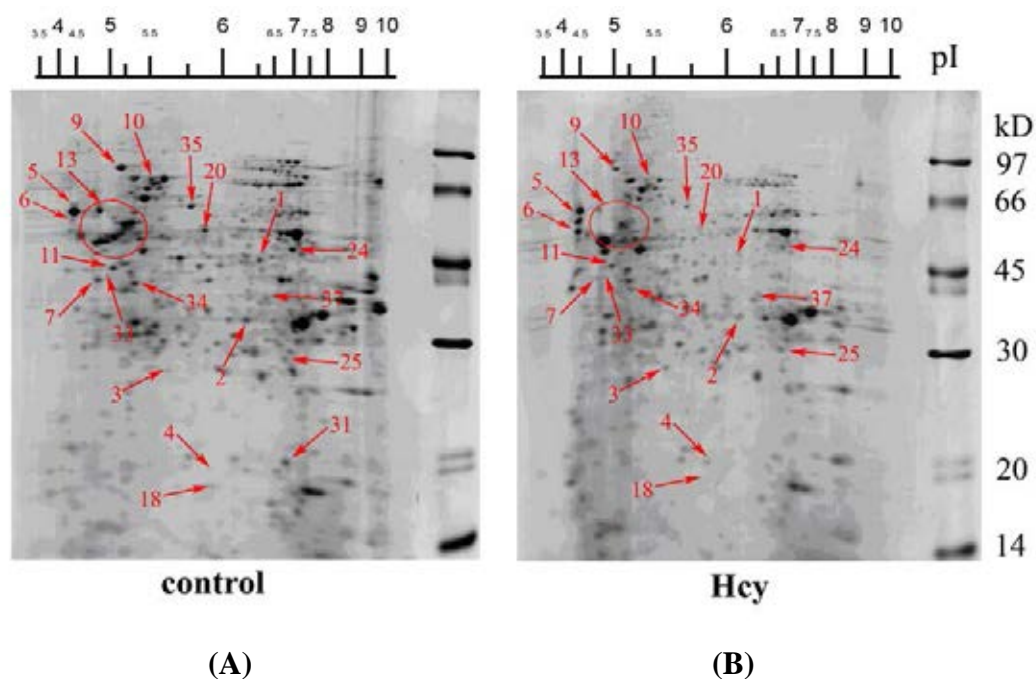


Figure 17. Representative 2-DE gels of proteins from cells exposed to Hcy. Proteins (150 μ g) were separated on non-linear IPG strips pH 3 - 10 NL for the first dimension and 12.5% SDS-PAGE for the second dimension of separation. Coomassie blue stained gels of proteins from (A) untreated cells (B) cells treated with Hcy (0.05 mM) for 12 h. The proteins spots numbered were excised, subjected to tryptic digestion and identified using LC/MS/MS analysis. Similar results were obtained in 3 independent experiments.

Table 4. Steady-state levels of proteins in Hcy-treated cells identified by LC/MS/MS.

Spot no.	Protein identity	UniProt no.	Theoretical		Fold change	MASCOT score	Cellular location
			MW (kD)	pI			
Annexin							
1	Annexin A1	P04083	39	6.6	lost	427	cell membrane; cytoplasm
2	Annexin A2	P07355	39	7.6	-1.43	153	cell membrane; cytoplasm
Redox regulation							
3	Glutathione <i>S</i> -transferase P	P09211	24	5.4	+1.51	134	cytoplasm; mitochondria
4	Superoxide dismutase [Cu-Zn]	P00441	16	5.7	+1.69	109	cytoplasm
Chaperones							
5	Calreticulin	P27797	48	4.3	+2.32	195	cytoplasm; ER
6	Calreticulin	P27798	48	4.3	+1.92	134	cytoplasm; ER
7	Endoplasmic	P14625	93	4.8	lost	267	ER
8	T-complex protein 1, subunit beta	P78371	58	6.0	lost	226	cytoplasm
9	78 kDa glucose-regulated protein	P11021	72	5.1	-1.65	127	cytoplasm; ER
10	Heat shock cognate 71 kD protein	P11142	71	5.4	-1.6	457	cytoplasm
11	Heat shock cognate 71 kD protein	P11142	71	5.4	+1.53	169	cytoplasm
12	Heat shock cognate 71 kD protein	P11142	71	5.4	-1.64	153	cytoplasm
32	Protein disulfide-isomerase	P07237	57	4.8	+1.89	548	cell membrane; ER
Cytoskeleton							

Table 4. (continued)

Spot no.	Protein identity	UniProt no.	Theoretical		Fold change	MASCOT score	Cellular location
			MW (kD)	pI			
13	Vimentin	P08670	54	5.1	change pattern	879	cytoplasm
14	Vimentin	P08670	54	5.1	change pattern	836	cytoplasm
18	Stathmin	P16949	17	5.8	lost	131	cytoplasm
	Metabolism						
20	Pyruvate kinase isozymes M1/M2	P14618	58	8.0	-1.78	164	cytoplasm; nucleus
24	Alpha-enolase	P06733	47	7.0	-.154	265	cytoplasm; nucleus
25	Triosephosphate isomerase	P60174	31	5.7	+1.68	152	cytoplasm
	Protein synthesis						
26	Heterogeneous nuclear ribonucleoprotein H	P31943	49	5.9	lost	227	nucleus
	Non-POU domain-containing octamer-binding protein		54	9	+1.71	64	nucleus
27		Q15233					
31	Heterogeneous nuclear ribonucleoprotein A1-like 2	Q32P51	34	9.1	-1.72	98	nucleus
35	Protein disulfide-isomerase A3	P30101	57	5.9	-1.76	123	cell membrane; ER
36	Elongation factor Tu, mitochondrial	P49411	50	7.3	-1.26	203	mitochondria
	Other proteins						
37	Lipocalin-1	P31025	19	5.4	+1.59	107	cytoplasm

UniProt: Universal Protein Resource (<http://www.uniprot.org/>)

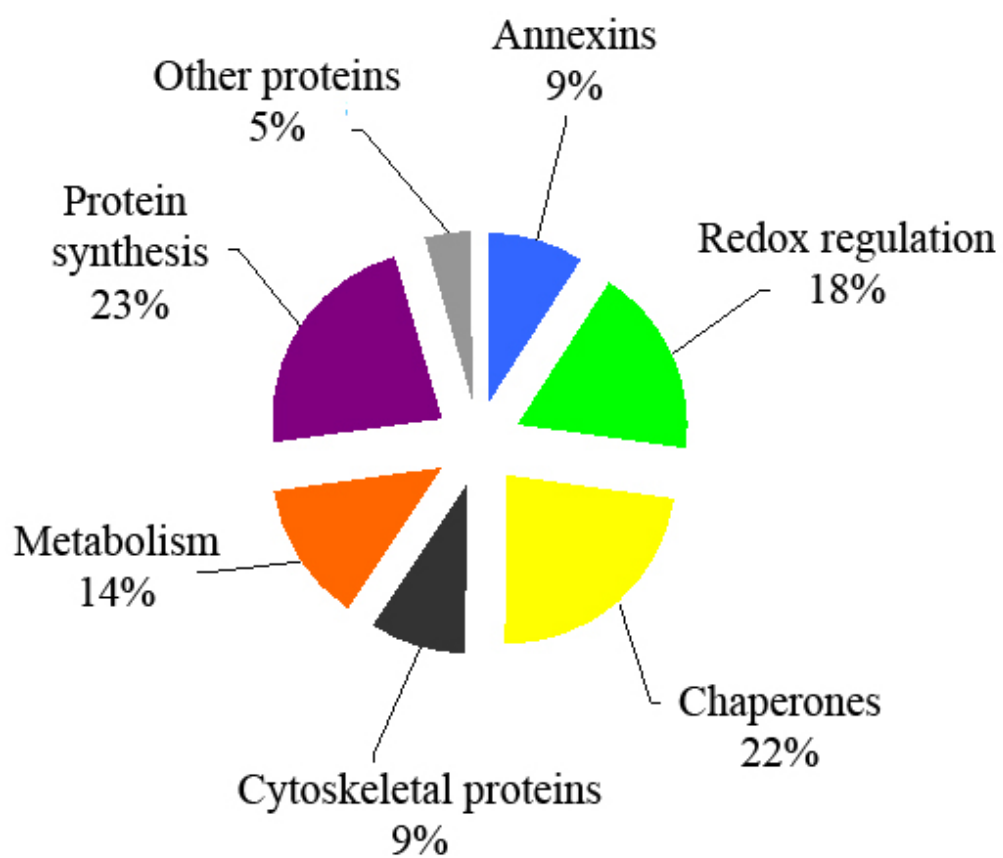


Figure 18. Functional categories of the changed proteins in Hcy-treated cells.

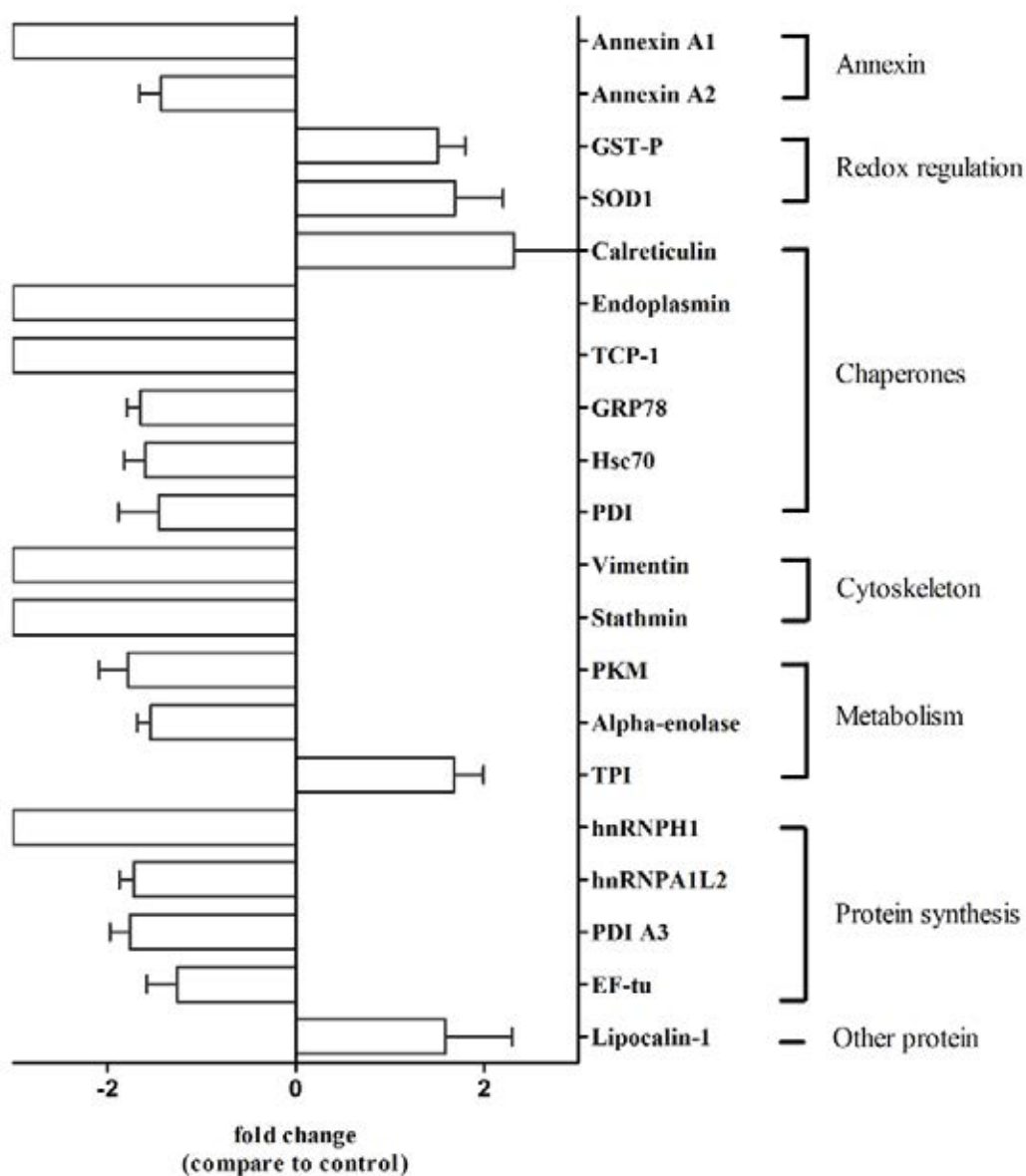


Figure 19. Relative spot intensities of identified proteins from Hcy-treated cells compared to control group (untreated).

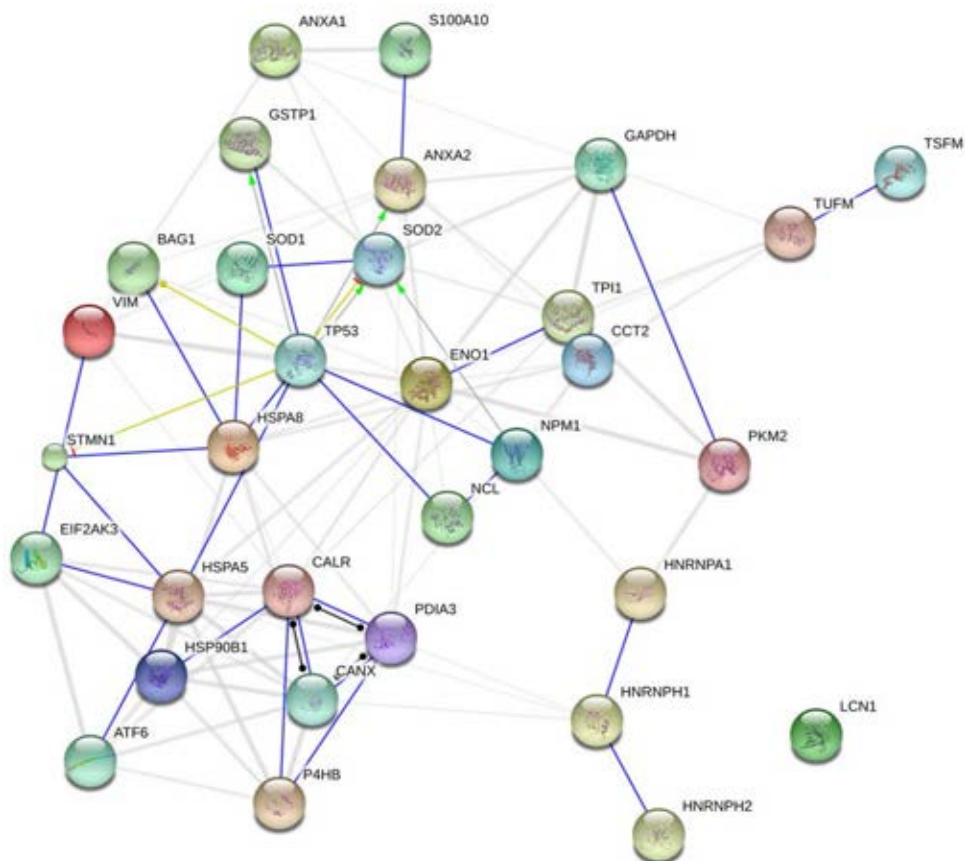


Figure 20. Network analysis of identified proteins from Hey-treated cells using STRING.

KOBAS analysis implicated that the altered proteins significantly involved in protein processing in ER, antigen presentation, aurora B signaling, glycolysis/gluconeogenesis, HIF-1 α transcription network and apoptosis signaling pathway ($p < 0.05$) (Table 5). However, due to small number of data obtained from 2-DE, the number of samples, which could be merged together into the same cellular pathways, was also less (Table 5). From our results, only one or two proteins could be merged into each pathway which consisting of a large number of molecules, resulting in low percent coverage in each pathway.

Our finding was in accordance with a previous study, revealing that many chaperone proteins such as endoplasmin and TCP-1 were down-regulated, while some redox regulation protein such as GST-P was up-regulated in Hcy-treated cells (Fuchs *et al.*, 2005). One of Hcy toxicities was induction of ER stress (Outinen *et al.*, 1999; Belal *et al.*, 2011). Disruption of protein folding in the ER resulted in accumulation of misfolded proteins. Endoplasmin, which had a protective role from ER stress and up-regulated in NVK-treated group, was down-regulated in Hcy-treated cells when compared to control (Figure 19). GRP78, also considered as protective protein in response to ER stress (Reddy *et al.*, 1999), was down-regulated in Hcy-treated group. Other proteins involving in unfold protein response were PDI and calreticulin. Calreticulin, a molecular calcium binding chaperone, played role in quality control of protein folding in ER via calreticulin/calnexin cycle (Nauseef *et al.*, 1995). The up-regulation of calreticulin in Hcy-treated cells might be due to the accumulation of misfolded proteins. ER stress in endothelial cells was considered as one of proatherogenic factors (Tabas, 2010) due to protein misfolding leading to endothelial dysfunction. One of the proteins involving in atherosclerosis was vimentin. Vimentin, a class-III intermediate filament, was attached to nucleus, ER and mitochondria (Challa, and Stefanovic, 2011). Vimentin also regulated proteins involving in cell adhesion, migration and stress-mediated cell signaling associated with atherosclerosis (Samanta *et al.*, 2012). Many studies revealed that Hcy induced the change in vimentin expression (Fuchs *et al.*, 2005; Lee *et al.*, 2007; Hung *et al.*, 2010), suggesting that Hcy exhibited a pro-apoptotic activity due to the altered expression of cytoskeleton proteins, which were known to be cleaved in initiation step of apoptosis (Zhang *et al.*, 2006).

Table 5. KOBAS analysis of differentially expressed proteins in Hcy-treated cells.

KOBAS pathway	Database	No. of sample	Background proteins	% coverage in pathway	<i>p</i> -value
Protein processing in endoplasmic reticulum	KEGG	6	166	3.61	0.001
Antigen processing and presentation	KEGG	4	76	5.26	0.005
Aurora B signaling	PID Curated	3	39	7.69	0.007
glycolysis I	BioCyc	3	22	13.64	0.014
HIF-1-alpha transcription factor network	PID Curated	3	65	4.62	0.016
Glycolysis / Gluconeogenesis	KEGG	3	65	4.62	0.019
Apoptosis signaling pathway	PANTHER	2	107	1.87	0.047

PID: Pathway Interaction Database (<http://pid.nci.nih.gov/>)

BioCyc (<http://biocyc.org/>)

PANTHER: Protein analysis through evolutionary relationships (<http://www.pantherdb.org/>)

KEGG: Kyoto Encyclopedia of Genes and Genomes (www.genome.jp/kegg/)

Our previous result showed that treatment of Hcy increased intracellular ROS in the cells (Figure 10) without affecting cell viability. However, proteomic profiles of Hcy-treated cells revealed that several proteins were regulated in response to cellular damage and pre-apoptosis due to Hcy treatment.

Proteomic profile of NVK in Hcy-treated cells

To investigate the action of NVK on Hcy-induced cellular stress, the proteins were separated and compared between Hcy-treated cells in the absence and presence of NVK. The results showed that approximately 331 and 328 protein spots were detected from gels of Hcy-treated control group and NVK-pretreated group, respectively. Total eight spots of protein significantly changed (Figure 21) which 4 spots were up-regulated and 4 spots were down-regulated. The down-regulated proteins were hnRNPH1, PDIA3, GRP78 and EF-Tu (Figure 22). The up-regulated proteins were annexin A2, stathmin, hnRNPA1L2 and Hsc70.

The result showed that only eight spots of proteins were changed when pre-treatment with NVK. This might be due to Hcy exposure which altered most of proteins in response to cellular damage (Table 6). Therefore, NVK prevented down-regulation of some proteins responsible for cellular protection.

Pathway analysis of identified proteins from NVK-treated cells under Hcy treatment

The list of 8 proteins was uploaded onto STRING and KOBAS. The network analysis using STRING showed the protein-protein interactions. The results showed that protein expression was related to oxidative stress, anti-apoptosis, cytoskeleton and chaperones (Figure 23).

The up-regulation of Hsc70 could prevent protein misfolding from ER stress which is induced by Hcy. This suggested the protective role of pre-treatment of NVK in Hcy-treated endothelial cells. Interestingly, NVK was able to restore in case of 4 proteins altered by Hcy-treatment. Annexin A2, which was down-regulated in Hcy-treated cells, increased by NVK pre-treatment. This finding was in contrast with the 2-DE result in NVK-treated group, which annexin A2 was also down-regulated. In

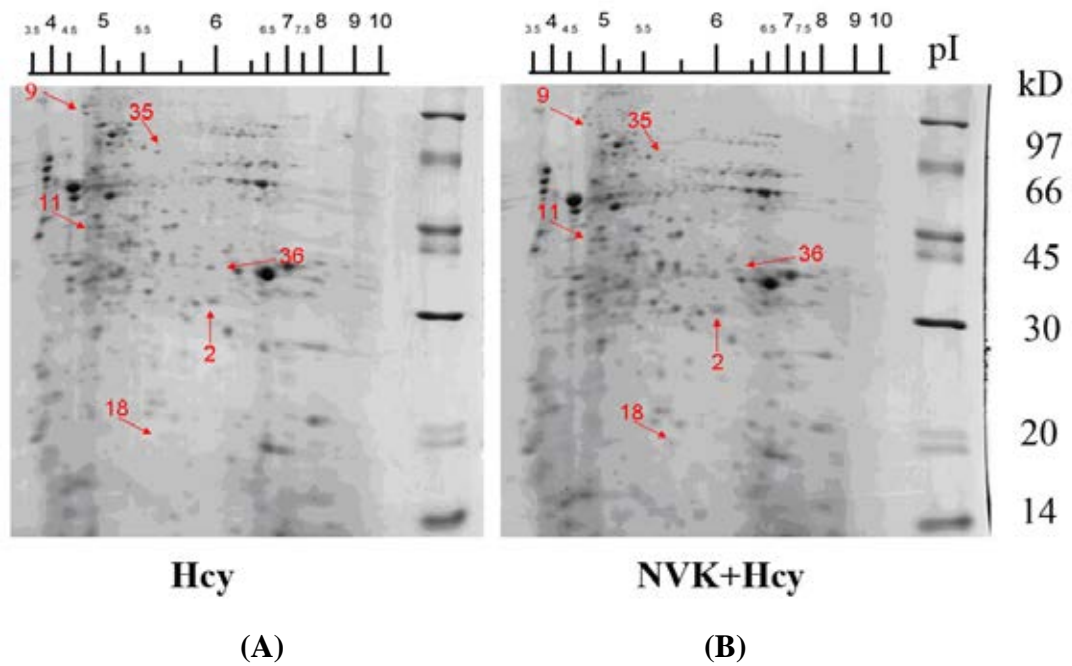


Figure 21. Representative 2-DE gels of proteins from the cells exposed to NVK before exposure to Hcy. Proteins (150 μ g) were separated on non-linear IPG strips pH 3 - 10 NL for the first dimension and 12.5% SDS-PAGE for the second dimension of separation. Coomassie blue stained gels of proteins from (A) cell treated with Hcy (0.05 mM) for 12 h (B) cells treated with NVK (0.05 mg/mL) followed by Hcy (0.05 mM) for 12 h. The proteins spots numbered were excised, subjected to tryptic digestion and identified using LC/MS/MS analysis. Similar results were obtained in 3 independent experiments.

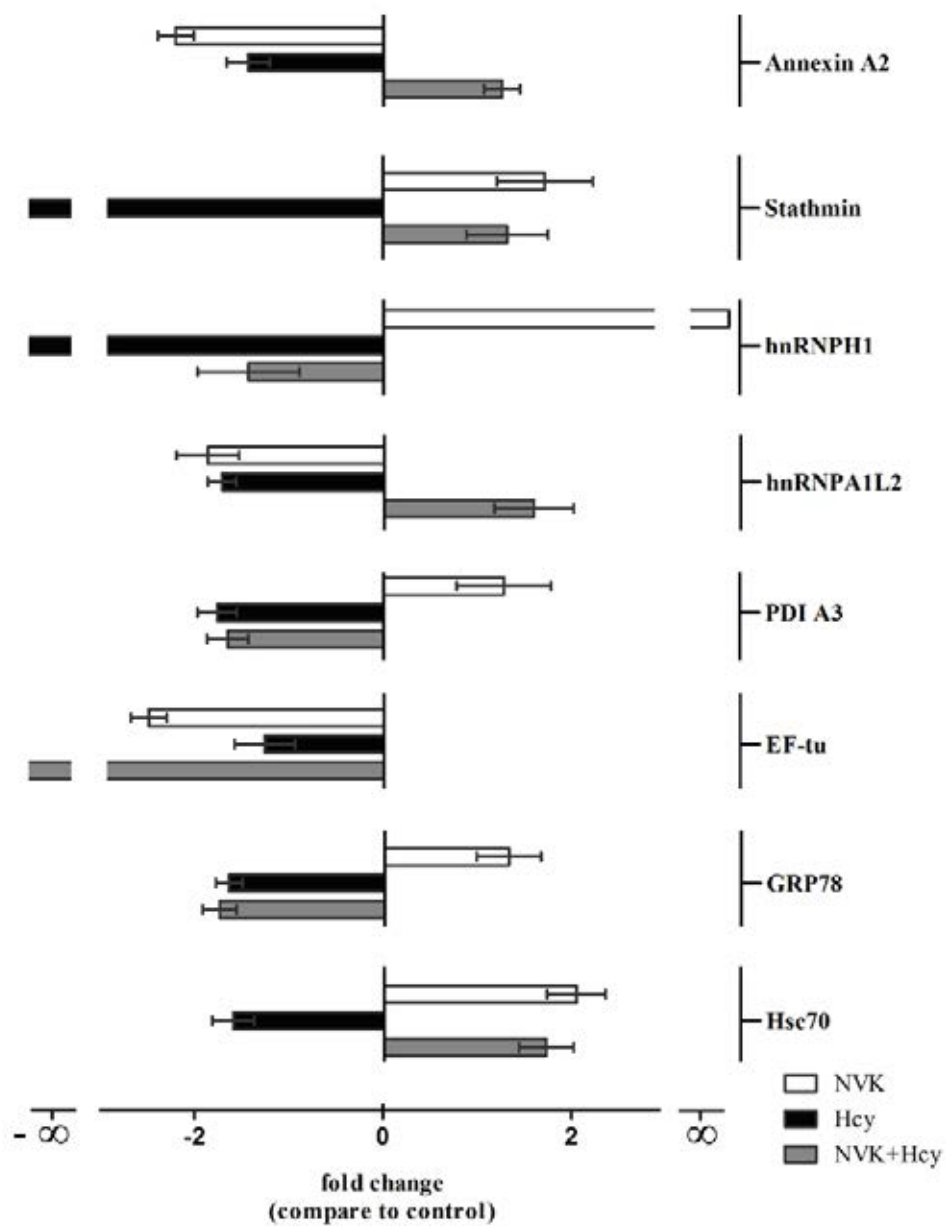


Figure 22. Relative spot intensities of same proteins in NVK pretreatment followed by Hcy group compared to either NVK or Hcy groups.

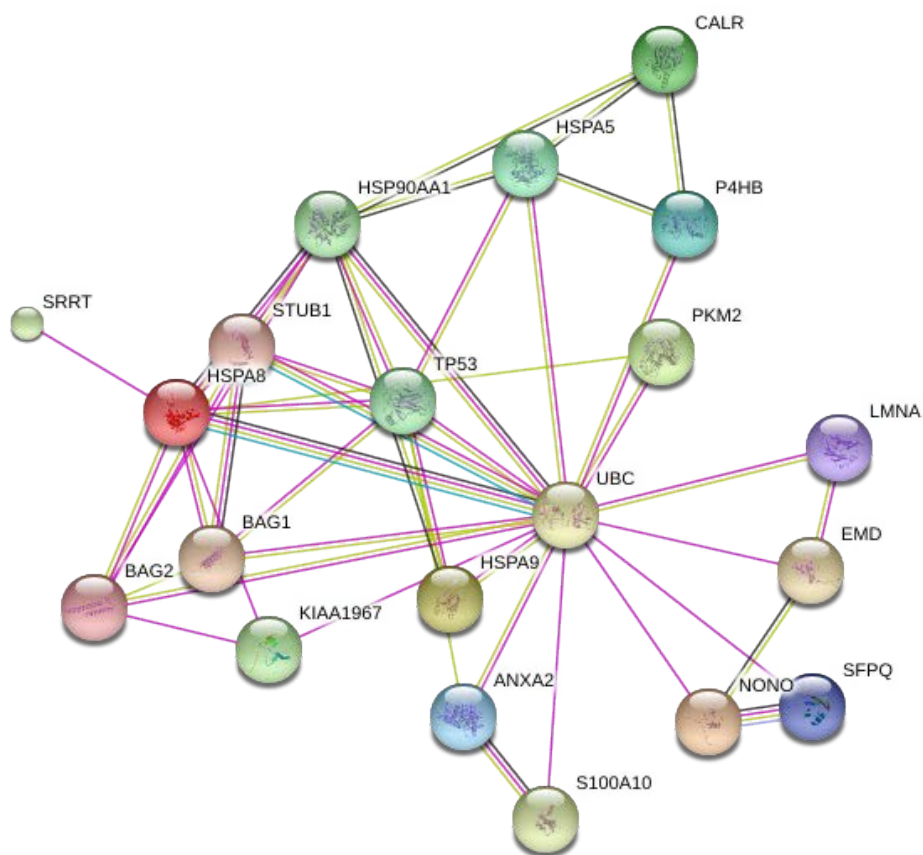


Figure 23. Network analysis of identified proteins from cells exposed to NVK before exposure to Hcy using STRING.

Table 6. Summary of changed proteins which affected by treatment of NVK, Hcy and NVK+Hcy.

Spot No.	Protein identity	UniProt No.	NVK/control	Hcy/control	NVK+ Hcy/Hcy
Annexins					
1	Annexin A1	P04083	-2.81	only in control	‡
2	Annexin A2	P07355	-2.20	-1.43	+1.26
Redox regulation					
3	Glutathione <i>S</i> -transferase P	P09211	+1.95	+1.51	‡
4	Superoxide dismutase [Cu-Zn]	P00441	+1.82	+1.69	+1.31
Chaperones					
5	Calreticulin	P27797	‡	+2.32	‡
6	Calreticulin	P27798	‡	+1.92	‡
7	Endoplasmin	P14625	+1.89	only in control	‡
8	T-complex protein 1	P78371	+1.87	only in control	‡
9	78 kDa glucose-regulated protein	P11021	‡	-1.65	-1.72
10	Heat shock cognate 71 kD	P11142	+ 2.04	-1.6	‡
11	Heat shock cognate 71 kD	P11142	‡	+1.53	-1.32
12	Heat shock cognate 71 kD	P11142	‡	-1.64	+1.72
Cytoskeletal proteins					
13	Vimentin	P08670	+6.25	pattern change	‡

Table 6. (continued)

Spot No.	Protein identity	UniProt No.	fold change		
			NVK/control	Hcy/control	NVK+ Hcy/Hcy
14	Vimentin	P08670	+2.16	pattern change	‡
15	β-Tubulin	P04350	+2.65	‡	‡
16	Vimentin	P08670	+2.49	pattern change	‡
17	β-Actin	P60709	+2.64	‡	‡
18	Stathmin	P16949	+1.72	only in control	+1.32
19	Prelamin-A/C	P02545	-1.69	‡	‡
Metabolism					
20	Pyruvate kinase isozymes M1/M2	P14618	‡	-1.78	‡
21	α-enolase	P06733	-1.75	‡	‡
22	α-enolase	P06733	-2.09	‡	‡
23	Pyruvate kinase isozymes M1/M2	P14618	+2.62	‡	‡
24	α-enolase	P06733	-1.87	-.154	‡
25	Triosephosphate isomerase	P60174	+1.90	+1.68	‡
Protein synthesis					
26	Heterogeneous nuclear ribonucleoprotein H	P31943	+3.02	only in control	‡

Table 6. (continued)

Spot No.	Protein identity	UniProt No.	fold change		
			NVK/control	Hcy/control	NVK+ Hcy/Hcy
27	Non-POU -binding protein	Q15233	‡	+1.71	‡
28	Splicing factor, proline- and glutamine-rich	P23246	-2.47	‡	‡
29	Heterogeneous nuclear ribonucleoprotein H	P31943	-1.78	‡	-1.43
30	Heterogeneous nuclear ribonucleoproteins A2/B1	P22626	-1.95	‡	‡
31	Heterogeneous nuclear ribonucleoprotein A1-like 2	Q32P51	-1.87	-1.72	+1.59
32	Protein disulfide-isomerase	P07237	+1.89	‡	‡
33	Nucleophosmin	P06748	only in treated	‡	‡
34	Protein disulfide-isomerase	P07237	‡	-1.45	‡
35	Protein disulfide-isomerase A3	P30101	‡	-1.76	-1.65
36	Elongation factor Tu,	P49411	-2.49	-1.26	only in Hcy
Other proteins					
37	Lipocalin-1	P31025	+2.01	+1.59	‡

UniProt: Universal Protein Resource (<http://www.uniprot.org/>)

‡ indicated no significant difference between compared groups.

normal condition, the generation of fibrin clot was in low level, down-regulated annexin A2 might have indistinctly effect. But in high Hcy level in plasma, endothelial cells were prone to be damaged and fibrin clots were more generated in wound healing process (Clark, 2001). Since annexin A2 was known to promote fibrinolytic activity, the excessive thrombosis might be lower in NVK-pretreated group, resulting in reduction of the circulatory disorder risk.

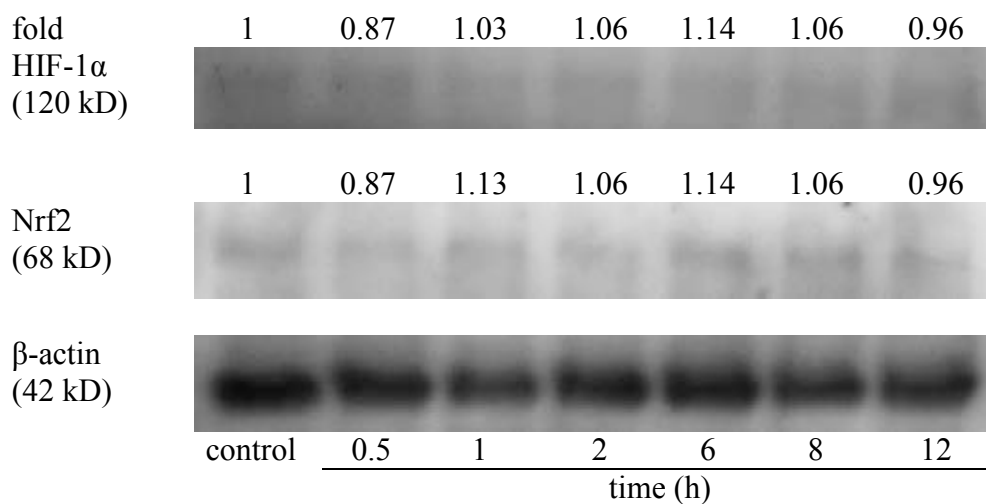
Immunoblot analysis of protein expression

The result from pathway analysis revealed that the altered proteins such as including antioxidant enzymes could be regulated by HIF-1 α and Nrf2. To confirm the protein expression changed by NVK in 2-DE and pathway analysis, immunoblot analysis of HIF-1 α , Nrf2 HO-1, SOD, GPx and CAT was then performed. The result showed that very low expression level of HIF-1 α was found in both control and NVK-treated group, while NVK (0.05 mg/mL) did not alter the expression level of HIF-1 α in time-dependent manner (Figure 24).

HIF-1 α in response to stimuli rapidly occurred by translocation from cytosol into nucleus. While it rapidly degraded in normoxic condition (Kallio *et al.*, 1998). Therefore, HIF-1 α in whole cell lysate could be not clearly detected at the tested condition. Nrf2 has been reported to be a highly unstable protein, which rapidly degraded by ubiquitin-dependent pathway (half-life \approx 15 min) (Nguyen *et al.*, 2003). In response to oxidative stress, Nrf2 was stabilized and translocated into nucleus. Therefore, the low level of Nrf2 was found in normal condition and was barely detected in whole cell lysate which might due to invalid method.

Although HIF-1 α and Nrf2 were failed to detect the expression change due to method invalidation, the expression of HO-1 significantly altered (Figure 25). Treatment of NVK at the concentrations to lower ROS level (0.05 and 0.2 mg/mL) (Figure 11) significantly up-regulated the expression of HO-1 in a concentration-dependent manner (Figure 25). Since Hcy could increase oxidative stress in the cells, the expression of antioxidant enzymes such as SOD1, GPx1 and CAT, which were reported to be regulated by Nrf2, was also determined. The result showed that SOD1 significantly decreased under NVK (0.2 mg/mL) treatment (Figure 26). Meanwhile,

(A)



(B)

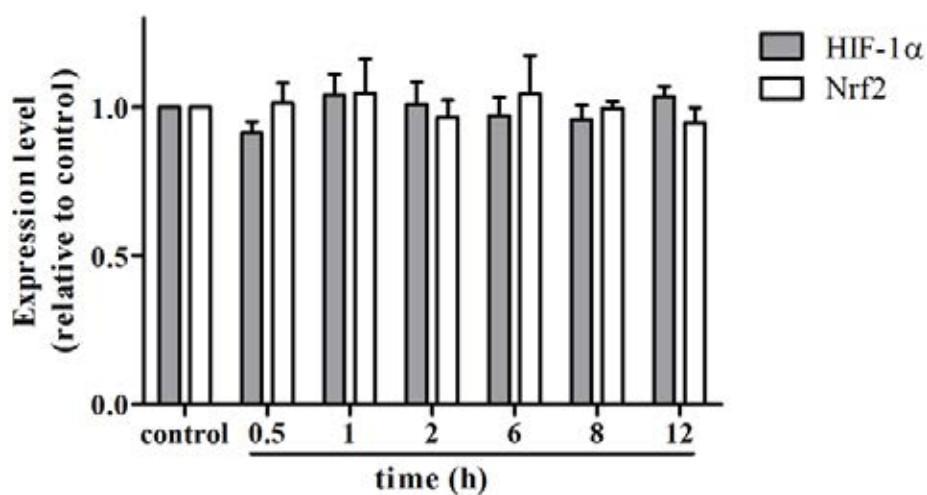
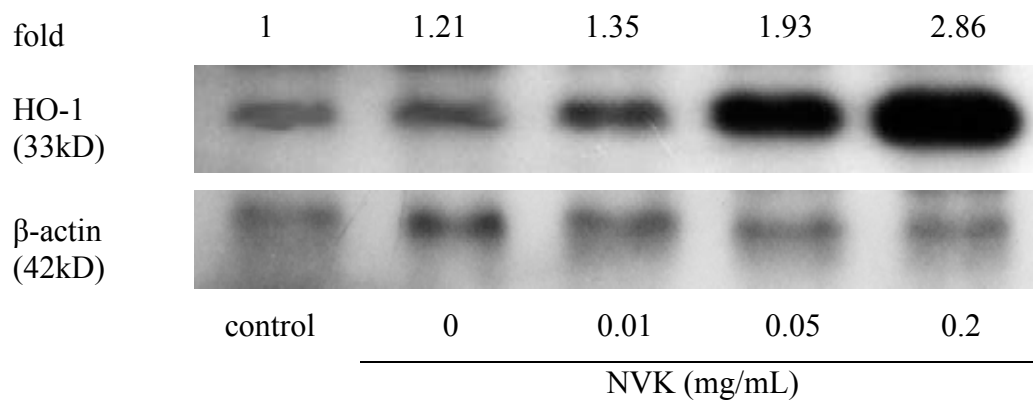


Figure 24. Time-dependent study of HIF-1 α and Nrf2 induction by NVK treatment. The cells were incubated with NVK (0.05 mg/mL) for 0.5, 1, 2, 6, 8 and 12 h. (A) Representative immunoblots of HIF-1 α at indicated times. (B) Densitometric analysis of immunoblot of HIF-1 α using ImageJ software. The histograms represented mean values \pm S.E.M. of at least three different experiments. Similar results were obtained in at least three independent experiments.

(A)



(B)

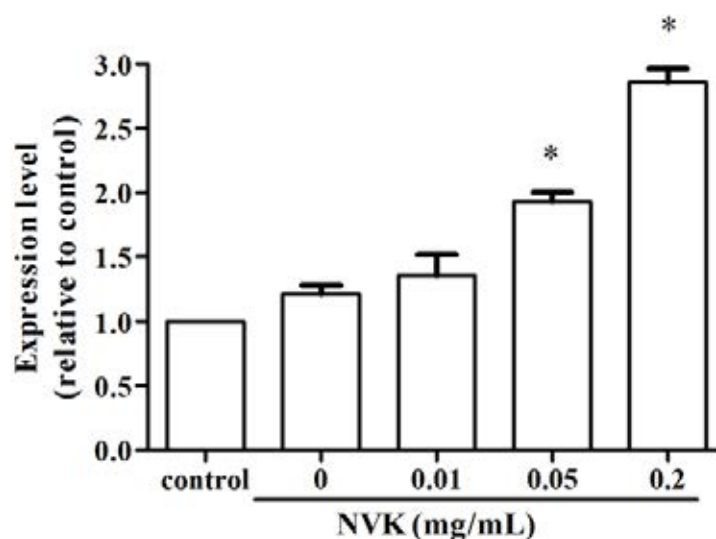
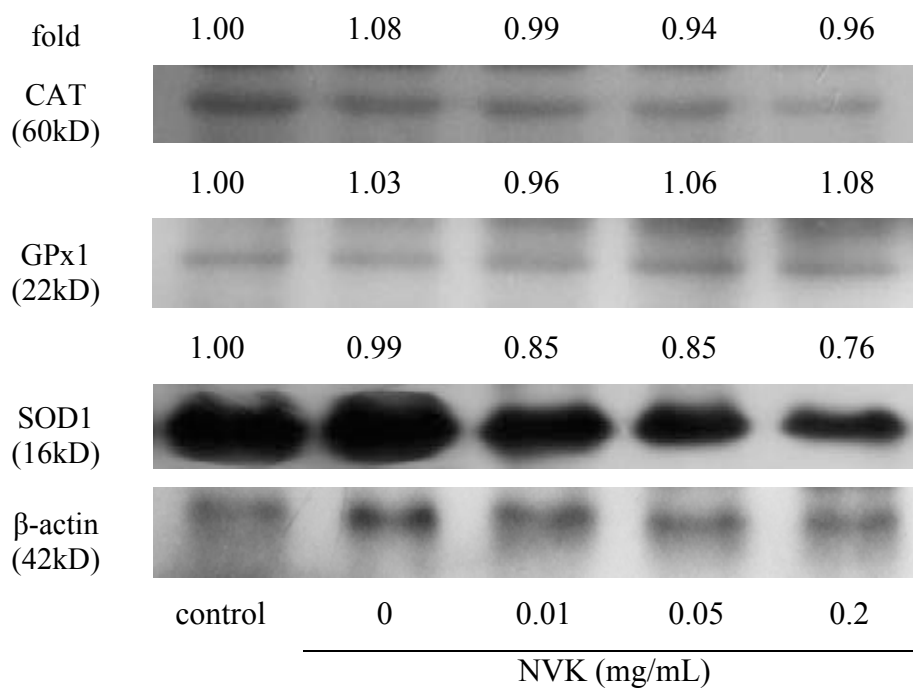


Figure 25. Concentration-dependent study of HO-1 expression by NVK treatment. The cells were incubated with NVK at the concentration of 0.01, 0.05 and 0.2 mg.mL for 12 h. (A) Representative immunoblots of HO-1. (B) Densitometric analysis of immunoblot of HO-1 using ImageJ software. The histograms represented mean \pm S.E.M. of at least three different experiments. Similar results were obtained in at least three independent experiments. * indicates the significant difference when compared to control group ($p < 0.05$).

(A)



(B)

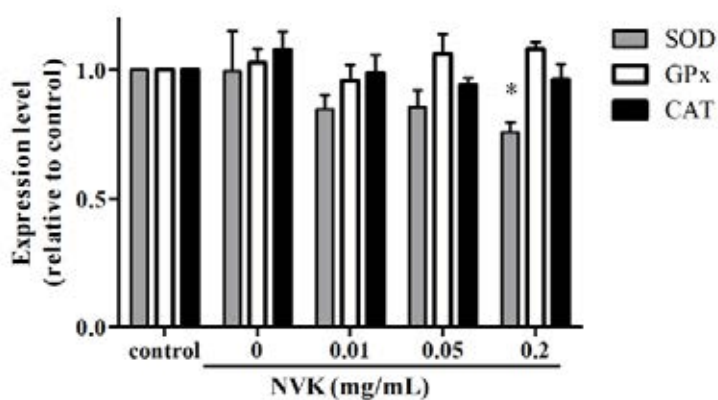


Figure 26. Concentration-dependent study of antioxidant enzyme expression by NVK treatment. The cells were incubated with NVK at the concentration of 0.01, 0.05 and 0.2 mg/mL for 12 h. (A) Representative immunoblots of SOD1, GPx and CAT. (B) Densitometric analysis of immunoblot of SOD1, GPx and CAT using ImageJ software. The histograms represented mean \pm S.E.M. of at least three different experiments. Similar results were obtained in at least three independent experiments. * indicates the significant difference when compared to control group ($p < 0.05$).

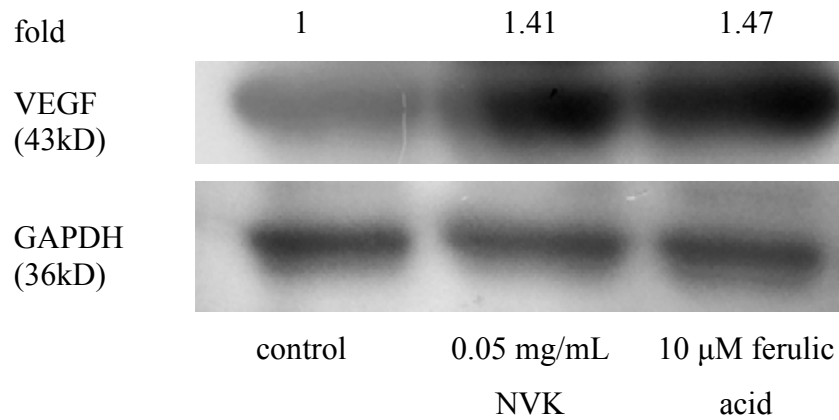
no significant alteration of GPx1 and CAT expression was observed. Therefore, protective effect of NVK might be mainly due to up-regulation of HO-1.

Previous studies reported the protective roles of HO-1 in atherosclerosis development due to its abilities to degrade the pro-oxidative heme, to biliverdin and bilirubin, both of which have antioxidant activities against oxidative stress (Morita *et al.*, 2005). VEGF regulated by HIF-1 α was the proteins responsible for endothelial cell growth, cell migration, and inhibition of apoptosis (Murphy *et al.*, 2001). Previous study reported that 10 μ M ferulic acid significantly increased mRNA expression of VEGF in HUVEC cells (Lin *et al.*, 2010). Therefore, ferulic acid, an active substance in AS and AP, was used as a positive control. The result showed that treatment of NVK (0.05 mg/mL) for 12 h also significantly increased the expression of VEGF (Figure 27).

The up-regulated VEGF was further secreted from endothelial cells and bound to the VEGF receptor on the endothelial cells, which called autocrine (Lee *et al.*, 2007). Once VEGF bound to VEGF receptor and triggered the intracellular signaling pathway through various pathways such as MEK/ERK pathway for cell proliferation and migration (Neufeld *et al.*, 1999) and PI3K/Akt pathway for cell survival and NO production (Gerber *et al.*, 1998).

The synthesis of NO, the essential mediator (Tai *et al.*, 2004), can be triggered by the activation of Akt in endothelial cells (Dimmeler *et al.*, 1999) which phosphorylates eNOS, resulting in the production of NO from L-arginine. Therefore, the effect of NVK on phosphorylation of Akt and eNOS was investigated. NVK (0.05 mg/mL) significantly increased eNOS phosphorylation in 45 min without activation of Akt (Figure 28). The result suggested that NVK increased phosphorylation of eNOS but not Akt. Akt-independent phosphorylation of eNOS was induced by quercetin (Li *et al.*, 2012). Increase of eNOS phosphorylation by NVK might result in an increase of NO, suggesting the vasoprotection in the treatment of circulatory disorder.

(A)



(B)

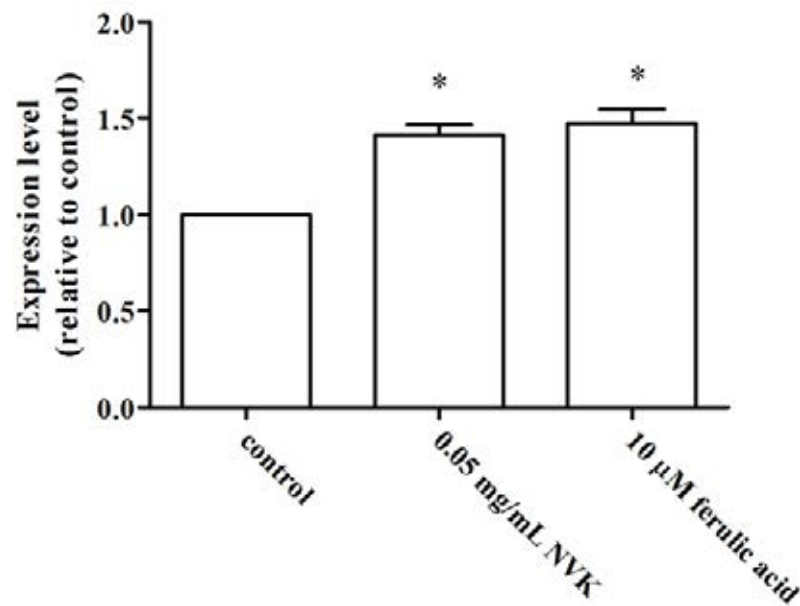
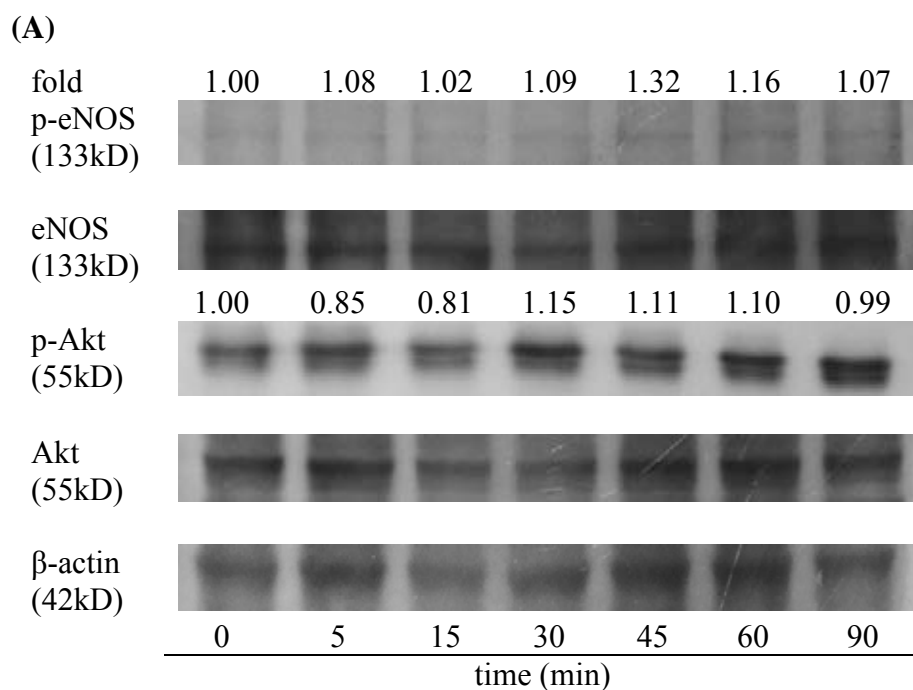


Figure 27. VEGF expression affected by NVK. Cells were incubated with NVK (0.05 mg/mL) or ferulic acid (10 μM) for 12 h. (A) Representative immunoblots of VEGF. (B) Densitometric analysis of immunoblot of VEGF using ImageJ software. Ferulic acid (10 μM) was used as a positive control. The histograms represented mean \pm S.E.M. of at least three different experiments. Similar results were obtained in at least three independent experiments. * indicates the significant difference when compared to control group ($p < 0.05$).



(B)

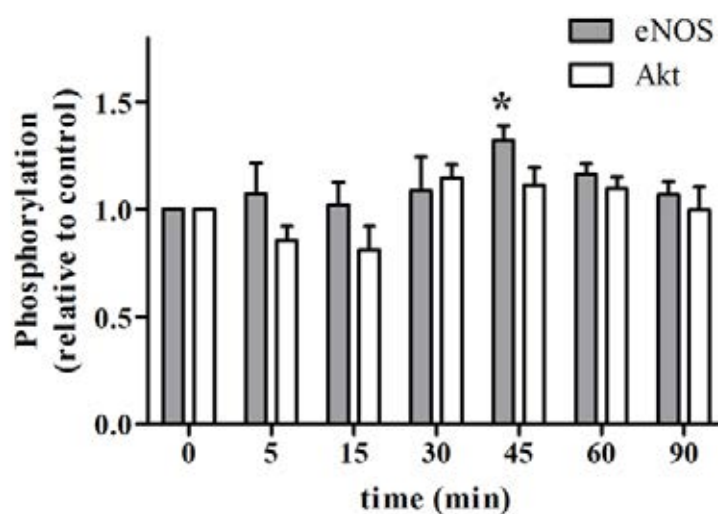


Figure 28. Time-dependent study on phosphorylation of eNOS and Akt by NVK treatment. The cells were incubated with NVK (0.05 mg/mL) for 5, 15, 30, 45, 60 and 90 min. (A) Representative immunoblots of p-eNOS/eNOS and p-Akt/Akt. (B) Densitometric analysis of immunoblot of p-eNOS/eNOS and p-Akt/Akt using ImageJ software. The histograms represented mean \pm S.E.M. of at least four different experiments. Similar results were obtained in at least three independent experiments. * indicates the significant difference when compared to control group ($p < 0.05$).

CHAPTER V

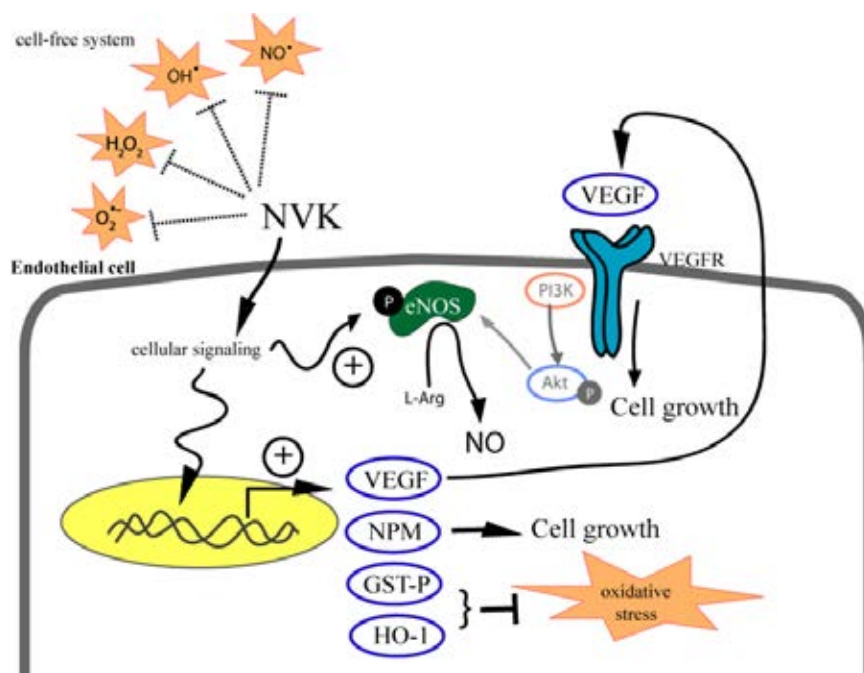
CONCLUSION

According to the traditional use of NVK, a polyherbal combination for the treatment of circulatory disorder, NVK was hypothesized to exhibit the protective role against Hcy-induced oxidative stress in endothelial cells. The ethanolic extract exhibited the potent scavenging activities against $O_2^{\bullet-}$, H_2O_2 , OH^{\bullet} and NO^{\bullet} in cell-free system (EC_{50} 26.99 – 132.32 $\mu\text{g/mL}$) which was more potent than the water extract (EC_{50} 40.42 - 248.52 $\mu\text{g/mL}$). Interestingly, the ethanolic extract exhibited the synergistic antioxidant effects in all tested ROS and RNS based on the analysis of combination index. In cell-based assay, EA.hy926 cells were used as a model for endothelial cell study.

In the absence of Hcy, an oxidative stressor, treatment with NVK (0.05 mg/mL) for 12 h did not affect both cell viability and intracellular ROS. Proteomic analysis using 2-DE and immunoblotting revealed that cytoprotective proteins such as GST-P, HO-1 and NPM were up-regulated by NVK (Figure 29A). GST-P and HO-1 played roles in oxidative homeostasis while NPM and VEGF involved in cell proliferation. Binding of VEGF to VEGF receptor also triggered phosphorylation of eNOS, resulting in an increase in NO production, which was essential for endothelial function.

Meanwhile, treatment with Hcy increased intracellular ROS (Figure 29B). The proteins involved in cytoprotection such as Hsc70 was down-regulated by Hcy treatment, resulting in ER stress. Moreover, Hcy down-regulated expression of annexin A2, leading to decrease in fibrinolytic activity which was considered as proatherogenic factor. Pre-treatment of NVK (0.05 mg/mL) for 12 h attenuated intracellular ROS in Hcy-treated cells. NVK restored the expression level of Hsc70 which prevented cellular damage from Hcy-induced ER stress. The restoration of

(A)



(B)

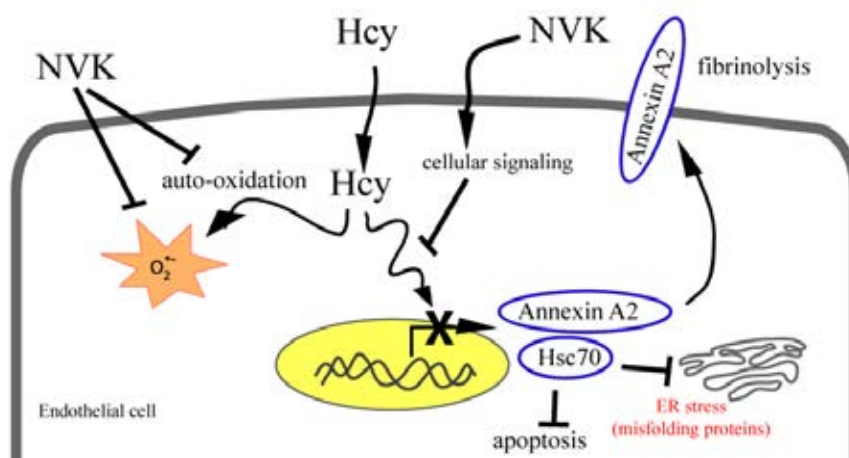


Figure 29. Possible mechanism of NVK in the (A) absence and (B) presence of Hcy in endothelial cells.

annexin A2 level by NVK suggested the promotion of fibrinolytic activity in Hcy-treated cells, resulting in reduction of circulatory disorder risk from thrombosis.

In summary, NVK, which possessed the potent *in vitro* antioxidant activities against $O_2^{\bullet-}$, H_2O_2 , OH^{\bullet} and NO^{\bullet} , attenuated intracellular ROS induced by Hcy. NVK prevented oxidative stress-induced endothelial dysfunction by up-regulation of GST-P, HO-1 and VEGF in normal condition, and Hsc70 and annexin A2 in Hcy-treated cells. Moreover, NVK prevented endothelial dysfunction by increase in phosphorylation of eNOS. Our finding might support the traditional use of Phikud Navakot, a polyherbal formula, in treatment of circulatory disorder.

REFERENCES

- Aguilar, B., Rojas, J. C., and Collados, M. T. 2004. Metabolism of homocysteine and its relationship with cardiovascular disease. Journal of Thrombosis and Thrombolysis 18 (2) : 75-87.
- Arya, A., Looi, C., Y., Wong, W. F., Noordin, M. I., Nyamathulla, S., Mustafa, M. R., and Ali Mohd, M. 2013. *In vitro* antioxidant, PTP-1B inhibitory effects and *in vivo* hypoglycemic potential of selected medicinal plants. International Journal of Pharmacology 9 (1) : 50-57.
- Austin, R. C., Sood, S. K., Dorward, A. M., Singh, G., Shaughnessy, S. G., Pamidi, S., Outinen, P. A., and Weitz, J. I. 1998. Homocysteine-dependent alterations in mitochondrial gene expression, function and structure. Journal of Biological Chemistry 273 (46) : 30808-30817.
- Bando, Y., Katayama, T., Aleshin, A. N., Manabe, T., and Tohyama, M. 2004. GRP94 reduces cell death in SH-SY5Y cells perturbed calcium homeostasis. Apoptosis 9 (4) : 501-508.
- Baranska, P., Jerczynska, H., Pawlowska, Z., Koziolkewicz, W., and Cierniewski, C. S. 2005. Expression of integrins and adhesive properties of human endothelial cell line EA.hy926. Cancer Genomics & Proteomics 2 (5) : 265-269.
- Bao, X. M., Wu, C. F., and Lu, G. P. 2009. Atorvastatin attenuates homocysteine-induced apoptosis in human umbilical vein endothelial cells via inhibiting NADPH oxidase-related oxidative stress-triggered p38MAPK signaling. Acta Pharmacologica Sinica 30 (10) : 1392-1398.
- Bautista, L. E., Arenas, I. A., Penuela, A., and Martinez, L. X. 2002. Total plasma homocysteine level and risk of cardiovascular disease: a meta-analysis of prospective cohort studies. Journal of Clinical Epidemiology 55 (9) : 882-887.
- Behrendt, D., and Ganz, P. 2002. Endothelial function. From vascular biology to clinical applications. American Journal of Cardiology 90 (10) : 40-48.
- Bouis, D., Hospers, G., Meijer, C., Molema, G., and Mulder, N. 2001. Endothelium *in vitro*: A review of human vascular endothelial cell lines for blood vessel-related research. Angiogenesis 4 (2) : 91-102.

- Brandes, R. P., Kim, D. Y., Schmitz-Winnenthal, F. H., Amidi, M., Godecke, A., Mulsch, A., and Busse, R. 2000. Increased nitrovasodilator sensitivity in endothelial nitric oxide synthase knockout mice: Role of soluble guanylyl cyclase. Hypertension 35 (1) : 231-236.
- Brix, B., Mesters, J. R., Pellerin, L., and Jöhren, O. 2012. Endothelial cell-derived nitric oxide enhances aerobic glycolysis in astrocytes via HIF-1 α -mediated target gene activation. Journal of Neuroscience 32 (28) : 9727-9735.
- Bureau of Policy and Strategy. 2011. Statistical Thailand. Thailand's Ministry of Public Health. Nontaburi: 2011 : 29-30.
- Butkhup, L., and Samappito, S. 2011. *In vitro* free radical scavenging and antimicrobial activity of some selected Thai medicinal plants. Research Journal of Medicinal Plant 5 (3) : 254-265.
- Cai, H. 2005. Hydrogen peroxide regulation of endothelial function: origins, mechanisms, and consequences. Cardiovascular Research 68 (1) : 26-36.
- Cai, Y., Luo, Q., Sun, M., and Corke, H. 2004. Antioxidant activity and phenolic compounds of 112 traditional Chinese medicinal plants associated with anticancer. Life Sciences 74 (17) : 2157-2184.
- Carmichael, J., DeGraff, W. G., Gazdar, A. F., Minna, J. D., and Mitchell, J. B. 1987. Evaluation of a tetrazolium-based semiautomated colorimetric assay: Assessment of chemosensitivity testing. Cancer Research 47 (4) : 936-942.
- Chander, R., Kapoor, N. K., and Dhawan, B. N. 1992. Picroliv, picroside-I and kutkoside from *Picrorhiza kurroa* are scavengers of superoxide anions. Biochemical Pharmacology 44 (1) : 180-183.
- Chang, C. L., and Lin, C. S. 2012. Phytochemical composition, antioxidant activity, and neuroprotective effect of *Terminalia chebula* Retzius extracts. Evidence-Based Complementary and Alternative Medicine 125247 : 1-7.
- Chang, K. M., Choi, S. I., and Kim, G. H. 2012. Anti-oxidant activity of *Saussurea lappa* C.B. Clarke roots. Preventive Nutrition and Food Science 17 (4) : 306-309.
- Chang, T. M., Shi, G. Y., Wu, H. L., Wu, C. H., Su, Y. D., Wang, H. L., Wen, H. Y., and Huang, H. C. 2011. Effects of salvianolic acid B on protein expression in

- human umbilical vein endothelial cells. Evidence-Based Complementary and Alternative Medicine 213050 :1-9.
- Chauhan, S., Nath, N., and Tule, V. 2008. Antidiabetic and antioxidant effects of *Picrorhiza kurrooa* rhizome extracts in diabetic rats. Indian Journal of Clinical Biochemistry 23 (3) : 238-242.
- Chen, Q., Li, P., Yang, H., Li, X., Zhu, J., and Chen, F. 2009. Identification of volatile compounds of *Atractylode lancea* rhizoma using supercritical fluid extraction and GC-MS. Journal of Separation Science 32 (18) : 3152-3156.
- Cheng, H. Y., Lin, T. C., Yu, K. H., Yang, C. M., and Lin, C. C. 2003. Antioxidant and free radical scavenging activities of *Terminalia chebula*. Biological & Pharmaceutical Bulletin 26 (9) : 1331-1335.
- Chilov, D., Camenisch, G., Kvietikova, I., Ziegler, U., Gassmann, M., and Wenger, R. H. 1999. Induction and nuclear translocation of hypoxia-inducible factor-1 (HIF-1): heterodimerization with ARNT is not necessary for nuclear accumulation of HIF-1alpha. Journal of Cell Science 112 (8) : 1203-1212.
- Choi, E. H., Chang, H. J., Cho, J. Y., and Chun, H. S. 2007. Cytoprotective effect of anthocyanins against doxorubicin-induced toxicity in H9c2 cardiomyocytes in relation to their antioxidant activities. Food and Chemical Toxicology 45 (10) : 1873-1881.
- Choi, H. G., Lee, D. S., Li, B., Choi, Y. H., Lee, S. H., and Kim, Y. C. 2012. Santamarin, a sesquiterpene lactone isolated from *Saussurea lappa*, represses LPS-induced inflammatory responses *via* expression of heme oxygenase-1 in murine macrophage cells. International Immunopharmacology 13 (3) : 271-279.
- Chou, T. C. 2006. Theoretical basis, experimental design, and computerized simulation of synergism and antagonism in drug combination studies. Pharmacological Reviews 58 (3) : 621-681.
- Comera, C., and Russo-Marie, F. 1995. Glucocorticoid-induced annexin 1 secretion by monocytes and peritoneal leukocytes. British Journal of Pharmacology 115 (6) : 1043-1047.
- Conn, K. J., Gao, W., McKee, A., Lan, M. S., Ullman, M. D., Eisenhauer, P. B., Fine, R. E., and Wells, J. M. 2004. Identification of the protein disulfide isomerase

- family member PDI in experimental Parkinson's disease and Lewy body pathology. Brain Research 1022 (1-2) : 164-172.
- Cumming, R. C., Andon, N. L., Haynes, P. A., Park, M., Fischer, W. H., and Schubert, D. 2004. Protein disulfide bond formation in the cytoplasm during oxidative stress. Journal of Biological Chemistry 279 (21) : 21749-21758.
- Dastoor, Z., and Dreyer, J. 2000. Nuclear translocation and aggregate formation of heat shock cognate protein 70 (Hsc70) in oxidative stress and apoptosis. Journal of Cell Science 113 (16) : 2845-2854.
- De Caterina, R., Libby, P., Peng, H. B., Thannickal, V. J., Rajavashisth, T. B., Gimbrone, M. A. Jr., Shin, W. S., and Liao, J. K. 1995. Nitric oxide decreases cytokine-induced endothelial activation. Nitric oxide selectively reduces endothelial expression of adhesion molecules and proinflammatory cytokines. Journal of Clinical Investigation 96 (1) : 60-68.
- Deora, A. B., Kreitzer, G., Jacovina, A. T., and Hajjar, K. A. 2004. An annexin 2 phosphorylation switch mediates p11-dependent translocation of annexin 2 to the cell surface. Journal of Biological Chemistry 279 (42) : 43411-43418.
- Dimmeler, S., Fleming, I., Fisslthaler, B., Hermann, C., Busse, R., and Zeiher, A. M. 1999. Activation of nitric oxide synthase in endothelial cells by Akt-dependent phosphorylation. Nature 399 (6736) : 601-605.
- Dhar, S. K., and St. Clair, D. K. 2009. Nucleophosmin blocks mitochondrial localization of p53 and apoptosis. Journal of Biological Chemistry 284 (24) : 16409-16418.
- Dhuna, K., Dhuna, V., Bhatia, G., Singh, J., and Kamboj, S. S. 2013. Cytoprotective effect of methanolic extract of *Nardostachys jatamansi* against hydrogen peroxide induced oxidative damage in C6 glioma cells. Acta Biochimica Polonica 60 (1) : 21-31.
- Domagala, T. B., Undas, A., Libura, M., and Szczeklik, A. 1998. Pathogenesis of vascular disease in hyperhomocysteinaemia. European Journal of Cardiovascular Prevention & Rehabilitation 5 (4) : 239-247.
- Dong, F., Zhang, X., Li, S. Y., Zhang, Z., Ren, Q., Culver, B., and Ren, J. 2005. Possible involvement of NADPH oxidase and JNK in homocysteine-induced

- oxidative stress and apoptosis in human umbilical vein endothelial cells. Cardiovascular Toxicology 5 (1) : 9-20.
- Dreger, H., Westphal, K., Weller, A., Baumann, G., Stangl, V., Meiners, S., and Stangl, K. 2009. Nrf2-dependent upregulation of antioxidative enzymes: a novel pathway for proteasome inhibitor-mediated cardioprotection. Cardiovascular Research 83 (2) : 354-361.
- Ebrahimzadeh, M. A., Nabavi, S. F., and Nabavi, S. M. 2009. Antioxidant activities of methanol extract of *Sambucus ebulus* L. flower. Pakistan Journal of Biological Sciences 12 (5) :447-450.
- Edgell, C. J., McDonald, C. C., and Graham, J. B. 1983. Permanent cell line expressing human factor VIII-related antigen established by hybridization. Proceedings of the National Academy of Sciences of the United States of America 80 (12) : 3734-3737.
- Ellis, R. J. 2006. Molecular chaperones: assisting assembly in addition to folding. Trends in Biochemical Sciences 31 (7) : 395-401.
- Fearnley, G. R., and Lackner, R. 2008. The fibrinolytic activity of normal blood. British Journal of Haematology 1 (2) : 189–198.
- Fernandes, E., Costa, D., Toste, S. A., Lima, J. L., and Reis, S. 2004. *In vitro* scavenging activity for reactive oxygen and nitrogen species by nonsteroidal anti-inflammatory indole, pyrrole, and oxazole derivative drugs. Free Radical Biology & Medicine 37 (11) : 1895-1905.
- Franceschini, A., Szklarczyk, D., Frankild, S., Kuhn, M., Simonovic, M., Roth, A., Lin, J., Minguez, P., Bork, P., von Mering, C., and Jensen, L. J. 2013. STRING v9.1: protein-protein interaction networks, with increased coverage and integration. Nucleic Acids Research 41 : 808-815.
- Friedman, M., and Jürgens, H. S. 2000. Effect of pH on the stability of plant phenolic compounds. Journal of Agricultural and Food Chemistry 48 (6) : 2101-2110.
- Feo, S., Arcuri, D., Piddini, E., Passantino, R., and Giallongo, A. 2000. *ENO1* gene product binds to the *c-myc* promoter and acts as a transcriptional repressor: relationship with Myc promoter-binding protein 1 (MBP-1). FEBS Letters 473 (1) : 47-52.

- Forstermann, U. 2010. Nitric oxide and oxidative stress in vascular disease. Pflugers Archiv - European Journal of Physiology 459 (6) : 923-939.
- Fuchs, D., Erhard, P., Rimbach, G., Daniel, H., and Wenzel, U. 2005. Genistein blocks homocysteine-induced alterations in the proteome of human endothelial cells. Proteomics 5 (11) : 2808-2818.
- Fuchs, D., Dirscherl, B., Schroot, J. H., Daniel, H., and Wenzel, U. 2006. Soy extract has different effects compared with the isolated isoflavones on the proteome of homocysteine-stressed endothelial cells. Molecular Nutrition and Food Research 50 (1) : 58-69.
- Gaddipati, J. P., Madhavan, S., Sidhu, G. S., Singh, A. K., Seth, P., and Maheshwari, R. K. 1999. Picroliv - a natural product protects cells and regulates the gene expression during hypoxia/reoxygenation. Molecular and Cellular Biochemistry 194 (1-2) : 271-281.
- Garai, S., Jaisankar, P., Singh, J. K., and Elango, A. 2012. A comprehensive study on crude methanolic extract of *Artemisia pallens* (Asteraceae) and its active component as effective corrosion inhibitors of mild steel in acid solution. Corrosion Science 60 : 193-204.
- Gerber, H. P., McMurtrey, A., Kowalski, J., Yan, M., Keyt, B. A., Dixit, V., and Ferrara, N. 1998. Vascular endothelial growth factor regulates endothelial cell survival through the phosphatidylinositol 3'-kinase/Akt signal transduction pathway. Requirement for Flk-1/KDR activation. Journal of Biological Chemistry 273 (46) : 30336-30343.
- Gil, C. D., La, M., Perretti, M., and Oliani, S. M. 2006. Interaction of human neutrophils with endothelial cells regulates the expression of endogenous proteins annexin 1, galectin-1 and galectin-3. Cell Biology International 30 (4) : 338-344.
- Gruber, C. W., Cemazar, M., Heras, B., Martin, J. L., and Craik, D. J. 2006. Protein disulfide isomerase: the structure of oxidative folding. Trends in Biochemical Sciences 31 (8) : 455-464.
- Goto, S., Kawakatsu, M., Izumi, S., Urata, Y., Kageyama, K., Ihara, Y., Koji, T., and Kondo, T. 2009. Glutathione S-transferase pi localizes in mitochondria and

- protects against oxidative stress. Free Radical Biology & Medicine 46 (10) : 1392-1403.
- Gousset-Dupont, A., Robert, V., Grynberg, A., Lacour, B., and Tardivel, S. 2007. The effect of n-3 PUFA on eNOS activity and expression in EA.hy926 cells. Prostaglandins Leukotrienes and Essential Fatty Acids 76 (3) : 131-139.
- Govindarajan, R., Vijayakumar, M., Rawat, A. K., and Mehrotra, S. 2003. Free radical scavenging potential of *Picrorhiza kurrooa* Royle ex Benth. Indian Journal of Experimental Biology 41 (8) : 875-879.
- Guleria, S., Tiku, A. K., Singh, G., Koul, A., Gupta, S., and Rana, S. 2013. *In vitro* antioxidant activity and phenolic contents in methanol extracts from medicinal plants. Journal of Plant Biochemistry and Biotechnology 22 (1) : 9-15.
- Gupta, S., Deepti, A., Deegan, S., Lisbona, F., Hetz, C., and Samali, A. 2010. HSP72 protects cells from ER stress-induced apoptosis via enhancement of IRE1 α -XBP1 signaling through a physical interaction. PLOS Biology 8 (7) : e1000410.
- Ha, M. K., Chung, K. Y., Bang, D., Park, Y. K., and Lee, K. H. 2005. Proteomic analysis of the proteins expressed by hydrogen peroxide treated cultured human dermal microvascular endothelial cells. Proteomics 5 (6) : 1507-1519.
- Haase, V. H. 2010. The sweet side of HIF. Kidney International 78 (1) : 10-13.
- Haddad, J. J., Olver, R. E., and Land, S. C. 2000. Antioxidant/pro-oxidant equilibrium regulates HIF-1 α and NF-kappa B redox sensitivity. Evidence for inhibition by glutathione oxidation in alveolar epithelial cells. Journal of Biological Chemistry 275 (28) : 21130-21139.
- Halliwell, B., Gutteridge, J. M., and Aruoma, O. I. 1987. The deoxyribose method: a simple "test-tube" assay for determination of rate constants for reactions of hydroxyl radicals. Analytical Biochemistry 165 (1) : 215-219.
- Hasada, K., Yoshida, T., Yamazaki, T., Sugimoto, N., Nishimura, T., Nagatsu, A., and Mizukami, H. 2010. Quantitative determination of atractylon in *Atractylodis rhizoma* and *Atractylodis lanceae* Rhizome by ¹H-NMR spectroscopy. Journal of Natural Medicines 64 (2) : 161-166.

- Hazra, B., Biswas, S., and Mandal, N. 2008. Antioxidant and free radical scavenging activity of *Spondias pinnata*. BMC Complementary and Alternative Medicine 9 (8) : 63.
- He, K. L., Deora, A. B., Xiong, H., Ling, Q., Weksler, B. B., Niesvizky, R., and Hajjar, K. A. 2008. Endothelial cell annexin A2 regulates polyubiquitination and degradation of its binding partner S100A10/p11. Journal of Biological Chemistry 283 (28) : 19192-19200.
- Heilmann, J., Resch, M., and Bauer, R. 1998. Antioxidant activity of constituents from *Atractylodes lancea*. Pharmaceutical and Pharmacological Letters 8 (2) : 69-71.
- Hidalgo, M., Sánchez-Moreno, C., and Pascual-Teresa, S. 2010. Flavonoid-flavonoid interaction and its effect on their antioxidant activity. Food Chemistry 121 (2) : 691-696.
- Hogg, N. 1999. The effect of cyst(e)ine on the auto-oxidation of homocysteine. Free Radical Biology & Medicine 27 (1-2) : 28-33.
- Houry, W. A. 2001. Chaperone-assisted protein folding in the cell cytoplasm. Current Protein & Peptide Science 2 (3) : 227-244.
- Huang, S. H., Chen, C. C., Lin, C. M., and Chiang, B. H. 2008. Antioxidant and flavor properties of *Angelica sinensis* extracts as affected by processing. Journal of Food Composition and Analysis 21 (5) : 402-409.
- Hung, Y. C., Wang, P. W., Pan, T. L., Bazylak, G., and Leu, Y. L. 2009. Proteomic screening of antioxidant effects exhibited by radix *Salvia miltiorrhiza* aqueous extract in cultured rat aortic smooth muscle cells under homocysteine treatment. Journal of Ethnopharmacology 124 (3) : 463-474.
- Hwang, J. M., Tseng, T. H., Hsieh, Y. S., Chou, F. P., Wang, C. J., and Chu, C. Y. 1996. Inhibitory effect of atractylon on tert-butyl hydroperoxide induced DNA damage and hepatic toxicity in rat hepatocytes. Archives of Toxicology 70 (10) : 640-644.
- Ikeda, U., Ikeda, M., Minota, S., and Shimada, K. 1999. Homocysteine increases nitric oxide synthesis in cytokine-stimulated vascular smooth muscle cells. Circulation 99 (9) : 1230-1235.

- Isoe, T., Makino, Y., Mizumoto, K., Sakagami, H., Fujita, Y., Honjo, J., Takiyama, Y., Itoh, H., and Haneda, M. 2010. High glucose activates HIF-1-mediated signal transduction in glomerular mesangial cells through a carbohydrate response element binding protein. Kidney International 78 (1) : 48-59.
- Itoh, K., Tong, K. I., and Yamamoto, M. 2004. Molecular mechanism activating Nrf2-Keap1 pathway in regulation of adaptive response to electrophiles. Free Radical Biology & Medicine 36 (10) : 1208-1013.
- Jariyapongskul, A., Pathumraj, S., and Niimi, H. 2006. Effects of Yahom on the regional cerebral blood flow in rat using fluorescence videomicroscopy. Clinical Hemorheology and Microcirculation 34 (1-2) : 139-144.
- Jin, L., Caldwell, R. B., Li-Masters, T., and Caldwell, R. W. 2007. Homocysteine induces endothelial dysfunction via inhibition of arginine transport. Journal of Physiology and Pharmacology 58 (2) : 191-206.
- Jin, M., Lee, H., Ryu, J., and Chung, K. 2000. Inhibition of LPS-induced NO production and NF-kB activation by a sesquiterpene from *Saussurea lappa*. Archives of Pharmacal Research 23 (1) : 54-58.
- Jeon, H., Kim, H., Choi, D., Kim, D., Park, S. Y., Kim, Y. J., Kim, Y. M., and Jung, Y. 2007. Quercetin activates an angiogenic pathway, hypoxia inducible factor (HIF)-1-vascular endothelial growth factor, by inhibiting HIF-prolyl hydroxylase: a structural analysis of quercetin for inhibiting HIF-prolyl hydroxylase. Molecular Pharmacology 71 (6) : 1676-1684.
- Jeong, J. B., Ju, S. Y., Park, J. H., Lee, J. R., Yun, K. W., Kwon, S. T., Lim, J. H., Chung, G. Y., and Jeong, H. J. 2009. Antioxidant activity in essential oils of *Cnidium officinale* makino and *Ligusticum chuanxiong* hort and their inhibitory effects on DNA damage and apoptosis induced by ultraviolet B in mammalian cell. Cancer Epidemiology 33 (1) : 41-46.
- Kallio, P. J., Okamoto, K., O'Brien, S., Carrero, P., Makino, Y., Tanaka, H., and Poellinger, L. 1998. Signal transduction in hypoxic cells: inducible nuclear translocation and recruitment of the CBP/p300 coactivator by the hypoxia-inducible factor-1alpha. EMBO Journal 17 (22) : 6573-6586.

- Kam, A., Li, K. M., Razmovski-Naumovski, V., Nammi, S., Chan, K., and Li, G. Q. 2012. Combination of TNF- α , homocysteine and adenosine exacerbated cytotoxicity in human cardiovascular and cerebrovascular endothelial cells. Cellular Physiology and Biochemistry 30 (3) : 805-814.
- Kamath, K. S., Vasavada, M. S., and Srivastava, S. 2011. Proteomic databases and tools to decipher post-translational modifications. Journal of Proteomics 75 (1) : 127-144.
- Kengkoom, K., Chaimongkolnukul, K., Cherdyu, S., Inpukaew, R., and Ampawong, S. 2012. Acute and sub-chronic oral toxicity studies of the extracts from herbs in Phikud Navakot. African Journal of Biotechnology 11 (48) : 10903-10911.
- Kim, K. M., Kim, D. K., Park, Y. M., Kim, C. K., and Na, D. S. 1994. Annexin-I inhibits phospholipase A2 by specific interaction, not by substrate depletion. FEBS Letters 343 (3) : 251-255.
- Kim, S. J., Kwon, D. Y., Kim, Y. S., and Kim, Y. C. 2010. Peroxyl radical scavenging capacity of extracts and isolated components from selected medicinal plants. Archives of Pharmacal Research 33 (6) : 867-873.
- Kitajima, J., Kamoshita, A., Ishikawa, T., Takano, A., Fukuda, T., Isoda, S., and Ida, Y. 2003. Glycosides of *Atractylodes lancea*. Chemical and Pharmaceutical Bulletin 51 (6) : 673-678.
- Kensler, T. W., Wakabayashi, N., and Biswal, S. 2007. Cell survival responses to environmental stresses *via* the Keap1-Nrf2-ARE pathway. Annual Review of Pharmacology and Toxicology 47 : 89-116.
- Kooistra, T., Lansink, M., Arts, J., Sitter, T., and Toet, K. 1995. Involvement of retinoic acid receptor alpha in the stimulation of tissue-type plasminogen-activator gene expression in human endothelial cells. European Journal of Biochemistry 232 (2) : 425-432.
- Laght, D. W., Carrier, M. J., and Anggard, E. E. 2000. Antioxidants, diabetes and endothelial dysfunction. Cardiovascular Research 47 (3) : 457-464.
- Lalouschek, W., Aull, S., Serles, W., Schnider, P., Mannhalter, C., Lang, T., Deecke, L., and Zeiler, K. 1999. Genetic and nongenetic factors influencing plasma homocysteine levels in patients with ischemic cerebrovascular disease and in

- healthy control subjects. Journal of Laboratory and Clinical Medicine 133 (6) : 575-582.
- Lee, H. S., Cho, H. Y., Park, K. W., Kim, I. H., Kim, J. T., Nam, M. H., and Lee, K. W. 2011. Inhibitory effects of *Terminalia chebula* extract on glycation and endothelial cell adhesion. Planta Medica 77 (10) : 1060-1067.
- Lee, H. S., Jung, S. H., Yun, B. S., and Lee, K. W. 2007. Isolation of chebulic acid from *Terminalia chebula* Retz. and its antioxidant effect in isolated rat hepatocytes. Archives of Toxicology 81 (3) : 211-218.
- Lee, H. S., Won, N. H., Kim, K. H., Lee, H., Jun, W., and Lee, K. W. 2005. Antioxidant effects of aqueous extract of *Terminalia chebula* in vivo and in vitro. Biological and Pharmaceutical Bulletin 28 (9) : 1639-1644.
- Lee, M. Y., Seo, C. S., Lee, J. A., Lee, N. H., Kim, J. H., Ha, H., Zheng, M. S., Son, J. K., and Shin, H. K. 2011. Anti-asthmatic effects of *Angelica dahurica* against ovalbumin-induced airway inflammation *via* upregulation of heme oxygenase-1. Food and Chemical Toxicology 49 (4) : 829-837.
- Lee, S. J., Kim, K. M., Namkoong, S., Kim, C. K., Kang, Y. C., Lee, H., Ha, K. S., Han, J. A., Chung, H. T., Kwon, Y. G., and Kim, Y. M. 2005. Nitric oxide inhibition of homocysteine-induced human endothelial cell apoptosis by down-regulation of p53-dependent Noxa expression through the formation of S-nitrosohomocysteine. Journal of Biological Chemistry 280 (7) : 5781-5788.
- Lee, S., Chen, T. T., Barber, C. L., Jordan, M. C., Murdock, J., Desai, S., Ferrara, N., Nagy, A., Roos, K. P., and Iruela-Arispe, M. L. 2007. Autocrine VEGF signaling is required for vascular homeostasis. Cell 130 (4) : 691-703.
- Lee, W. S., Yang, H. Y., Kao, P. F., Liu, J. C., Chen, C. H., Cheng, T. H., and Chan, P. 2005. Tetramethylpyrazine downregulates angiotensin II-induced endothelin-1 gene expression in vascular endothelial cells. Clinical and Experimental Pharmacology and Physiology 32 (10) : 845-850.
- Lee, Y. S., Jang, S. M., and Kim, N. W. 2007. Antioxidative activity and physiological function of the *Angelica dahurica* roots. Journal of the Korean Society of Food Science and Nutrition 36 (1) : 20-26.

- Lee, Y. S., and Kim, N. W. 2011. Antioxidant activity and irritation test of extracts obtained from *Angelica dahurica*. Journal of Food Science Nutrition 16 (1) : 8-11.
- Lengqvist, J., Eriksson, H., Gry, M., Uhlén, K., Björklund, C., Bjellqvist, B., Jakobsson, P. J., and Lehtiö, J. 2011. Observed peptide pI and retention time shifts as a result of post-translational modifications in multidimensional separations using narrow-range IPG-IEF. Amino Acids 40 (2) : 697-711.
- Leung, D. W., Cachianes, G., Kuang, W. J., Goeddel, D. V., and Ferrara, N. 1989. Vascular endothelial growth factor is a secreted angiogenic mitogen. Science 246 (4935) : 1306-1309.
- Li, H., and Wang, Q. 2004. Evaluation of free hydroxyl radical scavenging activities of some Chinese herbs by capillary zone electrophoresis with amperometric detection. Analytical and Bioanalytical Chemistry 378 (7) : 1801-1805.
- Li, H., Xia, N., Brausch, I., Yao, Y., and Förstermann, U. 2004. Flavonoids from artichoke (*Cynara scolymus* L.) up-regulate endothelial-type nitric-oxide synthase gene expression in human endothelial cells. Journal of Pharmacology and Experimental Therapeutics 310 (3) : 926-932.
- Li, J., Zhang, X., Sejas, D. P., Bagby, G. C., and Pang, Q. 2004. Hypoxia-induced nucleophosmin protects cell death through inhibition of p53. Journal of Biological Chemistry 279 (40) : 41275-41279.
- Li, K., Diao, Y., Zhang, H., Wang, S., Zhang, Z., Yu, B., Huang, S., and Yang, H. 2011. Tannin extracts from immature fruits of *Terminalia chebula* Fructus Retz. promote cutaneous wound healing in rats. BMC Complementary and Alternative Medicine 11 : 86.
- Li, M., Xu, Y., Yang, W., Li, J., Xu, X., Zhang, X., Chen, F., and Li, D. 2011. *In vitro* synergistic anti-oxidant activities of solvent-extracted fractions from *Astragalus membranaceus* and *Glycyrrhiza uralensis*. LWT- Food Science and Technology 44 (8) : 1745-1751.
- Li, P. G., Sun, L., Han, X., Ling, S., Gan, W. T., and Xu, J. W. 2012. Quercetin induces rapid eNOS phosphorylation and vasodilation by an Akt-independent and PKA-dependent mechanism. Pharmacology 89 (3-4) : 220-228.

- Li, S. Y., Yu, Y., and Li, S. P. 2007. Identification of antioxidants in essential oil of radix *Angelicae sinensis* using HPLC coupled with DAD-MS and ABTS-based assay. Journal of Agricultural and Food Chemistry 55 (9) : 3358-3362.
- Li, W., Wu, Y., Liu, X., Yan, C., Liu, D., Pan, Y., Yang, G., Yin, F., Weng, Z., Zhao, D., Chen, Z., and Cai, B. 2013. Antioxidant properties of cis-Z,Z'-3a,7a',7a,3a'-dihydroxyiligustilide on human umbilical vein endothelial cells in vitro. Molecules 18 (1) : 520-534.
- Li, Z., Boone, D., and Hann, S. R. 2008. Nucleophosmin interacts directly with c-Myc and controls c-Myc-induced hyperproliferation and transformation. Proceedings of the National Academy of Sciences of the United States of America 105 (48) : 18794-18799.
- Liang, P., and MacRae, T. H. 1997. Molecular chaperones and the cytoskeleton. Journal of Cell Science 110 (13) : 1431-1440.
- Liao, H., Banbury, L. K., and Leach, D. N. 2008. Antioxidant activity of 45 Chinese herbs and the relationship with their TCM characteristics. Evidence-Based Complementary and Alternative Medicine 5 (4) : 429-434.
- Lin, C. M., Chiu, J. H., Wu, I. H., Wang, B. W., Pan, C. M., and Chen, Y. H. 2010. Ferulic acid augments angiogenesis via VEGF, PDGF and HIF-1 alpha. Journal of Nutritional Biochemistry 21 (7) : 627-633.
- Lin, R., Liu, J., Gan, W., and Ding, C. 2007. Protective effect of quercetin on the homocysteine-injured human umbilical vein vascular endothelial cell line (ECV304). Basic & Clinical Pharmacology & Toxicology 101 (3) : 197-202.
- Liu, D. P., Luo, Q., Wang, G. H., Xu, Y., Zhang, X. K., Chen, Q. C., and Chen, H. F. 2011. Furocoumarin derivatives from radix *Angelicae dahuricae* and their effects on RXR alpha transcriptional regulation. Molecules 16 (8) : 6339-6348.
- Lyle, N., Gomes, A., Sur, T., Munshi, S., Paul, S., Chatterjee, S., and Bhattacharyya, D. 2009. The role of antioxidant properties of *Nardostachys jatamansi* in alleviation of the symptoms of the chronic fatigue syndrome. Behavioural Brain Research 202 (2) : 285-290.
- Ma, Z. C., Hong, Q., Wang, Y. G., Tan, H. L., Xiao, C. R., Liang, Q. D., Zhang, B. L., and Gao, Y. 2010. Ferulic acid protects human umbilical vein endothelial

- cells from radiation induced oxidative stress by phosphatidylinositol 3-kinase and extracellular signal-regulated kinase pathways. Biological and Pharmaceutical Bulletin 33 (1) : 29-34.
- Mahesh, R., Bhuvana, S., and Begum, V. M. 2009. Effect of *Terminalia chebula* aqueous extract on oxidative stress and antioxidant status in the liver and kidney of young and aged rats. Cell Biochemistry and Function 27 (6) : 358-363.
- Manda, G., Nechifor, M. T., and Neagu, T. M. 2009. Reactive oxygen species, cancer and anti-cancer therapies. Current Chemical Biology 3 (1) : 22-46.
- Mandal, S., Hazra, B., Sarkar, R., Biswas, S., and Mandal, N. 2009. Assessment of the antioxidant and reactive oxygen species scavenging activity of methanolic extract of *Caesalpinia crista* Leaf. Evidence-Based Complementary and Alternative Medicine 2011 :173768.
- Manna, C., Napoli, D., Cacciapuoti, G., Porcelli, M., and Zappia, V. 2009. Olive oil phenolic compounds inhibit homocysteine-induced endothelial cell adhesion regardless of their different antioxidant activity. Journal of Agricultural and Food Chemistry 57 (9) : 3478-3482.
- Manosroi, A., Jantrawut, P., Akazawa, H., Akihisa, T., and Manosroi, J. 2010. Biological activities of phenolic compounds isolated from galls of *Terminalia chebula* Retz. (Combretaceae). Natural Product Research 24 (20) : 1915-1926.
- Manosroi, A., Jantrawut, P., Akihisa, T., Manosroi, W., and Manosroi, J. 2010. *In vitro* anti-aging activities of *Terminalia chebula* gall extract. Pharmaceutical Biology 48 (4) : 469-481.
- Maurya, D. K., and Devasagayam, T. P. 2010. Antioxidant and prooxidant nature of hydroxycinnamic acid derivatives ferulic and caffeic acids. Food and Chemical Toxicology 48 (12) : 3369-3373.
- McDowell, I. F., and Lang, D. 2000. Homocysteine and endothelial dysfunction: a link with cardiovascular disease. Journal of Nutrition 130 (2S) : 369S-372S.
- Menell, J. S., Cesarman, G. M., Jacovina, A. T., McLaughlin, M. A., Lev, E. A., and Hajjar, K. A. 1999. Annexin II and bleeding in acute promyelocytic leukemia. New England Journal of Medicine 340 (13) : 994-1004.

- Morris, G. E., Nelson, C. P., Standen, N. B., Challiss, R. A. J., and Willets, J. M. 2010. Endothelin signaling in arterial smooth muscle is tightly regulated by G protein-coupled receptor kinase 2. Cardiovascular Research 85 (3) : 424-433.
- Morita, T., Imai, T., Sugiyama, T., Katayama, S., and Yoshino, G. 2005. Heme oxygenase-1 in vascular smooth muscle cells counteracts cardiovascular damage induced by angiotensin II. Current Neurovascular Research 2 (2) : 113-120.
- Mosser, D. D., Caron, A. W., Bourget, L., Meriin, A. B., Sherman, M. Y., Morimoto, R. I., and Massie, B. 2000. The chaperone function of hsp70 is required for protection against stress-induced apoptosis. Molecular and Cellular Biology 20 (19) : 7146-7159.
- Mujumdar, V. S., Aru, G. M., and Tyagi, S. C. 2001. Induction of oxidative stress by homocyst(e)ine impairs endothelial function. Journal of Cellular Biochemistry 82 (3) : 491-500.
- Murphy, J. F., and Fitzgerald, D. J. 2001. Vascular endothelial growth factor induces cyclooxygenase-dependent proliferation of endothelial cells via the VEGF-2 receptor. FASEB Journal 15 (9) : 1667-1669.
- Naik, G. H., Priyadarsini, K. I., Naik, D. B., Gangabhagirathi, R., and Mohan, H. 2004. Studies on the aqueous extract of *Terminalia chebula* as a potent antioxidant and a probable radioprotector. Phytomedicine 11 (6) : 530-538.
- National Drug Committee of Thailand. 2011. List of Herbal Medicinal Products A.D. 2011. Bangkok: 2011 : 19-28.
- Niranjan, A., Barthwal, J., Lehri, A., Singh, D. P., Govindrajan, R., Rawat, A. K. S., and Amla, D. V. 2009. Development and validation of an HPLC-UV-MS-MS method for identification and quantification of polyphenols in *Artemisia pallens* L. Acta Chromatographica 21 (1) : 105-116.
- Neufeld, G., Cohen, T., Gengrinovitch, S., and Poltorak, Z. 1999. Vascular endothelial growth factor (VEGF) and its receptors. FASEB Journal 13 (1) : 9-22.
- Nguyen, T., Sherratt, P. J., Huang, H. C., Yang, C. S., and Pickett, C. B. 2003. Increased protein stability as a mechanism that enhances Nrf2-mediated transcriptional activation of the antioxidant response element: degradation of

- Nrf2 by the 26S proteasome. Journal of Biological Chemistry 278 (7) : 4536-4541.
- Nguyen, T., Sherratt, P. J., and Pickett, C. B. 2003. Regulatory mechanisms controlling gene expression mediated by the antioxidant response element. Annual Review of Pharmacology and Toxicology 43 : 233-260.
- Ning, W., Chu, T. J., Li, C. J., Choi, A. M. K., and Peters, D. G. 2004. Genome-wide analysis of the endothelial transcriptome under short-term chronic hypoxia. Physiological Genomics 18 (1) : 70-78.
- Okar, D. A., Manzano, A., Navarro-Sabatè, A., Riera, L., Bartrons, R., and Lange, A. J. 2001. PFK-2/FBPase-2: maker and breaker of the essential biofactor fructose-2,6-bisphosphate. Trends in Biochemical Sciences 26 (1) : 30-35.
- Ohno, M., Gibbons, G., Dzau, V., and Cooke, J. 1993. Shear stress elevates endothelial cGMP. Role of a potassium channel and G protein coupling. Circulation 88 (1) : 193-197.
- Østergaard, L., Simonsen, U., Eskildsen-Helmond, Y., Vorum, H., Uldbjerg, N., Honoré, B., and Mulvany, M. J. 2009. Proteomics reveals lowering oxygen alters cytoskeletal and endoplasmic stress proteins in human endothelial cells. Proteomics 9 (19) : 4457-4467.
- Palmer, L. A., Gaston, B., and Johns, R. A. 2000. Normoxic stabilization of hypoxia-inducible factor-1 expression and activity: redox-dependent effect of nitrogen oxides. Molecular Pharmacology 58 (6) : 1197-1203.
- Paris, S., Denis, H., Delaive, E., Dieu, M., Dumont, V., Ninane, N., Raes, M., and Michiels, C. 2005. Up-regulation of 94-kDa glucose-regulated protein by hypoxia-inducible factor-1 in human endothelial cells in response to hypoxia. FEBS Letters 579 (1) : 105-114.
- Parveen, Z., Siddique, S., Shafique, M., Khan, S. J., and Khanum, R. 2011. Volatile constituents, antibacterial and antioxidant activities of essential oil from *Nardostachys jatamansi* DC. roots. Pharmacology Online 3 : 329-337.
- Perla-Kajan, J., Twardowski, T., and Jakubowski, H. 2007. Mechanisms of homocysteine toxicity in humans. Amino Acids 32 (4) : 561-572.
- Perna, A. F., Ingrosso, D., and De Santo, N. G. 2003. Homocysteine and oxidative stress. Amino Acids 25 (3-4) : 409-417.

- Perretti, M., Ingegnoli, F., Wheller, S. K., Blades, M. C., Solito, E., and Pitzalis, C. 2002. Annexin 1 modulates monocyte-endothelial cell interaction in vitro and cell migration in vivo in the human SCID mouse transplantation model. Journal of Immunology 169 (4) : 2085-2092.
- Peterson, E. A., Sutherland, M. R., Nesheim, M. E., and Pryzdial, E. L. G. 2003. Thrombin induces endothelial cell-surface exposure of the plasminogen receptor annexin 2. Journal of Cell Science 116 (12) : 2399-2408.
- Piao, X. L., Park, I. H., Baek, S. H., Kim, H. Y., Park, M. K., and Park, J. H. 2004. Antioxidative activity of furanocoumarins isolated from *Angelicae dahuricae*. Journal of Ethnopharmacology 93(2-3) : 243-246.
- Pujar, P. P., Sawaikar, D. D., Rojatkar, S. R., and Nagasampagi, B. A. 2000. A new germacranolide from *Artemisia pallens*. Fitoterapia 71 (5) : 590-592.
- Qiu, J., Gao, H. Q., Zhou, R. H., Liang, Y., Zhang, X. H., Wang, X. P., You, B. A., and Cheng, M. 2007. Proteomics analysis of the proliferative effect of low-dose ouabain on human endothelial cells. Biological and Pharmaceutical Bulletin 30 (2) : 247-253.
- Radreau, P., Rhodes, J. D., Mithen, R. F., Kroon, P. A., and Sanderson, J. 2009. Hypoxia-inducible factor-1 (HIF-1) pathway activation by quercetin in human lens epithelial cells. Experimental Eye Research 89 (6) : 995-1002.
- Rajkumar, V., Guha, G., and Kumar, R. A. 2011. Antioxidant and anti-neoplastic activities of *Picrorhiza kurroa* extracts. Food and Chemical Toxicology 49 (2) : 363-369.
- Rasheed, A. S., Venkataraman, S., Jayaveera, K. N., Fazil, A. M., Yasodha, K. J., Aleem, M. A., Mohammed, M., Khaja, Z., Ushasri, B., Pradeep, H. A., and Ibrahim, M. 2010. Evaluation of toxicological and antioxidant potential of *Nardostachys jatamansi* in reversing haloperidol-induced catalepsy in rats. International Journal of General Medicine 3 : 127-136.
- Ray, A., Chaudhuri, S. R., Majumdar, B., and Bandyopadhyay, S. K. 2002. Antioxidant activity of ethanol extract of rhizome of *Picrorhiza kurroa* on indomethacin induced gastric ulcer during healing. Indian Journal of Clinical Biochemistry 17 (2) : 44-51.

- Reddy, R. K., Lu, J., and Lee, A. S. 1999. The endoplasmic reticulum chaperone glycoprotein GRP94 with Ca²⁺-binding and antiapoptotic properties is a novel proteolytic target of calpain during etoposide-induced apoptosis. Journal of Biological Chemistry 274 (40) : 28476-28483.
- Resch, M., Heilmann, J., Steigel, A., and Bauer, R. 2001. Further phenols and polyacetylenes from the rhizomes of *Atractylodes lancea* and their anti-inflammatory activity. Planta Medica 67 (5) : 437-442.
- Rodrigo, J. P., Garcia-Pedrero, J. M., Gonzalez, M. V., Fernandez, M. P., Suarez, C., and Herrero, A. 2004. Expression of annexin A1 in normal and chronically inflamed nasal mucosa. Archives of Otolaryngology - Head and Neck Surgery 130 (2) : 211-215.
- Rubporn, A., Srisomsap, C., Subhasitanont, P., Chokchaichamnankit, D., Chiablaem, K., Svasti, J., and Sangvanich, P. 2009. Comparative proteomic analysis of lung cancer cell line and lung fibroblast cell line. Cancer Genomics and Proteomics 6 (4) : 229-237.
- Ruikar, A., Khatiwora, E., Ghayal, N., Misar, A., Mujumdar, A., Puranik, V., and Deshpande, N. 2011. Studies on aerial parts of *Artemisia pallens* wall for phenol, flavonoid and evaluation of antioxidant activity. Journal of Pharmacy and Bioallied Sciences 3 (2) : 302-305.
- Russo, A., Izzo, A. A., Cardile, V., Borrelli, F., and Vanella, A. 2001. Indian medicinal plants as antiradicals and DNA cleavage protectors. Phytomedicine 8 (2) : 125-132.
- Sabu, M. C., and Kuttan, R. 2002. Anti-diabetic activity of medicinal plants and its relationship with their antioxidant property. Journal of Ethnopharmacology 81 (2) : 155-160.
- Saleem, A., Husheem, M., Härkönen, P., and Pihlaja, K. 2002. Inhibition of cancer cell growth by crude extract and the phenolics of *Terminalia chebula* retz. fruit. Journal of Ethnopharmacology 81 (3) : 327-336.
- Selhub, J. 1999. Homocysteine metabolism. Annual Review of Nutrition 19 : 217-246.

- Semenza, G. L. 1999. Regulation of mammalian O₂ homeostasis by hypoxia-inducible factor 1. Annual Review of Cell and Developmental Biology 15 : 551-578.
- Seo, S., Baye, L. M., Schulz, N. P., Beck, J. S., Zhang, Q., Slusarski, D. C., and Sheffield, V. C. 2010. BBS6, BBS10, and BBS12 form a complex with CCT/TRiC family chaperonins and mediate BBSome assembly. Proceedings of the National Academy of Sciences of the United States of America 107 (4) : 1488-1493.
- Sevier, C. S., and Kaiser, C. A. 2002. Formation and transfer of disulphide bonds in living cells. Nature Reviews Molecular Cell Biology 3 (11) : 836-847.
- Shao, B., Tang, M., Li, Z., Zhou, R., Deng, Y., Nie, C., Yuan, Z., Zhou, L., Tong, A., and Wei, Y. 2012. Proteomics analysis of human umbilical vein endothelial cells treated with resveratrol. Amino Acids 43 (4) : 1671-1678.
- Sharma, S. K., and Singh, A. P. 2012. *In vitro* antioxidant and free radical scavenging activity of *Nardostachys jatamansi* DC. Journal of Acupuncture and Meridian Studies 5 (3) : 112-118.
- Shiota, M., Kusakabe, H., Izumi, Y., Hikita, Y., Nakao, T., Funae, Y., Miura, K., and Iwao, H. 2010. Heat shock cognate protein 70 is essential for Akt signaling in endothelial function. Arteriosclerosis, Thrombosis & Vascular Biology 30 (3) : 491-497.
- Singh, A. K., Sharma, A., Warren, J., Madhavan, S., Steele, K., RajeshKumar, N. V., Thangapazham, R. L., Sharma, S. C., Kulshreshtha, D. K., Gaddipati, J., and Maheshwari, R. K. 2007. Picroliv accelerates epithelialization and angiogenesis in rat wounds. Planta Medica 73 (3) : 251-256.
- Singh, R., Singh, B., Kumar, N., and Arora, S. 2010. Antioxidant activity of triphala a combination of *Terminalia chebula*, *Terminalia bellerica* and *Emblica officinalis*. Journal of Food Biochemistry 34 : 222-232.
- Sipkens, J. A., Hahn, N., van den Brand, C. S., Meischl, C., Cillessen, S. A., Smith, D. E., Juffermans, L. J., Musters, R. J., Roos, D., Jakobs, C., Blom, H. J., Smulders, Y. M., Krijnen, P. A., Stehouwer, C. D., Rauwerda, J. A., van Hinsbergh, V. W., and Niessen, H. W. 2011. Homocysteine-induced apoptosis

- in endothelial cells coincides with nuclear NOX2 and peri-nuclear NOX4 activity. Cell Biochemistry and Biophysics 30: [Epub ahead of print].
- Srisomsap, C., Sawangareetrakul, P., Subhasitanont, P., Chokchaichamnankit, D., Chiablaem, K., Bhudhisawasdi, V., Wongkham, S., and Svasti, J. 2010. Proteomic studies of cholangiocarcinoma and hepatocellular carcinoma cell secretomes. Journal of Biomedicine and Biotechnology 2010 : 437143.
- Subashini, R., Yogeta, S., Gnanapragasam, A., and Devaki, T. 2006. Protective effect of *Nardostachys jatamansi* on oxidative injury and cellular abnormalities during doxorubicin-induced cardiac damage in rats. Journal of Pharmacy and Pharmacology 58 (2) : 257-262.
- Subramanian, A., and Miller, D. M. 2000. Structural analysis of alpha-enolase. Mapping the functional domains involved in down-regulation of the c-myc protoonco gene. Journal of Biological Chemistry 275 (8) : 5958-5965.
- Subramoniam, A., Pushpangadan, P., Rajasekharan, S., Evans, D. A., Latha, P. G., and Valsaraj, R. 1996. Effects of *Artemisia pallens* Wall. on blood glucose levels in normal and alloxan-induced diabetic rats. Journal of Ethnopharmacology 50 (1) : 13-17.
- Sue, Y. M., Cheng, C. F., Chang, C. C., Chou, Y., Chen, C. H., and Juan, S. H. 2009. Antioxidation and anti-inflammation by heme oxygenase-1 contribute to protection by tetramethylpyrazine against gentamicin-induced apoptosis in murine renal tubular cells. Nephrology Dialysis Transplantation 24 (3) : 769-777.
- Suresh, J., Reddy, A. S. V., Ahuja, J., Sebastian, M., and Rajan, S. K. 2011. Antioxidant and antimicrobial activity of *Artemisia pallens*. IJPI's Journal of Pharmacognosy and Herbal Formulations 1 (2) : 12-18.
- Surh, Y. J., Kundu, J. K., and Na, H. K. 2008. Nrf2 as a master redox switch in turning on the cellular signaling involved in the induction of cytoprotective genes by some chemopreventive phytochemicals. Planta Medica 74 (13) : 1526-1539.
- Suvitayavat, W., Tunlert, S., Thirawarapan, S. S., Kitpati, C., and Bunyapraphatsara, N. 2005. Actions of Ya-hom, a herbal drug combination, on isolated rat aortic ring and atrial contractions. Phytomedicine 12 (8) : 561-569.

- Tai, S. C., Robb, G. B., and Marsden, P. A. 2004. Endothelial nitric oxide synthase: A new paradigm for gene regulation in the injured blood vessel. Arteriosclerosis, Thrombosis & Vascular Biology 24 (3) : 405-412.
- Tew, K. D., Manevich, Y., Grek, C., Xiong, Y., Uys, J., and Townsend, D. M. 2011. The role of glutathione S-transferase P in signaling pathways and S-glutathionylation in cancer. Free Radical Biology & Medicine 51 (2) : 299-313.
- Tyagi, N., Sedoris, K. C., Steed, M., Ovechkin, A. V., Moshal, K. S., and Tyagi, S. C. 2005. Mechanisms of homocysteine-induced oxidative stress. Heart and Circulatory Physiology: American Journal of Physiology 289 (6) : H2649-2656.
- Topal, G., Brunet, A., Millanvoeye, E., Boucher, J. L., Rendu, F., Devynck, M. A., and David-Duffilho, M. 2004. Homocysteine induces oxidative stress by uncoupling of no synthase activity through reduction of tetrahydrobiopterin. Free Radical Biology & Medicine 36 (12) : 1532-1541.
- Tsukahara, F., Yoshioka, T., and Muraki, T. 2000. Molecular and functional characterization of HSC54, a novel variant of human heat-shock cognate protein 70. Molecular Pharmacology 58 (6) : 1257-1263.
- Tsuneki, H., Ma, E. L., Kobayashi, S., Sekizaki, N., Maekawa, K., Sasaoka, T., Wang, M. W., and Kimura, I. 2005. Antiangiogenic activity of beta-eudesmol in vitro and in vivo. European Journal of Pharmacology 512 (2-3) : 105-115.
- Unger, R. E., Krump-Konvalinkova, V., Peters, K., and Kirkpatrick, C. J. 2002. *In vitro* expression of the endothelial phenotype: comparative study of primary isolated cells and cell lines, including the novel cell line HPMEC-ST1.6R. Microvascular Research 64 (3) : 384-397.
- van Acker, S. A., van den Berg, D. J., Tromp, M. N., Griffioen, D. H., van Bennekom, W. P., van der Vijgh, W. J., and Bast, A. 1996. Structural aspects of antioxidant activity of flavonoids. Free Radical Biology & Medicine 20 (3) : 331-342.
- Venema, R. C., Sayegh, H. S., Kent, J. D., and Harrison, D. G. 1996. Identification, characterization, and comparison of the calmodulin-binding domains of the

- endothelial and inducible nitric oxide synthases. Journal of Biological Chemistry 271 (11) : 6435-6440.
- Walia, H., Kumar, S., and Arora, S. 2009. Antiradical efficacy and protective effect of water extract/fractions of *Terminalia chebula* on DNA cleavage. Journal of Chinese Clinical Medicine 4 (12) : 661-673.
- Wallerath, T., Deckert, G., Ternes, T., Anderson, H., Li, H., Witte, K., and Förstermann U. 2002. Resveratrol, a polyphenolic phytoalexin present in red wine, enhances expression and activity of endothelial nitric oxide synthase. Circulation 106 (13) : 1652-1658.
- Wang, H., and Joseph, J. A. 1999. Quantifying cellular oxidative stress by dichlorofluorescein assay using microplate reader. Free Radical Biology & Medicine 27 (5-6) : 612-616.
- Weiss, N., Ide, N., Abahji, T., Nill, L., Keller, C., and Hoffmann, U. 2006. Aged garlic extract improves homocysteine-induced endothelial dysfunction in macro- and microcirculation. Journal of Nutrition 136 (3) : 750S-754S.
- Wiesener, M. S., and Maxwell, P. H. 2003. HIF and oxygen sensing; as important to life as the air we breathe? Annals of Medicine 35 (3) : 183-190.
- Williamson, E. M. 2001. Synergy and other interactions in hytomedicines. Phytomedicine 8 (5) : 401-409.
- Wolin, M. S. 1996. Reactive oxygen species and vascular signal transduction mechanisms. Microcirculation 3 (1) : 1-17.
- Wu, H. L., Li, Y. H., Lin, Y. H., Wang, R., Li, Y. B., Tie, L., Song, Q. L., Guo, D. A., Yu, H. M., and Li, X. J. 2009. Salvianolic acid B protects human endothelial cells from oxidative stress damage: A possible protective role of glucose-regulated protein 78 induction. Cardiovascular Research 81 (1) : 148-158.
- Wu, M. H., and Yung, B. Y. M. 2002. UV Stimulation of nucleophosmin/B23 expression is an immediate-early gene response induced by damaged DNA. Journal of Biological Chemistry 277 (50) : 48234-48240.
- Xia, N., Bollinger, L., Steinkamp-Fenske, K., Förstermann, U., and Li, H. 2010. *Prunella vulgaris* L. upregulates eNOS expression in human endothelial cells. American Journal of Chinese Medicine 38 (3) : 599-611.

- Xie, C., Mao, X., Huang, J., Ding, Y., Wu, J., Dong, S., Kong, L., Gao, G., Li, C. Y., and Wei, L. 2011. KOBAS 2.0: a web server for annotation and identification of enriched pathways and diseases. Nucleic Acids Research 39 : W316-322.
- Xu, S. F., Ye, Y. P., Li, X. Y., and Chen, F. Y. 2011. Chemical composition and antioxidant activities of different polysaccharides from the roots of *Angelica dahurica*. Chemistry & Biodiversity 8 (6) : 1121-1131.
- Yan, R., Li, S. L., Chung, H. S., Tam, Y. K., and Lin, G. 2005. Simultaneous quantification of 12 bioactive components of *Ligusticum chuanxiong* Hort. by high-performance liquid chromatography. Journal of Pharmaceutical and Biomedical Analysis 37 (1) : 87-95.
- Yan, T., Li, Q., Zhang, X. H., Wu, W. K., Sun, J., Li, L., Zhang, Q., and Tan, H. M. 2010. Homocysteine impaired endothelial function through compromised vascular endothelial growth factor/Akt/endothelial nitric oxide synthase signaling. Clinical and Experimental Pharmacology and Physiology 37 (11) : 1071-1077.
- Yan, X., Nagata, T., and Fan, X. 1998. Antioxidative activities in some common seaweeds. Plant Foods for Human Nutrition 52 (3) : 253-262.
- Yi, F., Zhang, A. Y., Janscha, J. L., Li, P. L., and Zou, A. P. 2004. Homocysteine activates NADH/NADPH oxidase through ceramide-stimulated Rac GTPase activity in rat mesangial cells. Kidney International 66 (5) : 1977-1987.
- Yoshiki, Y., Kahara, T., Okubo, K., Sakabe, T., and Yamasaki, T. 2001. Superoxide- and 1,1-diphenyl-2-picrylhydrazyl radical-scavenging activities of soyasaponin beta related to gallic acid. Bioscience, Biotechnology, and Biochemistry 65 (10) : 2162-2165.
- Yu, F., Li, H., Meng, Y., and Yang, D. 2013. Extraction optimization of *Angelica sinensis* polysaccharides and its antioxidant activity in vivo. Carbohydrate Polymers 94 (1) : 114-119.
- Yuan, J. F., Zhang, Z. Q., Fan, Z. C., and Yang, J. X. 2008. Antioxidant effects and cytotoxicity of three purified polysaccharides from *Ligusticum chuanxiong* Hort. Carbohydrate Polymers 74 (4) : 822-827.
- Zhang, B. Q., Hu, S. J., Qiu, L. H., Zhu, J. H., Xie, X. J., Sun, J., Zhu, Z. H., Xia, Q., and Bian, K. 2007. Effects of *Astragalus membranaceus* and its main

- components on the acute phase endothelial dysfunction induced by homocysteine. Vascular Pharmacology 46 (4) : 278-285.
- Zhang, C., Cai, Y., Adachi, M. T., Oshiro, S., Aso, T., Kaufman, R. J., and Kitajima, S. 2001. Homocysteine induces programmed cell death in human vascular endothelial cells through activation of the unfolded protein response. Journal of Biological Chemistry 276 (38) : 35867-35874.
- Zhang, M. H., Lee, J. S., Kim, H. J., Jin, D. I., Kim, J. I., Lee, K. J., and Seo, J. S. 2006. HSP90 protects apoptotic cleavage of vimentin in geldanamycin-induced apoptosis. Molecular and Cellular Biochemistry 281 (1-2) : 111-121.
- Zhang, Q., Zeng, X., Guo, J., and Wang, X. 2002. Oxidant stress mechanism of homocysteine potentiating Con A-induced proliferation in murine splenic T lymphocytes. Cardiovascular Research 53 (4) : 1035-1042.
- Zhang, S., He, B., Ge, J., Li, H., Luo, X., Zhang, H., Li, Y., Zhai, C., Liu, P., Liu, X., and Fei, X. 2010. Extraction, chemical analysis of *Angelica sinensis* polysaccharides and antioxidant activity of the polysaccharides in ischemia-reperfusion rats. International Journal of Biological Macromolecules 47 (4) : 546-550.
- Zhang, X., Xiao, H., Xu, Q., Li, X., Wang, J., and Liang, X. 2003. Characterization of phthalides in *Ligusticum chuanxiong* by liquid chromatographic-atmospheric pressure chemical ionization-mass spectrometry. Journal of Chromatographic Science 41 (8) : 428-433.
- Zhang, Y., DeWitt, D. L., Murugesan, S., and Nair, M. G. 2004. Novel lipid-peroxidation- and cyclooxygenase-inhibitory tannins from *Picrorhiza kurroa* seeds. Chemistry & Biodiversity 1 (3) : 426-441.
- Zheng, K. Y. Z., Guo, A. J. Y., Bi, C. W. C., Zhu, K. Y., Chan, G. K. L., Fu, Q., Xu, S. L., Zhan, J. Y. Z., Lau, D. T. W., Dong, T. T. X., Choi, R. C. Y., and Tsim, K. W. K. 2011. The extract of *Rhodiola crenulatae* Radix et Rhizoma induces the accumulation of HIF-1 α via blocking the degradation pathway in cultured kidney fibroblasts. Planta Medica 77 (9) : 894-899.
- Zhou, W., Chai, H., Lin, P. H., Lumsden, A. B., Yao, Q., and Chen, C. 2005. Ginsenoside Rb1 blocks homocysteine-induced endothelial dysfunction in porcine coronary arteries. Journal of Vascular Surgery 41 (5) : 861-868.

Zou, T., Liu, W. J., Li, S. D., Zhou, W., Yang, J. F., and Zou, C. G. 2011. TRB3 mediates homocysteine-induced inhibition of endothelial cell proliferation. Journal of Cellular Physiology 226 (11) : 2782-2789.

APPENDICES

APPENDIX A

PREPARATION OF REAGENTS

Acrylamide solution

To make 100 mL of 30% acrylamide solution, 30.0 g of acrylamide and 0.8 g of N,N'-bis-methyleneacrylamide were dissolved in 30 mL of ultrapure water. The solution was stirred until completely solubilized, then adjusted volume to 100 mL. Store the solution in the dark at 4° C.

0.5% Agarose

To make 1 mL of 0.5% agarose, 5 mg of agarose was dispersed in 1 mL of 1× running buffer. Add 0.1% Coomassie blue solution 2 µL. Boiled for at least 5 min until completely solubilized.

10% APS solution

To make 300 µL of 10% APS solution, 30 mg of APS was dissolved in 300 µL of ultrapure water. The solution was mixed until completely solubilized. Prepare freshly before use.

1× blotting buffer (25 mM Tris-base, 192 mM glycine, 20% MeOH)

To make 1 L of 1× blotting buffer, the ingredients were:

5× blotting buffer	200	mL
MeOH	200	mL
Adjust volume with ultrapure to	1	L

5× blotting buffer (125 mM Tris-base, 960 mM glycine)

To make 1 L of 5× blotting buffer, the ingredients were:

Tris-base	15.1	g
Glycine	72	g

All ingredients were dissolved in ultrapure water. The solution was stirred until completely solubilized. Finally, adjust the total volume to 1 L. Store the buffer at room temperature. Dilute to 1× before use.

Coomassie destaining solution

	10% MeOH		40% MeOH	
MeOH	200	mL	800	mL
Acetic acid	100	mL	200	mL
R.O. water	1700	mL	1000	mL

Coomassie staining solution

Coomassie Blue R250	1	g
MeOH	400	mL
Acetic acid	100	mL
R.O. water	500	mL

Equilibration buffer no. 1 for 2-DE analysis

	for 4 strips	
SDS	60	mg
DTT	60	mg
Urea	2.16	g
0.5 M Tris-HCl pH 6.8	0.6	mL
Glycerol	1.8	mL
Adjust volume with ultrapure to	500	μL

Equilibration buffer no. 2 for 2-DE analysis

	for 4 strips	
SDS	60	mg
iodacetamide	150	mg
Urea	2.16	g
0.5 M Tris-HCl pH 6.8	0.6	mL
Glycerol	1.8	mL
Adjust volume with ultrapure to	500	μ L

Growth medium DMEM

DMEM powder (1 package) was dissolved with 900 mL of ultrapure water and the g of sodium bicarbonate was added. The medium was mixed until completely dissolved and adjusted pH to 7.2 - 7.3 with 6N HCl. The medium was then adjusted volume to 1 L and further filtered through 0.22 μ m Bottle-Top Vacuum Filters. Before use, medium was supplemented with 10% FBS and 1% penicillin-streptomycin under aseptic condition.

Lysis buffer for 2-DE analysis

DTT	10	mg
CHAPS	20	mg
Thiourea	76.25	mg
Urea	0.21	g
Ampholytes	25	μ L
Protease inhibitor (Cocktail)	5	μ L
Adjust volume with ultrapure to	500	μ L

Phosphate-buffer saline (PBS)

To make 1 L of PBS, the ingredients including 8.00 g of NaCl, 0.20 g of KCl, 1.15 g of Na₂HPO₄ and 0.20 g of KH₂PO₄ were dissolved in 800 mL of ultrapure water and adjusted the pH to 7.2 - 7.4 with 6N HCl. The solution was then adjusted volume to 1000 mL and sterilized by autoclave. Store the buffer at room temperature.

Rehydration buffer for 2-DE analysis

DTT	14	mg
CHAPS	10	mg
Urea	0.24	g
IPG buffer pH 3.10	2.5	μL
Adjust volume with ultrapure to	500	μL

RIPA lysis buffer for immunoblotting

1 M Tris-HCl pH 8.0	50	μL
1 M NaCl	150	μL
10% SDS	10	μL
10% Na deoxycholate	50	μL
Triton-X100	10	μL
R.O. water	630	μL

Freshly add the 100 \times cocktail protease inhibitor in ratio of 1 μL per 100 μL of RIPA buffer before use.

10 \times running buffer for SDS-PAGE (250 mM Tris-base, 1.92 M glycine, 1% SDS)

To make 1 L of 10 \times Tris-glycine running buffer, the ingredients were:

Tris-base	30.2	g
Glycine	144	g
SDS	10	g

All ingredients were dissolved in ultrapure water. The solution was stirred until completely solubilized. Finally, adjust the total volume to 1 L. Store the buffer at room temperature. Dilute to 1 \times before use.

1× running buffer for SDS-PAGE (25 mM Tris-base, 192 mM glycine, 0.1% SDS)

To make 1 L of 1× Tris-glycine running buffer, the ingredients were:

10× running buffer	100	mL
Adjust volume with ultrapure to	1	L

10% SDS solution

To make 100 mL of 10% SDS solution, 10 g of SDS was dissolved in 80 mL of ultrapure water. The solution was stirred until completely solubilized. Carefully adjust the total volume to 100 mL. Store the solution at room temperature.

Separating gel

To prepare 2 separating gels for Mighty small II SE250/SE260, the ingredients of separating gel were:

	8%	12.5%	
Ultrapure water	10.2	14.464	mL
1.5 M Tris-HCl pH 8.8	5.5	11	mL
10% SDS	0.22	0.44	mL
30% acrylamide solution	5.86	17.856	mL
10% APS	220	220	μL
TEMED	13.2	22	μL

All ingredients were thoroughly mixed and immediately pour gel between the glass plates. Ultrapure water was immediately layered the top of the gel. The gels were leaved overnight for complete polymerization.

Stacking gel

Once the separating gel has completely polymerized, ultrapure was removed from the top of the polymerized gel. To prepare 2 stacking gels for Mighty small II SE250/SE260, the ingredients of stacking gel were:

Ultrapure water	3.06	mL
0.5 M Tris-HCl pH 6.8	1.26	mL
10% SDS	50	μ L
30% acrylamide solution	0.66	mL
10% APS	31.2	μ L
TEMED	5	μ L

All ingredients were thoroughly mixed and immediately pour gel between the glass plates. Combs were inserted between the glass plates to make sample loading wells. The gels were leaved at least 40 min to polymerize.

0.25 M Sucrose

To make 500 mL of 0.25 M sucrose solution, 48.78 g of sucrose was dissolved in 450 mL of ultrapure water. The solution was stirred until completely solubilized, then adjusted volume to 500 mL. Store at 4°C.

10× TBS

To make 1 L of 10× TBS buffer, the ingredients were:

Tris-base	24.23	g
NaCl	80.06	g

All ingredients were dissolved in ultrapure water. The solution was stirred until completely solubilized. Finally, adjust the total volume to 1 L. Store the buffer at room temperature. Dilute to 1× before use.

1× TBS-T

To make 1 L of 1× TBS-T buffer, the ingredients were:

10× TBS	100	mL
Tween 20	1	mL
Adjust volume with ultrapure to	1	L

0.5 M Tris-HCl pH 6.8

To make 100 mL of 0.5 M Tris-HCl pH 6.8 buffer, 6.1 g of Tris-base was dissolved in 80 mL of ultrapure water. The solution was stirred until completely solubilized. Adjust to pH 6.8 with 6N HCl. Finally, adjust the total volume to 100 mL. Store the buffer at 4°C.

1.5 M Tris-HCl pH 8.8

To make 100 mL of 1.5 M Tris-HCl pH 8.8 buffer, 18.15 g of Tris-base was dissolved in 80 mL of ultrapure water. The solution was stirred until completely solubilized. Adjust to pH 8.8 with 6N HCl. Finally, adjust the total volume to 100 mL. Store the buffer at 4°C.

0.25% Trypsin/ 0.038% EDTA solution

To prepare 100 mL of trypsin/EDTA solution, 0.25 g of trypsin and 0.038 g of EDTA were dissolved in PBS. Solution was filtered through 0.22 µm syring filter for sterilization.

APPENDIX B
TABLE OF EXPERIMENTAL RESULTS

Table 7. The percentage of $O_2^{\cdot-}$ scavenging activities of AD. Each value represented the mean \pm S.E.M. of three independent experiments. Each performed in triplicate.

AD ($\mu\text{g/mL}$)	% Scavenging	
	ethanolic extract	water extract
0.32	3.98 \pm 3.83	1.34 \pm 9.59
1.60	4.43 \pm 3.93	7.37 \pm 9.44
8	12.34 \pm 8.33	17.93 \pm 9.78
40	32.96 \pm 7.28	28.34 \pm 8.43
200	51.45 \pm 4.35	40.58 \pm 8.39
1000	76.45 \pm 12.34	69.38 \pm 4.34
2000	85.34 \pm 6.93	81.93 \pm 9.34

Table 8. The percentage of $O_2^{\cdot-}$ scavenging activities of AL. Each value represented the mean \pm S.E.M. of three independent experiments. Each performed in triplicate.

AL ($\mu\text{g/mL}$)	% Scavenging	
	ethanolic extract	water extract
8	3.04 \pm 2.98	6.34 \pm 9.43
40	12.93 \pm 8.34	16.37 \pm 10.23
200	31.09 \pm 7.34	29.34 \pm 13.45
1000	43.29 \pm 11.23	46.34 \pm 19.23
2000	56.93 \pm 12.34	62.93 \pm 9.34
3000	78.93 \pm 9.38	74.54 \pm 12.34

Table 9. The percentage of $O_2^{\cdot-}$ scavenging activities of AP. Each value represented the mean \pm S.E.M. of three independent experiments. Each performed in triplicate.

AP ($\mu\text{g/mL}$)	% Scavenging	
	ethanolic extract	water extract
1.60	12.98 \pm 3.44	16.89 \pm 8.34
8	26.83 \pm 2.98	23.84 \pm 8.37
40	45.94 \pm 3.84	48.93 \pm 5.30
200	59.37 \pm 2.97	65.43 \pm 9.98
1000	78.38 \pm 8.93	76.38 \pm 9.34

Table 10. The percentage of $O_2^{\cdot-}$ scavenging activities of AS. Each value represented the mean \pm S.E.M. of three independent experiments. Each performed in triplicate.

AS ($\mu\text{g/mL}$)	% Scavenging	
	ethanolic extract	water extract
1.60	6.92 \pm 5.87	8.83 \pm 7.54
8	12.34 \pm 2.93	15.38 \pm 2.93
40	32.93 \pm 9.83	30.98 \pm 2.74
200	45.94 \pm 8.37	41.93 \pm 4.33
1000	65.43 \pm 8.39	64.33 \pm 9.34
2000	89.39 \pm 6.22	87.94 \pm 5.29

Table 11. The percentage of $O_2^{\cdot -}$ scavenging activities of LC. Each value represented the mean \pm S.E.M. of three independent experiments. Each performed in triplicate.

LC ($\mu\text{g/mL}$)	% Scavenging	
	ethanolic extract	water extract
1.60	8.32 \pm 6.83	4.93 \pm 9.83
8	16.34 \pm 7.32	20.34 \pm 10.34
40	31.98 \pm 9.83	37.23 \pm 10.93
200	54.54 \pm 9.44	59.34 \pm 12.93
1000	72.34 \pm 12.94	76.34 \pm 2.93
2000	89.93 \pm 18.33	84.45 \pm 8.33

Table 12. The percentage of $O_2^{\cdot -}$ scavenging activities of NJ. Each value represented the mean \pm S.E.M. of three independent experiments. Each performed in triplicate.

NJ ($\mu\text{g/mL}$)	% Scavenging	
	ethanolic extract	water extract
0.32	3.98 \pm 2.98	3.94 \pm 1.23
1.60	10.93 \pm 7.43	12.83 \pm 8.37
8	28.98 \pm 10.98	30.93 \pm 5.44
40	40.83 \pm 2.98	45.98 \pm 6.67
200	60.39 \pm 12.34	60.98 \pm 4.30
1000	89.02 \pm 4.32	76.74 \pm 7.53

Table 13. The percentage of $O_2^{\cdot-}$ scavenging activities of PK. Each value represented the mean \pm S.E.M. of three independent experiments. Each performed in triplicate.

PK ($\mu\text{g/mL}$)	% Scavenging	
	ethanolic extract	water extract
0.32	6.34 \pm 4.08	12.93 \pm 9.33
1.60	20.93 \pm 6.33	27.49 \pm 10.83
8	31.93 \pm 7.63	38.94 \pm 5.42
40	49.37 \pm 8.22	54.34 \pm 6.93
200	61.23 \pm 8.63	65.93 \pm 7.34
1000	98.38 \pm 9.45	79.93 \pm 12.93

Table 14. The percentage of $O_2^{\cdot-}$ scavenging activities of SC. Each value represented the mean \pm S.E.M. of three independent experiments. Each performed in triplicate.

SC ($\mu\text{g/mL}$)	% Scavenging	
	ethanolic extract	water extract
8	12.98 \pm 7.83	7.89 \pm 6.33
40	23.83 \pm 4.09	17.65 \pm 3.33
200	40.56 \pm 2.84	35.98 \pm 7.88
1000	47.94 \pm 9.38	42.93 \pm 6.72
2000	76.34 \pm 8.37	68.28 \pm 9.37

Table 15. The percentage of $O_2^{\cdot-}$ scavenging activities of TC. Each value represented the mean \pm S.E.M. of three independent experiments. Each performed in triplicate.

TC ($\mu\text{g/mL}$)	% Scavenging	
	ethanolic extract	water extract
0.32	14.83 \pm 8.21	9.93 \pm 9.02
1.60	32.56 \pm 3.92	23.48 \pm 1.92
8	47.52 \pm 5.93	39.94 \pm 1.28
40	60.37 \pm 8.63	56.73 \pm 3.76
200	87.09 \pm 6.39	88.92 \pm 4.42
1000	98.03 \pm 2.93	96.93 \pm 4.39

Table 16. The percentage of $O_2^{\cdot-}$ scavenging activities of NVK. Each value represented the mean \pm S.E.M. of three independent experiments. Each performed in triplicate.

NVK ($\mu\text{g/mL}$)	% Scavenging	
	ethanolic extract	water extract
0.32	1.92 \pm 1.23	1.34 \pm 0.45
1.60	5.43 \pm 1.93	1.98 \pm 0.94
8	15.71 \pm 9.32	13.83 \pm 6.33
40	51.63 \pm 4.09	43.65 \pm 2.93
200	94.93 \pm 10.92	89.76 \pm 6.34
1000	102.03 \pm 4.87	96.23 \pm 5.63

Table 17. The percentage of H₂O₂ scavenging activities of AD. Each value represented the mean \pm S.E.M. of three independent experiments. Each performed in triplicate.

AD ($\mu\text{g/mL}$)	% Scavenging	
	ethanolic extract	water extract
8	12.83 \pm 6.01	14.93 \pm 8.34
40	32.93 \pm 3.94	26.49 \pm 1.93
200	40.38 \pm 4.99	42.87 \pm 7.83
1000	67.93 \pm 9.34	54.93 \pm 0.34
2000	89.43 \pm 6.34	79.94 \pm 2.22

Table 18. The percentage of H₂O₂ scavenging activities of AL. Each value represented the mean \pm S.E.M. of three independent experiments. Each performed in triplicate.

AL ($\mu\text{g/mL}$)	% Scavenging	
	ethanolic extract	water extract
200	8.34 \pm 3.44	12.83 \pm 5.33
1000	12.67 \pm 6.33	21.85 \pm 4.86
2000	32.93 \pm 13.03	37.93 \pm 7.34
3000	49.95 \pm 12.47	54.82 \pm 1.22
4000	59.73 \pm 8.96	67.55 \pm 6.34

Table 19. The percentage of H₂O₂ scavenging activities of AP. Each value represented the mean \pm S.E.M. of three independent experiments. Each performed in triplicate.

AP ($\mu\text{g/mL}$)	% Scavenging	
	ethanolic extract	water extract
1.60	2.74 \pm 0.43	7.45 \pm 2.34
8	14.83 \pm 4.98	16.03 \pm 3.93
40	23.39 \pm 9.38	20.84 \pm 6.22
200	36.74 \pm 4.93	39.63 \pm 6.98
1000	75.33 \pm 1.34	70.32 \pm 4.33

Table 20. The percentage of H₂O₂ scavenging activities of AS. Each value represented the mean \pm S.E.M. of three independent experiments. Each performed in triplicate.

AS ($\mu\text{g/mL}$)	% Scavenging	
	ethanolic extract	water extract
8	10.93 \pm 0.47	7.83 \pm 0.89
40	21.56 \pm 4.33	17.43 \pm 8.09
200	34.76 \pm 7.89	30.56 \pm 13.44
1000	48.39 \pm 5.67	52.09 \pm 0.94
2000	72.93 \pm 6.98	70.39 \pm 6.29

Table 21. The percentage of H₂O₂ scavenging activities of LC. Each value represented the mean \pm S.E.M. of three independent experiments. Each performed in triplicate.

LC ($\mu\text{g/mL}$)	% Scavenging	
	ethanolic extract	water extract
8	4.39 \pm 8.22	6.23 \pm 1.93
40	11.83 \pm 5.92	17.53 \pm 8.48
200	36.65 \pm 6.93	30.47 \pm 4.34
1000	58.93 \pm 4.39	59.22 \pm 4.63
2000	79.33 \pm 8.36	81.29 \pm 3.99

Table 22. The percentage of H₂O₂ scavenging activities of NJ. Each value represented the mean \pm S.E.M. of three independent experiments. Each performed in triplicate.

NJ ($\mu\text{g/mL}$)	% Scavenging	
	ethanolic extract	water extract
8	7.93 \pm 0.33	8.34 \pm 1.23
40	18.83 \pm 7.01	21.93 \pm 6.34
200	38.94 \pm 9.33	40.37 \pm 3.98
1000	68.39 \pm 4.59	65.39 \pm 6.94
2000	89.54 \pm 10.91	87.93 \pm 0.34

Table 23. The percentage of H₂O₂ scavenging activities of PK. Each value represented the mean \pm S.E.M. of three independent experiments. Each performed in triplicate.

PK ($\mu\text{g/mL}$)	% Scavenging	
	ethanolic extract	water extract
1.60	3.94 \pm 0.68	7.93 \pm 7.39
8	20.15 \pm 0.16	17.38 \pm 8.37
40	39.10 \pm 2.34	32.84 \pm 7.33
200	43.93 \pm 0.23	44.78 \pm 2.94
1000	63.93 \pm 9.33	58.44 \pm 3.98

Table 24. The percentage of H₂O₂ scavenging activities of SC. Each value represented the mean \pm S.E.M. of three independent experiments. Each performed in triplicate.

SC ($\mu\text{g/mL}$)	% Scavenging	
	ethanolic extract	water extract
8	5.93 \pm 1.34	1.93 \pm 0.73
40	21.94 \pm 8.34	25.93 \pm 9.34
200	31.83 \pm 7.34	34.98 \pm 6.34
1000	43.65 \pm 2.45	49.93 \pm 2.34
2000	56.34 \pm 8.43	60.93 \pm 10.34

Table 25. The percentage of H₂O₂ scavenging activities of TC. Each value represented the mean \pm S.E.M. of three independent experiments. Each performed in triplicate.

TC ($\mu\text{g/mL}$)	% Scavenging	
	ethanolic extract	water extract
0.32	7.56 \pm 4.39	4.93 \pm 0.34
1.60	12.93 \pm 0.78	16.93 \pm 3.44
8	41.93 \pm 0.39	40.97 \pm 6.34
40	65.93 \pm 12.33	63.12 \pm 0.34
200	72.98 \pm 12.93	83.83 \pm 8.22
1000	98.93 \pm 8.22	109.23 \pm 10.28

Table 26. The percentage of H₂O₂ scavenging activities of NVK. Each value represented the mean \pm S.E.M. of three independent experiments. Each performed in triplicate.

NVK ($\mu\text{g/mL}$)	% Scavenging	
	ethanolic extract	water extract
0.32	4.83 \pm 0.93	1.29 \pm 0.89
1.60	13.34 \pm 7.34	5.34 \pm 3.54
8	34.83 \pm 3.45	15.34 \pm 6.79
40	42.57 \pm 9.23	31.98 \pm 5.73
200	56.78 \pm 0.34	48.93 \pm 6.34
1000	78.49 \pm 5.39	64.35 \pm 8.34

Table 27. The percentage of OH[•] scavenging activities of AD. Each value represented the mean \pm S.E.M. of three independent experiments. Each performed in triplicate.

AD ($\mu\text{g/mL}$)	% Scavenging	
	ethanolic extract	water extract
8	12.03 \pm 7.34	3.45 \pm 8.33
40	34.22 \pm 1.38	30.48 \pm 0.34
200	52.34 \pm 3.94	46.39 \pm 9.23
1000	67.34 \pm 5.46	60.23 \pm 0.83
2000	78.98 \pm 4.98	75.34 \pm 4.21

Table 28. The percentage of OH[•] scavenging activities of AL. Each value represented the mean \pm S.E.M. of three independent experiments. Each performed in triplicate.

AL ($\mu\text{g/mL}$)	% Scavenging	
	ethanolic extract	water extract
8	5.67 \pm 4.34	8.34 \pm 3.22
40	23.73 \pm 6.77	16.73 \pm 6.39
200	39.23 \pm 4.82	40.34 \pm 1.38
1000	53.34 \pm 6.59	61.93 \pm 4.56
2000	76.39 \pm 4.94	79.03 \pm 5.41

Table 29. The percentage of OH[•] scavenging activities of AP. Each value represented the mean \pm S.E.M. of three independent experiments. Each performed in triplicate.

AP ($\mu\text{g/mL}$)	% Scavenging	
	ethanolic extract	water extract
8	12.34 \pm 9.34	7.08 \pm 6.98
40	31.93 \pm 0.65	27.54 \pm 8.34
200	44.57 \pm 3.45	49.45 \pm 3.45
1000	57.98 \pm 3.97	59.32 \pm 2.34
2000	80.34 \pm 6.83	76.34 \pm 1.22

Table 30. The percentage of OH[•] scavenging activities of AS. Each value represented the mean \pm S.E.M. of three independent experiments. Each performed in triplicate.

AS ($\mu\text{g/mL}$)	% Scavenging	
	ethanolic extract	water extract
8	9.34 \pm 5.66	5.34 \pm 0.34
40	23.94 \pm 1.23	21.83 \pm 5.41
200	38.45 \pm 3.34	41.34 \pm 4.33
1000	54.56 \pm 9.34	51.34 \pm 8.34
2000	78.45 \pm 0.34	85.63 \pm 5.34

Table 31. The percentage of OH[•] scavenging activities of LC. Each value represented the mean \pm S.E.M. of three independent experiments. Each performed in triplicate.

LC ($\mu\text{g/mL}$)	% Scavenging	
	ethanolic extract	water extract
8	12.03 \pm 6.11	16.34 \pm 2.93
40	23.84 \pm 6.45	21.09 \pm 0.22
200	40.12 \pm 4.34	36.76 \pm 0.34
1000	56.78 \pm 3.48	54.93 \pm 3.55
2000	82.34 \pm 3.55	78.34 \pm 2.93

Table 32. The percentage of OH[•] scavenging activities of NJ. Each value represented the mean \pm S.E.M. of three independent experiments. Each performed in triplicate.

NJ ($\mu\text{g/mL}$)	% Scavenging	
	ethanolic extract	water extract
8	12.89 \pm 4.59	11.09 \pm 7.69
40	30.49 \pm 7.15	25.29 \pm 4.98
200	45.69 \pm 7.19	40.69 \pm 6.23
1000	69.19 \pm 5.19	62.19 \pm 4.69
2000	89.29 \pm 4.22	82.19 \pm 4.42

Table 33. The percentage of OH[•] scavenging activities of PK. Each value represented the mean \pm S.E.M. of three independent experiments. Each performed in triplicate.

PK ($\mu\text{g/mL}$)	% Scavenging	
	ethanolic extract	water extract
8	18.51 \pm 5.26	10.26 \pm 5.15
40	30.21 \pm 5.46	43.46 \pm 7.15
200	48.25 \pm 5.29	49.25 \pm 2.59
1000	61.28 \pm 5.15	63.15 \pm 1.89
2000	79.82 \pm 4.69	83.58 \pm 4.25

Table 34. The percentage of OH[•] scavenging activities of SC. Each value represented the mean \pm S.E.M. of three independent experiments. Each performed in triplicate.

SC ($\mu\text{g/mL}$)	% Scavenging	
	ethanolic extract	water extract
1.6	12.03 \pm 4.73	14.16 \pm 0.58
8	26.83 \pm 1.34	30.15 \pm 4.89
40	41.23 \pm 4.03	45.69 \pm 1.28
200	59.45 \pm 1.34	58.29 \pm 6.39
1000	73.95 \pm 9.34	76.58 \pm 4.15

Table 35. The percentage of OH[•] scavenging activities of TC. Each value represented the mean \pm S.E.M. of three independent experiments. Each performed in triplicate.

TC ($\mu\text{g/mL}$)	% Scavenging	
	ethanolic extract	water extract
0.32	14.09 \pm 8.46	15.29 \pm 9.25
1.60	30.29 \pm 1.59	35.19 \pm 5.98
8	47.29 \pm 5.98	51.69 \pm 7.59
40	59.19 \pm 2.97	60.49 \pm 4.29
200	86.29 \pm 4.98	76.49 \pm 9.58
1000	106.59 \pm 7.19	98.79 \pm 4.98

Table 36. The percentage of OH[•] scavenging activities of NVK. Each value represented the mean \pm S.E.M. of three independent experiments. Each performed in triplicate.

NVK ($\mu\text{g/mL}$)	% Scavenging	
	ethanolic extract	water extract
0.32	9.18 \pm 2.39	11.89 \pm 0.19
1.60	23.17 \pm 4.19	20.34 \pm 6.78
8	40.59 \pm 3.29	37.08 \pm 4.80
40	59.19 \pm 5.10	53.29 \pm 4.19
200	76.29 \pm 1.29	70.39 \pm 5.00
1000	89.78 \pm 1.29	91.05 \pm 0.29

Table 37. The percentage of NO[•] scavenging activities of AD. Each value represented the mean ± S.E.M. of three independent experiments. Each performed in triplicate.

AD (µg/mL)	% Scavenging	
	ethanolic extract	water extract
1.6	20.18 ± 4.98	16.21 ± 4.00
8	39.48 ± 5.89	30.89 ± 1.97
40	56.89 ± 1.44	45.69 ± 1.89
200	69.49 ± 1.22	59.18 ± 4.01
1000	86.18 ± 6.49	83.29 ± 1.09

Table 38. The percentage of NO[•] scavenging activities of AL. Each value represented the mean ± S.E.M. of three independent experiments. Each performed in triplicate.

AL (µg/mL)	% Scavenging	
	ethanolic extract	water extract
8	11.98 ± 2.98	12.56 ± 0.16
40	23.09 ± 7.00	21.91 ± 7.10
200	40.29 ± 3.29	39.49 ± 3.50
1000	59.42 ± 2.10	61.39 ± 1.29
2000	73.19 ± 2.98	78.16 ± 6.15

Table 39. The percentage of NO[•] scavenging activities of AP. Each value represented the mean \pm S.E.M. of three independent experiments. Each performed in triplicate.

AP ($\mu\text{g/mL}$)	% Scavenging	
	ethanolic extract	water extract
8	20.98 \pm 4.09	17.98 \pm 2.29
40	38.74 \pm 9.58	40.21 \pm 3.09
200	58.16 \pm 0.98	63.29 \pm 4.02
1000	71.29 \pm 5.98	75.29 \pm 1.29
2000	89.82 \pm 4.09	92.39 \pm 4.19

Table 40. The percentage of OH[•] scavenging activities of AS. Each value represented the mean \pm S.E.M. of three independent experiments. Each performed in triplicate.

AS ($\mu\text{g/mL}$)	% Scavenging	
	ethanolic extract	water extract
8	5.19 \pm 0.94	6.98 \pm 0.92
40	14.33 \pm 6.91	10.98 \pm 4.50
200	32.19 \pm 0.89	26.19 \pm 0.95
1000	65.98 \pm 0.77	55.29 \pm 4.09
2000	81.59 \pm 0.47	76.09 \pm 4.29

Table 41. The percentage of NO[•] scavenging activities of LC. Each value represented the mean \pm S.E.M. of three independent experiments. Each performed in triplicate.

LC ($\mu\text{g/mL}$)	% Scavenging	
	ethanolic extract	water extract
1.6	5.98 \pm 1.09	9.12 \pm 0.13
8	20.15 \pm 4.09	19.19 \pm 5.08
40	39.19 \pm 5.18	42.98 \pm 5.39
200	66.08 \pm 0.89	71.98 \pm 0.89
1000	86.19 \pm 7.02	84.19 \pm 9.12

Table 42. The percentage of NO[•] scavenging activities of NJ. Each value represented the mean \pm S.E.M. of three independent experiments. Each performed in triplicate.

NJ ($\mu\text{g/mL}$)	% Scavenging	
	ethanolic extract	water extract
8	16.36 \pm 3.10	12.39 \pm 4.16
40	30.48 \pm 1.24	34.94 \pm 1.23
200	46.29 \pm 9.08	50.19 \pm 4.03
1000	60.23 \pm 4.22	62.98 \pm 4.02
2000	78.45 \pm 1.03	79.34 \pm 0.35

Table 43. The percentage of NO[•] scavenging activities of PK. Each value represented the mean \pm S.E.M. of three independent experiments. Each performed in triplicate.

PK ($\mu\text{g/mL}$)	% Scavenging	
	ethanolic extract	water extract
8	12.17 \pm 1.82	14.36 \pm 0.82
40	30.17 \pm 0.38	32.25 \pm 2.04
200	46.58 \pm 4.98	52.31 \pm 0.08
1000	59.23 \pm 0.18	65.28 \pm 3.02
2000	71.29 \pm 4.02	75.18 \pm 1.08

Table 44. The percentage of NO[•] scavenging activities of SC. Each value represented the mean \pm S.E.M. of three independent experiments. Each performed in triplicate.

SC ($\mu\text{g/mL}$)	% Scavenging	
	ethanolic extract	water extract
1.6	12.37 \pm 0.24	10.26 \pm 4.30
8	30.19 \pm 1.09	24.53 \pm 4.01
40	47.29 \pm 2.19	49.29 \pm 4.59
200	59.13 \pm 0.28	63.15 \pm 1.09
1000	71.33 \pm 4.21	73.04 \pm 2.61

Table 45. The percentage of NO[•] scavenging activities of TC. Each value represented the mean \pm S.E.M. of three independent experiments. Each performed in triplicate.

TC ($\mu\text{g/mL}$)	% Scavenging	
	ethanolic extract	water extract
0.32	10.18 \pm 0.58	8.16 \pm 0.16
1.60	20.12 \pm 4.05	16.15 \pm 5.01
8	31.08 \pm 1.09	35.28 \pm 4.06
40	42.08 \pm 1.54	46.24 \pm 1.58
200	79.25 \pm 1.05	73.05 \pm 4.21
1000	92.15 \pm 12.09	105.18 \pm 0.28

Table 46. The percentage of NO[•] scavenging activities of NVK. Each value represented the mean \pm S.E.M. of three independent experiments. Each performed in triplicate.

NVK ($\mu\text{g/mL}$)	% Scavenging	
	ethanolic extract	water extract
1.60	6.99 \pm 1.17	6.71 \pm 5.79
8	15.34 \pm 0.38	19.46 \pm 1.05
40	40.23 \pm 2.03	43.44 \pm 1.53
200	62.31 \pm 2.33	56.72 \pm 4.12
1000	86.45 \pm 1.66	78.34 \pm 1.03

Table 47. The EC₅₀ values of O₂^{•-}, H₂O₂, OH[•] and NO[•] scavenging activities of ethanolic extracts of individual herbs and NVK. Each value represented the mean ± S.E.M. of three independent experiments. Each performed in triplicate.

Extract	EC ₅₀ values (µg/mL)			
	O ₂ ^{•-}	H ₂ O ₂	OH [•]	NO [•]
AD	201.20 ± 23.82	629.32 ± 22.91	183.70 ± 44.37	30.67 ± 4.16
AL	1599.84 ± 45.64	3016.00 ± 170.94	868.77 ± 150.63	353.33 ± 85.05
AP	75.29 ± 4.65	515.34 ± 29.84	308.71 ± 18.73	106.00 ± 20.66
AS	358.78 ± 21.76	1190.00 ± 113.65	489.94 ± 51.33	546.67 ± 102.55
LC	150.54 ± 5.79	733.67 ± 60.52	440.62 ± 57.37	81.67 ± 11.68
NJ	80.69 ± 0.06	645.36 ± 18.70	325.54 ± 12.78	226.00 ± 28.84
PK	45.35 ± 3.87	501.91 ± 14.95	216.33 ± 14.79	269.33 ± 33.08
SC	1083.73 ± 41.01	1774.67 ± 152.06	80.86 ± 2.81	288.00 ± 28.93
TC	12.00 ± 1.14	21.28 ± 0.29	9.99 ± 1.03	68.33 ± 13.65
NVK	47.26 ± 6.23	132.32 ± 15.16	26.99 ± 1.47	82.33 ± 9.45

Table 48. The EC₅₀ values of O₂^{•-}, H₂O₂, OH[•] and NO[•] scavenging activities of water extracts of individual herbs and NVK. Each value represented the mean ± S.E.M. of three independent experiments. Each performed in triplicate.

Extract	EC ₅₀ values (µg/mL)			
	O ₂ ^{•-}	H ₂ O ₂	OH [•]	NO [•]
AD	355.60 ± 13.02	896.71 ± 25.33	296.67 ± 15.31	70.00 ± 13.53
AL	1392.30 ± 26.66	2726.00 ± 272.19	584.89 ± 87.24	368.67 ± 36.64
AP	61.16 ± 2.30	559.14 ± 19.42	218.84 ± 36.51	83.00 ± 10.54
AS	378.31 ± 6.80	994.67 ± 141.85	487.12 ± 48.38	781.33 ± 46.69
LC	130.99 ± 5.06	708.67 ± 17.21	474.70 ± 42.39	76.33 ± 9.87
NJ	67.16 ± 1.45	645.64 ± 11.96	310.40 ± 13.12	195.00 ± 22.11
PK	28.70 ± 3.51	579.58 ± 31.36	231.37 ± 20.63	182.00 ± 26.89
SC	1559.22 ± 97.18	1133.00 ± 92.59	109.06 ± 3.65	217.00 ± 26.23
TC	12.00 ± 1.14	22.35 ± 0.48	7.63 ± 0.36	75.67 ± 12.22
NVK	57.81 ± 8.56	248.52 ± 7.65	40.42 ± 2.51	135.67 ± 8.14

Table 49. CI values of $O_2^{\cdot-}$, H_2O_2 , OH^{\cdot} and NO^{\cdot} scavenging activities of ethanolic and water extracts. Each value represented the mean \pm S.E.M. of three independent experiments. Each performed in triplicate. Significance of CI values lower than 1 was indicated as * $p < 0.05$ and ** $p < 0.01$. # indicated the significance of CI values higher than 1 ($p < 0.05$).

radical	ethanolic extract	water extract
$O_2^{\cdot-}$	0.84 \pm 0.09*	1.06 \pm 0.11
H_2O_2	0.84 \pm 0.06*	1.51 \pm 0.03#
OH^{\cdot}	0.41 \pm 0.03**	0.73 \pm 0.01**
NO^{\cdot}	0.79 \pm 0.08*	1.10 \pm 0.09

Table 50. The percentage of cell viability of NVK at various concentrations and incubation times measured by MTT reduction assay. Each value represented the mean \pm S.E.M. of three independent experiments. Each performed in triplicate. * indicated the significant difference when compared to the vehicle control group ($p < 0.05$).

NVK (mg/mL)	% Cell viability		
	6 h	12 h	24 h
0.000	100.00	100.00	100.00
0.002	100.22 \pm 4.74	102.64 \pm 4.04	96.42 \pm 2.16
0.008	91.71 \pm 3.36	92.64 \pm 1.76	98.91 \pm 2.50
0.031	94.44 \pm 2.06	94.15 \pm 2.40	92.49 \pm 2.93
0.125	98.04 \pm 6.35	98.09 \pm 5.51	83.52 \pm 3.24
0.500	97.81 \pm 2.99	94.93 \pm 3.15	52.99 \pm 3.65*
1.000	89.81 \pm 1.42	89.75 \pm 1.82	30.14 \pm 7.55*

Table 51. The percentage of DCF fluorescence of NVK at various concentrations and incubation times measured by DCFH-DA assay. Each value represented the mean \pm S.E.M. of three independent experiments. Each performed in triplicate. * indicated the significant difference when compared to the vehicle control group ($p < 0.05$).

NVK (mg/mL)	% DCF fluorescence		
	6 h	12 h	24 h
0.000	100.00	100.00	100.00
0.002	90.66 \pm 2.98	89.21 \pm 4.16	93.81 \pm 6.79
0.008	89.31 \pm 5.60	93.31 \pm 1.67	84.35 \pm 2.66
0.031	98.25 \pm 1.10	97.91 \pm 2.10	91.58 \pm 2.71
0.125	86.28 \pm 5.78	88.83 \pm 5.09	68.34 \pm 4.80*
0.500	93.56 \pm 3.08	95.19 \pm 6.10	40.78 \pm 2.64*
1.000	87.94 \pm 5.81	98.07 \pm 2.59	39.74 \pm 4.50*

Table 52. The percentage of cell viability of Hcy at various concentrations and incubation times measured by MTT reduction assay. Each value represented the mean \pm S.E.M. of three independent experiments. Each performed in triplicate. * indicated the significant difference when compared to the vehicle control group ($p < 0.05$).

Hcy (μ M)	% Cell viability		
	6 h	12 h	24 h
0.000	100.00	100.00	100.00
0.005	94.23 \pm 3.87	88.14 \pm 5.69	92.54 \pm 4.91
0.01	93.45 \pm 6.13	87.12 \pm 4.69	99.47 \pm 0.56
0.05	88.97 \pm 4.88	87.00 \pm 6.20	93.04 \pm 0.39
0.1	93.92 \pm 4.60	94.22 \pm 2.21	98.40 \pm 1.38
0.5	91.06 \pm 4.04	89.24 \pm 9.39	93.56 \pm 6.18
1	89.87 \pm 1.04	92.94 \pm 5.83	95.30 \pm 7.04
2	86.91 \pm 2.67	86.28 \pm 3.77	87.96 \pm 3.82
5	89.98 \pm 2.05	90.06 \pm 3.50	76.81 \pm 2.00*

Table 53. The percentage of DCF fluorescence of Hcy at various concentrations for 0.5, 1, 2 and 3 h measured by DCFH-DA assay. Each value represented the mean \pm S.E.M. of three independent experiments. Each performed in triplicate. * indicated the significant difference when compared to the control group ($p < 0.05$).

Hcy (mM)	% DCF fluorescence			
	0.5 h	1 h	2 h	3 h
0.005	106.31 \pm 4.58	99.45 \pm 1.29	101.76 \pm 5.87	90.52 \pm 5.43
0.01	103.72 \pm 2.48	98.57 \pm 3.38	104.07 \pm 6.33	96.81 \pm 5.33
0.02	98.86 \pm 1.88	97.01 \pm 2.48	99.59 \pm 4.80	91.15 \pm 5.32
0.05	100.39 \pm 2.34	102.90 \pm 3.24	101.54 \pm 4.52	98.36 \pm 1.00
0.1	96.22 \pm 6.69	102.32 \pm 4.68	103.92 \pm 4.67	98.40 \pm 3.35
0.5	100.02 \pm 3.44	110.09 \pm 0.57	104.69 \pm 8.50	100.13 \pm 2.41
1	103.67 \pm 5.00	119.43 \pm 1.45*	108.69 \pm 4.99	104.33 \pm 0.86
2	113.06 \pm 12.97	131.77 \pm 6.47*	106.59 \pm 3.10	113.77 \pm 0.95

Table 54. The percentage of DCF fluorescence of Hcy at various concentrations for 6, 12 and 24 h measured by DCFH-DA assay. Each value represented the mean \pm S.E.M. of three independent experiments. Each performed in triplicate. * indicated the significant difference when compared to the control group ($p < 0.05$).

Hcy (mM)	% DCF fluorescence		
	6 h	12 h	24 h
0.005	97.99 \pm 4.51	106.13 \pm 2.28	102.43 \pm 5.94
0.01	98.82 \pm 3.72	120.01 \pm 5.00*	103.20 \pm 3.55
0.02	95.26 \pm 3.36	116.72 \pm 2.09*	98.96 \pm 2.69
0.05	102.85 \pm 3.80	105.44 \pm 5.40	100.78 \pm 5.87
0.1	97.82 \pm 3.97	93.96 \pm 1.86	101.73 \pm 1.46
0.5	106.36 \pm 5.04	84.80 \pm 2.84	101.96 \pm 3.37
1	105.49 \pm 1.13	88.62 \pm 1.69	97.44 \pm 2.80
2	110.58 \pm 1.01	80.55 \pm 0.34	96.53 \pm 2.15

Table 55. The percentage of DCF fluorescence of NVK pre-treatment at the various concentrations for 12 h prior to 1 mM Hcy for 1 h measured by DCFH-DA assay. Each value represented the mean \pm S.E.M. of three independent experiments. Each performed in triplicate. * indicated the significant difference when compared to the untreated group ($p < 0.05$).

NVK (mg/mL)	% DCF fluorescence
control	100.00
0.000	116.54 \pm 1.28
0.001	106.51 \pm 2.58
0.005	98.31 \pm 6.30*
0.01	97.34 \pm 6.44*
0.05	98.94 \pm 4.21*
0.1	107.34 \pm 6.25
0.2	89.54 \pm 2.18*
0.5	71.59 \pm 1.28*

Table 56. The percentage of cell viability of NVK pre-treatment at the various concentrations for 12 h prior to 0.05 mM Hcy for 12 h measured by MTT reduction assay. Each value represented the mean \pm S.E.M. of three independent experiments. Each performed in triplicate. * indicated the significant difference when compared to the untreated group ($p < 0.05$).

NVK (mg/mL)	% Cell viability
control	100.00
0.000	92.15 \pm 0.85
0.001	94.46 \pm 0.92
0.005	94.62 \pm 4.56
0.01	93.28 \pm 3.92
0.05	92.89 \pm 0.59
0.1	93.21 \pm 0.91
0.2	84.56 \pm 2.94
0.5	78.38 \pm 3.02*

Table 57. The percentage of DCF fluorescence of NVK pre-treatment at the various concentrations for 12 h prior to 0.05 mM Hcy for 12 h measured by DCFH-DA assay. Each value represented the mean \pm S.E.M. of three independent experiments. Each performed in triplicate. * indicated the significant difference when compared to the untreated group ($p < 0.05$).

NVK (mg/mL)	% DCF fluorescence
control	100.00
0.000	113.59 \pm 4.58
0.001	96.29 \pm 3.46
0.005	94.59 \pm 2.45
0.01	94.01 \pm 2.91
0.05	90.25 \pm 4.02*
0.1	101.33 \pm 2.19
0.2	102.30 \pm 2.01
0.5	80.41 \pm 2.46*

Table 58. Identified proteins obtained from LC/MS/MS and MASCOT database.

Spot no.	Protein identity	SwissProt no.	Mascot score	Sequence coverage (%)	Peptide
1	Annexin A1	P04083	427	28	K.GVDEATHIDILTK.R K.AAYLQETGKPLDETLK.K K.TPAQFDADEL.R.A K.DITSDTSGDFR.N R.NALLSLAK.G R.ALYEAGER.R K.GTDVNVFNTILTTR.S K.CLTAIVK.C
2	Annexin A2	P07355	153	8	R.SEIDMNDIK.A R.DALNIETAIK.T R.QDIAFAYQR.R
3	Glutathione S-transferase P	P09211	134	10	K.TPAQYDASELK.A K.ASCLYGQLPK.F R.MLLADQGSWK.E

Table 58. (Continued)

Spot no.	Protein identity	SwissProt no.	Mascot score	Sequence coverage (%)	Peptide
4	Superoxide dismutase [Cu-Zn]	P00441	89	7	R.HVGDLDGNVTADK.D
5	Calreticulin	P27797	195	10	K.EQFLDGDGWTSR.W K.FVLSSGK.F K.FYGDEEK.D K.FYGDEEKDK.G K.VHVIFNYK.G K.NVLINK.D
6	Calreticulin	P27797	134	5	K.GQTLVVQFTVK.H K.VHVIFNYK.G K.NVLINK.D
7	Endoplasmin	P14625	267	6	K.IYFMAGSSR.K K.EAESSPFVER.L K.DISTNYYASQK.K K.TFEINPR.H R.SGYLLPDTK.A R.LSLNIDPDAK.V
8	T-complex protein 1, subunit beta	P78371	226	13	K.LAVEAVLR.L K.GSGNLEAIHIK.K K.ILIANTGMDTDK.I R.GATQQILDEAER.S R.EALLSSAVDHGSDEVK.F
9	78 kD glucose-regulated protein	P11021	127	6	K.TKPYIQVDIGGGQTK.T K.VTHAVVTVPAYFNDAQR.Q K.ITITNDQNR.L
10	Heat shock cognate 71 kD protein	P11142	457	15	K.VEIIANDQGNR.T K.NQVAMNPTNTVFDAK.R R.FDDAVVQSDMK.H K.EIAEAYLGK.T K.DAGTIAGLNVL.R.I R.FEELNADLFR.G R.GTLDPVEK.A K.LLQDFENGK.E K.ITITNDK.G K.VCNPIITK.L
12	Heat shock cognate 71 kD protein	P11142	169	5	R.GTLDPVEK.A K.LLQDFENGK.E K.VCNPIITK.L

Table 58. (Continued)

Spot no.	Protein identity	SwissProt no.	Mascot score	Sequence coverage (%)	Peptide
13	Vimentin	P08670	879	45	R.LDLER.K R.FANYIDK.V R.FLEQQNK.I R.SYVTTSTR.T K.LLEGEESR.I R.QQYESVAAK.N R.QVDQLTNDK.A R.DNLAEDIMR.L K.FADLSEAAANR.N K.VELQELNDR.F R.LQDEIQNMK.E R.EYQDLLNVK.M R.LGDLYEEEMR.E K.MALDIEIATYR.K K.NLQEAEWYK.S R.EEAENTLQSFR.Q K.VESLQEEIAFLK.K R.QVQSLTCEVDALK.G R.TYSLGSALRPSTSR.S R.DGQVINETSQHDDLE.-
15	Tubulin beta-4A	P04350	172	6	R.IMNTFSVVPSPK.V K.LAVNMVPPFR.L K.TAVCDIPPR.G
17	Actin, beta	P60709	260	13	K.AGFAGDDAPR.A K.DSYVGDEAQSK.R R.DLTDYLMK.I R.GYSFTTTAER.E K.EITALAPSTMK.I
18	Stathmin	P16949	131	21	R.ASGQAFELILSPR.S K.DLSLEEIQK.K K.AIEENNNFSK.M
19	Prelamin-A/C	P02545	103	2	R.SSFSQHAR.T R.VAVEEVDEEGK.F
21	Alpha-enolase	P06733	243	13	K.YDLDFK.S K.TIAPALVSK.K K.KLNVTEQEK.I R.IGAEVYHNLK.N K.LMIEMDGTENK.S R.YISPDQLADLYK.S
22	Alpha-enolase	P06733	181	6	K.TIAPALVSK.K K.LNVTEQEK.I K.KLNVTEQEK.I R.IGAEVYHNLK.N

Table 58. (Continued)

Spot no.	Protein identity	SwissProt no.	Mascot score	Sequence coverage (%)	Peptide
23	Pyruvate kinase isozymes M1/M2	P14618	215	8	K.GSGTAEVELK.K K.GSGTAEVELKK.G R.GDLGIEIPAEK.V K.CCSGAIIVLTK.S R.NTGIICTIGPASR.S
24	Alpha-enolase	P06733	265	12	K.YDLDFK.S R.IEELGSK.A K.LNVTEQEK.I K.SCNCLLLK.V K.KLVNTEQEK.I R.IGAEVYHNLK.N R.YISPDQLADLYK.S
25	Triosephosphate isomerase	P60174	152	8	K.SNVSDAVAQSTRI R.IIYGGSVTGATCK.E
26	Heterogeneous nuclear ribonucleoprotein H	P31943	227	16	R.FIYTR.E R.YIEIFK.S K.IQNGAQGIR.F R.VHIEIGPDGR.V R.VHIEIGPDGR.V R.GLPWSCSADEVQR.F R.DLNYCFSGMSDHR.Y K.HTGPNSPDTANDGFVR.L
28	Splicing factor, proline- and glutamine-rich	P23246	128	4	R.AVVIVDDR.G R.EMEEQMR.R R.FGQGGAGPVGGQGPR.G
29	Heterogeneous nuclear ribonucleoprotein H	P31943	121	5	R.FIYTR.E K.IQNGAQGIR.F K.SNNVEMDWVLK.H
30	Heterogeneous nuclear ribonucleoproteins A2/B1	P22626	201	14	R.GGNFGFGDSR.G R.DYFEEYGK.I K.IDTIEIITDR.Q R.QEMQEVQSSR.S K.YHTINGHNAEVR.K
31	Heterogeneous nuclear ribonucleoprotein A1-like 2	Q32P51	98	5	R.DYFEQYQK.I R.DYFEQYQK.I K.IEVIEIMTDR.G

Table 58. (Continued)

Spot no.	Protein identity	SwissProt no.	Mascot score	Sequence coverage (%)	Peptide
32	Protein disulfide-isomerase	P07237	548	26	K.EECPAVR.L K.FFPASADR.T K.VHSFPTLK.F R.ITEFCHR.F R.ILEFFGLK.K K.DHENIVIAK.M R.TVIDYNGER.T K.THILLFLPK.S R.EADDIVNWLK.K R.LITLEEEMTK.Y K.NFEDVAFDEK.K K.MDSTANEVEAVK.V
33	Nucleophosmin	P06748	78	7	K.LLSISGK.R K.GPSSVEDIK.A
36	Elongation factor Tu, mitochondrial	P49411	203	9	K.FINYVK.N K.TTLTAAITK.I K.YEEIDNAPEER.A R.AEAGDNLGALVR.G
37	Lipocalin-1	P31025	107	12	K.VEAQVYILSK.E R.GLSTESILIPR.Q K.NNLEALEDFEK.A

Table 59. Relative ratio of NVK on induction of HIF-1 α in EA.hy926 cells. Intensity was quantified using ImageJ software and normalized with β -actin. Each value represented the mean \pm S.E.M. of three independent experiments. Each performed in triplicate. * indicated the significant difference when compared to the untreated group ($p < 0.05$).

Induction time (h)	Relative intensity
control	1.00
0.5	0.913 \pm 0.038
1	1.040 \pm 0.072
2	1.010 \pm 0.076
6	0.973 \pm 0.060
8	0.960 \pm 0.047
12	1.037 \pm 0.032

Table 60. Relative ratio of NVK on induction of Nrf2 in EA.hy926 cells. Intensity was quantified using ImageJ software and normalized with β -actin. Each value represented the mean \pm S.E.M. of three independent experiments. Each performed in triplicate. * indicated the significant difference when compared to the untreated group ($p < 0.05$).

Induction time (h)	Relative intensity
control	1.00
0.5	1.013 \pm 0.067
1	1.047 \pm 0.117
2	0.967 \pm 0.058
6	1.043 \pm 0.130
8	0.998 \pm 0.022
12	0.950 \pm 0.049

Table 61. Relative intensity ratio of HO-1 expression by NVK treatment. Intensity was quantified using ImageJ software and normalized with β -actin. Each value represented the mean \pm S.E.M. of three independent experiments. Each performed in triplicate. * indicated the significant difference when compared to the untreated group ($p < 0.05$).

NVK (mg/mL)	Relative intensity
control	1.00
0	1.213 \pm 0.069
0.01	1.353 \pm 0.166
0.05	1.930 \pm 0.074*
0.2	2.860 \pm 0.107*

Table 62. Relative intensity ratio of expression of antioxidant enzymes by NVK treatment. Intensity was quantified using ImageJ software and normalized with β -actin. Each value represented the mean \pm S.E.M. of three independent experiments. Each performed in triplicate. * indicated the significant difference when compared to the untreated group ($p < 0.05$).

NVK (mg/mL)	Relative intensity		
	SOD	GPx	CAT
control	1.00	1.00	1.00
0	0.993 \pm 0.156	1.027 \pm 0.055	1.077 \pm 0.069
0.01	0.847 \pm 0.055	0.957 \pm 0.063	0.987 \pm 0.069
0.05	0.853 \pm 0.067	1.060 \pm 0.079	0.940 \pm 0.026
0.2	0.757 \pm 0.039*	1.080 \pm 0.029	0.960 \pm 0.062

Table 63. Relative intensity ratio of VEGF expression by NVK treatment. Intensity was quantified using ImageJ software and normalized with GAPDH. Each value represented the mean \pm S.E.M. of three independent experiments. Each performed in triplicate. * indicated the significant difference when compared to the untreated group ($p < 0.05$).

Sample	Relative intensity
control	1.00
0.05 mg/mL NVK	1.413 \pm 0.052
10 μ M ferulic acid	1.473 \pm 0.074

Table 64. Relative intensity ratio of Akt phosphorylation by NVK treatment. Intensity was quantified using ImageJ software and normalized with β -actin. Each value represented the mean \pm S.E.M. of three independent experiments. Each performed in triplicate. * indicated the significant difference when compared to the untreated group ($p < 0.05$).

Induction time (min)	Relative intensity
control	1.00
5	0.835 \pm 0.067
15	0.810 \pm 0.111
30	1.147 \pm 0.061
45	1.113 \pm 0.080
60	1.097 \pm 0.057
90	0.997 \pm 0.107

Table 65. Relative intensity ratio of eNOS phosphorylation by NVK treatment. Intensity was quantified using ImageJ software and normalized with β -actin. Each value represented the mean \pm S.E.M. of three independent experiments. Each performed in triplicate. * indicated the significant difference when compared to the untreated group ($p < 0.05$).

Induction time (min)	Relative intensity
control	1.00
5	1.072 \pm 0.144
15	1.020 \pm 0.106
30	1.087 \pm 0.157
45	1.320 \pm 0.070*
60	1.163 \pm 0.048
90	1.067 \pm 0.063

VITA

Mr. Nonthaneth Nalinratana was born on April 18, 1986 in Bangkok, Thailand. In 2009, he received Bachelor of Science in Pharm. from Chulalongkorn University. After graduation, he entered the Master's degree program in Biomedical Chemistry at the Faculty of Pharmaceutical Sciences, Chulalongkorn University.